UNIVERSITY OF LONDON THESIS

Degree PhD Year 2006 Name of Author SILVA
Elizabeth

The role of the tumour suppressor Fat in the patterning and development of the *Drosophila* eye

Elizabeth Silva

Developmental Patterning Laboratory
London Research Institute
Cancer Research UK, London

A thesis submitted for the degree of
Doctor of Philosophy
at the University of London

ProQuest LLC
789 East Eisenhower Parkway
P.O. Box 1346
Ann Arbor, MI 48106-1346

I, Elizabeth Silva, declare that the work presented in this thesis is my own, except where acknowledged.

Abstract

The atypical cadherin and tumour suppressor, Fat, is a molecule with a well-defined role in planar cell polarity. Specifically, it is one of a number of molecules that provides directional cues to cells in the establishment of tissue polarity in a variety of systems and organisms. Less understood is its function as a tumour suppressor. The work presented here is a characterisation of the *fat* phenotypes, with a view to understanding the mechanisms underlying Fat's ability to restrict proliferation. Using the *Drosophila* eye as a model system, I have addressed this problem in three ways.

First, I examined the patterns of expression of various cell cycle molecules, as well as markers of various stages of the cell cycle. This analysis led me to propose that mutations in *fat* result in a de-sensitisation of cells to the signalling cascades that are responsible for triggering a transition from proliferation to differentiation in the course of development.

As such, I then looked at the ways in which Fat affects the activities of the main signalling pathways involved in *Drosophila* eye development: Notch, EGFR, Hedgehog, Dpp, and Wingless. From this analysis I found that Fat function can be connected to EGFR, Hedgehog and Wingless signalling. However, I found no evidence to implicate these pathways in Fat-related overgrowth.

Finally, I present evidence of parallels between phenotypes of *fat* and those of components of the Hippo signalling pathway. I show that Fat is required for localisation of Expanded, the most upstream component of this pathway identified to date. I further demonstrate that this localisation is necessary for the function of this pathway and that compromises to this

function contribute to Ft-related overgrowth. I also present evidence that suggests this role in growth suppression is independent of Fat's role in dorsal-ventral polarity in the eye.

Acknowledgements

First, thank you to my supervisor, Helen McNeill, whose unquenchable enthusiasm for science has made my degree so genuinely enjoyable. Thank you also to Sally Leevers and to Nic Tapon who have both been like surrogate supervisors in Helen's absence.

Thank you to the members of the McNeill Lab, past and present, in London and in Toronto. In particular, Lesley Clayton, Joseph Bateman, Afifa Khan, Ruth Wheeler, Sakura Saburi and Manolis Fanto, who were all there at the start and who were great company along the way. And I can't forget a few of the later arrivals: Nadja Muncke, Natalia Arbuzova and Nancy Amin who were there for a brief, but memorable, time.

Thank you to the members of the Developmental supergroup who have provided invaluable insight and feedback over the course of this project, as well as some delicious teatime snacks. In particular, thank you to Inbal Ringel, Ditte Andersen, Rhian Walther, Jon Leslie, Megan Cully, Mariam Orme and Mary Wu, and the honorary members of CRUK, Joana Novais and Nick Hutchinson, for invaluable and (I hope) enduring friendships.

Thank you to Terence Gilbank, Steve Murray and Francis Earl for taking such good care of our flies, and for making those long hours in the fly room so much more enjoyable.

Living in London has provided me with some amazing experiences and opportunities, but one of the hardest things about being here is saying goodbye to so many friends when they move on. In particular, Aphrodite Bilioni, a colleague and one of the most wonderful people I've ever had the privilege to call my friend; François Giudicelli, not always the easiest person to know, but well worth the effort; Mike Mohns and Bruno Contreras-Moreira, whose infectious laughs can lift anyone's spirits; and Saori Kitao, who is furthest away and who is missed a great deal. You were, and are, like family.

I would also like to thank my friends and family in Canada. In particular, thank you to my parents and my sister, who have always been so supportive and who have made me the person I am. Thank you to my grandparents, from whose strength I draw inspiration. Thank you to Leigh, Jill, Kathy, Wing, Jennifer and Rhonda for your invaluable friendship. I think of you all often and miss you all very much!

Finally, and most importantly, I would like to thank Jordan Ward, my husband, my friend and my partner, for his support, love, encouragement and humour.

Table of Contents

List of Figures

List of Tables

List of abbreviations

APF	after puparium formation
arm	armadillo
ato	atonal
atro	atrophin
β-Gal	beta-galactosidase
BrdU	bromo-deoxyribouridine
ci	cubitus interruptus
CKI	casein kinase I
cyc	cyclin
dco	discs overgrown
diap1	*Drosophila* inhibitor of apoptosis 1
dpERK	dual phosphorylated mitogen activated protein kinase
dpp	decapentaplegic
ds	dachsous
D-V	dorsal-ventral
EGF(R)	Epidermal Growth Factor (Receptor)
ex	expanded
ey	eyeless
fj	four-jointed
FRT	Flp recombination target
ft	fat
fz	frizzled
GFP	green fluorescent protein
GMR	glass multimer reporter
hh	hedgehog
hpo	hippo
LMB	leptomycin-B
Mad	Mothers against Dpp
MAP(K)	mitogen activated protein (kinase)
mats	mob as tumour suppressor
mer	merlin
MF	morphogenetic furrow
moe	moesin
mst1	mammalian sterile twenty (kinase) 1
PCNA	proliferating cell nuclear antigen
PCP	planar cell polarity

List of abbreviations

PKA	protein kinase A
pro	prospero
RTK	receptor tyrosine kinase
sav	salvador
sens	senseless
smo	smoothened
SMW	second mitotic wave
stg	string
sty	sprouty
tsc1	tuberous sclerosis 1
UAS	upstream activating sequence
wg	wingless
wt	wild-type
wts	warts
yki	yorkie

1 CHAPTER 1: INTRODUCTION

1.1 Planar cell polarity (PCP) as a model for tissue organization

Coordinated organisation of cells into tissues is critical for the development of all metazoans, and loss of tissue organisation is a hallmark of cancer. Planar cell polarity (PCP) is the coordinated organisation of cells within the plane of a tissue, the result of which is the polarisation of all cells within that plane in an axis perpendicular to the apical-basal axis. The most visible examples of PCP are in the vertebrate epidermis where, for example, all cells are polarised so that hairs or feathers are aligned along a single axis.

One of the most avidly studied models for PCP is the arrangement of the hair cells of the vertebrate inner ear, where loss of polarity compromises aural function and balance (reviewed in Hawkins and Lovett, 2004). Various signalling pathways and molecules that are required for PCP have also been implicated in a number of other cellular events critical to development, including migration of tissues in processes such as dorsal closure and oriented cell divisions that determine axes of growth (Baena-Lopez *et al.*, 2005; Kaltschmidt *et al.*, 2002).

1.1.1 PCP models in *Drosophila*

There are several models used in the study of PCP in *Drosophila*. Bristles in the adult wing are oriented along the proximal-distal axis, a model

that has provided a great deal of insight into the directional cues for PCP and the cellular responses they elicit (Tree *et al.*, 2002). Polarity in the adult cuticle is revealed by hairs and bristles oriented along the anterior posterior axis, which is a model system that is favoured by some geneticists (Lawrence *et al.*, 2004). Finally, there is the coordinated orientation of cells in the larval and adult eye, the model system on which I will focus here.

1.1.1.1 Morphology of the adult ommatidium

The adult *Drosophila* eye (Figure 1.1A) consists of about 800 repeating units, each with its own lens and complement of photoreceptors. Each unit, or ommatidium, consists of eight photoreceptors. Sections through the ommatidium reveal seven visible cells arranged in a trapezoid: the trapezoid shape is most apparent in the arrangement of the rhabdomeres, the photosensitive organelles of each photoreceptive cell (Figure 1.1B); the eighth photoreceptor exists below R7, out of the plane of this section. Each photoreceptor is morphologically distinct, and in the adult can be identified according to its relative position within the ommatidium. There are a further seven accessory cells per ommatidium that contribute to the overall structure as it exists in the adult. In all images of adult eyes and eye imaginal discs presented throughout this work, unless otherwise indicated, anterior is left.

Polarity of the ommatidia is visible in sections

The orientation of the trapezoids that are apparent in adult sections depends on each one's location within the eye field: dorsal ommatidia point dorsally; ventral ommatidia point ventrally (Figure 1.1C). The interface

between these two fields is referred to as the equator. Note that ommatidia in each of the two halves of the eye have opposite chirality: ventral and dorsal ommatidia are mirror images of each other and cannot be superimposed. Disruption of the signalling pathways that mediate this organisation can result in a range of defects. These defects include a failure of ommatidia to orient along the dorsal-ventral (D-V) axis, or an inability of ommatidia to recognise their locations within the eye field, resulting in the existence of ommatidia with dorsal chirality in the ventral field or vice versa. I will, for the most part, refer to the former phenotype as a rotation defect, the reasons for which will become clear below. The latter phenotype is referred to as a D-V flip, since ommatidia have the appearance of having flipped in the D-V axis.

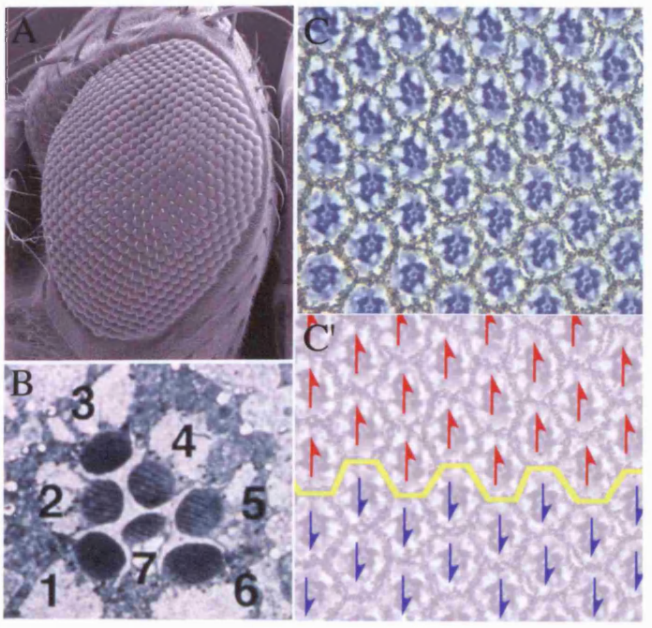

Figure 1.1 The *Drosophila* adult eye. (A) SEM of the adult *Drosophila* eye. (B) Cross-section through a single ommatidium revealing the trapezoid arrangement of the rhabdomeres, labelled R1 through R7. (C) Cross-section through the eye revealing the opposite chiralities of the dorsal and ventral ommatidia; red arrows represent ommatidia of dorsal chirality, blue arrows represent ommatidia of ventral chiralities. The equator is represented in yellow. In all images, both here and throughout the remainder of this work, anterior is left.

1.2 Development of the *Drosophila* eye

The processes that underlie the development of such an elegant structure require complex mechanisms of control. While the earliest events that are responsible for specifying the adult structures occur in the embryo, differentiation in the eye does not really begin until early third instar.

1.2.1 The Morphogenetic Furrow (MF) and larval eye imaginal disc development

All adult structures, including the eye, arise from the larval imaginal discs. These discs exist, throughout the majority of larval life, as undifferentiated masses of cells that are fated to become particular adult structures. However, it is not until third instar that detectable changes in morphology indicate the beginnings of differentiation. This process is particularly unique in the eye.

Differentiation of the eye begins in the posterior. Throughout third instar development, successive rows of cells, each more anterior than the last, initiate the differentiation process. Cells that have yet to experience this transition, those in the anterior eye disc, continue to proliferate. The progression of this transition from proliferation to differentiation is demarcated by a physical indentation in the disc referred to as the morphogenetic furrow (MF). Eye imaginal discs taken from wandering third instar larvae have progressed halfway through this process, and thus consist of cells in the anterior that are

continuing to proliferate and cells in the posterior that have started differentiating (Ready *et al.*, 1976) (Figure 1.2A,B).

1.2.1.1 Cell cycle regulation and morphological events of MF progression

The transition from proliferation to differentiation is accompanied by tight regulation of cell cycle events (Figure 1.2B). This regulation begins when randomly proliferating cells are synchronised in G1 upon entry into the furrow. This synchronisation is characterised by a prevalence of mitotic figures just anterior to the furrow, which is indicative of cells completing their final cell division cycle prior to G1 arrest (Baker and Yu, 2001).

G1 arrest is maintained within the furrow by the Cyclin dependent kinase inhibitor (CKI), Roughex (Thomas *et al.*, 1994). At this stage, single cells are selected from the undifferentiated field at regular intervals along the MF. These cells are fated to become the R8 photoreceptors for each future ommatidium. At this point, each future ommatidium is referred to as an ommatidial pre-cluster. Signalling from the R8 cells, the details of which are discussed below, recruits a further four cells per ommatidial pre-cluster to become R2 to R5 (Ready *et al.*, 1976). All remaining unrecruited cells then exit G1 arrest and undergo synchronised S phase. This synchronous S phase, visible as a tight band of BrdU incorporating cells just posterior to the MF, is referred to as the second mitotic wave (SMW). The SMW and the accompanying mitoses are required to generate sufficient numbers necessary for a full complement of ommatidial cells (Ready *et al.*, 1976; Wolff and Ready, 1991a) (Figure 1.2B).

Following the SMW, recruitment of the remaining photoreceptors continues, first with R1 and R6, and finally with R7 (Ready *et al.*, 1976; Wolff and Ready, 1991a). This later recruitment is accompanied and followed by the specification of cells fated to become cone cells and pigment cells. Throughout this process, each photoreceptor and cell type can be identified by a specific complement of transcription factors. For example, I will present data in which I examine Senseless expression as a marker for R8 cells (Frankfort *et al.*, 2001; Nolo *et al.*, 2000), BarH1 expression as a marker for R1 and R6 (Higashijima *et al.*, 1992), and Prospero expression as a marker for R7 and cone cells (Kauffmann *et al.*, 1996).

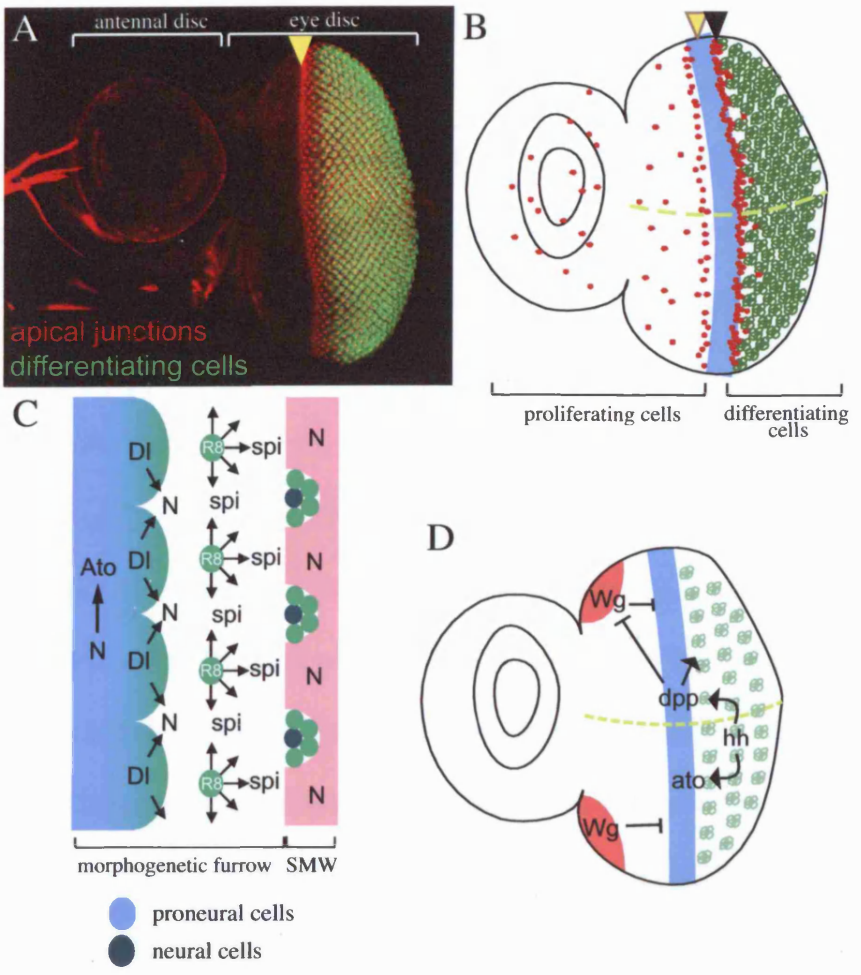

Figure 1.2 Patterning in the third larval instar. (A) Eye-antennal imaginal disc from the third larval instar; apical junctions are labelled in red, revealing the constriction of cells that result in the physical indentation of the morphogenetic furrow (MF, yellow arrowhead); differentiating neurons are labelled in green. (B) Schematic of the eye-imaginal disc revealing patterns of mitoses in red, differentiating neurons in green, the domain of G1 arrest in blue and the equator in yellow. The yellow arrowhead indicates the position of the MF, the black arrowhead indicates the second mitotic wave (SMW). (C) The roles of Notch and EGFR signalling in initiating neural development and specifying cell fates in the MF and SMW. (D) The roles of Wingless, Hedgehog and Dpp signalling in the propogation of the MF.

1.2.1.2 The signalling pathways involved in MF progression

The processes described above are subject to regulation by several signalling pathways known to be involved in diverse developmental processes from embryo to adult, from flies to humans. Here I will discuss the roles of these pathways in MF progression in the order in which they will be discussed later.

Notch

Notch is a transmembrane receptor whose function is required for a myriad of developmental processes. Notch signalling is best characterised in its role in lateral inhibition, a phenomenon whereby a particular fate is restricted to a single cell within a field through inhibition of that fate in its neighbours. In this phenomenon, Notch (N) and its ligand Delta (Dl) are initially expressed at similar levels in all cells. When a small elevation of Dl in one cell triggers increased activity of N in its neighbour, there is a transcriptional repression of Dl in that neighbouring cell. This repression results in a feedback loop that amplifies initially small differences in N activity that exist between neighbouring cells; differences in N activity then trigger different cell fates (for an example of Dl-N lateral inhibition see Figure 1.3C).

Lateral inhibition is not the only mechanism of function for Notch signalling, and while this mechanism is involved in some processes of *Drosophila* eye development, Notch signalling is required in other events and in other capacities. For example, it is required early in eye patterning where its activation defines the equator, separating the dorsal and ventral fields. This

activation also defines the initiation point for differentiation, which occurs at the posterior margin at the junction between dorsal and ventral fields.

There is a further requirement for Notch signalling in the expression of neurogenic factors. All cells in the morphogenetic furrow express the neuronal transcription factor, Atonal (Ato). However, shortly thereafter Ato expression becomes restricted to a single cell. This resolution begins with the selection of groups of cells in which Ato expression is maintained, called the intermediate groups. In the intermediate groups, Notch signalling is necessary for the elevation of Atonal (Ato) and Senseless (Sens) expression resulting in a 'pro-neural' state (Baker and Yu, 1997; Baonza and Freeman, 2001; Li and Baker, 2001). From these intermediate groups, Notch signalling is again required to select a single founder cell per precluster, this time through what is thought to be its classic function in lateral inhibition: individual cells with higher levels of Delta relative to all others in the field are selected and fated to become R8s (Baker *et al.*, 1990; Baker and Zitron, 1995; Jarman *et al.*, 1994); in the remaining cells, Notch activity, through induction of Enhancer of Split, represses Ato expression and thus neuronal cell fate (Figure 1.2C).

More recently it has been demonstrated that Notch function is also required for unrecruited cells to overcome G1 arrest and enter into the SMW (Baonza and Freeman, 2005; Firth and Baker, 2005) (Figure 1.2C). In the proposed model, activation of EGF signalling in the preclusters, which is known to result in upregulation of Delta expression (Tsuda *et al.*, 2002), in turn results in activation of Notch in the surrounding field. Further roles for EGF signalling in the progression of the MF are discussed below.

Epidermal Growth Factor

The key function of Epidermal Growth Factor Receptor (EGFR) signalling is in the subsequent recruitment of the majority of all other cell types to the pre-clusters. Differentiation triggers secretion of the EGF receptor ligand, Spitz, from each R8 cell, which in turn triggers the Ras/MAP Kinase signalling cascade in adjacent cells. Initially this signalling recruits four cells into the pre-cluster, R2-R5. However, later EGFR activity is initiated in waves and is required for further photoreceptor and accessory cell recruitment (Freeman, 1996) (Figure 1.2C).

Activity of this signalling cascade is mediated by a number of factors, but I will introduce only those that are relevant to the work presented here. In particular, Sprouty and Argos are antagonists of EGFR signalling. Sprouty is a general intracellular inhibitor of receptor tyrosine kinase (RTK) signalling (Reich *et al.*, 1999) and Argos is an EGFR ligand that acts as an intercellular competitor for EGF agonists (Klein *et al.*, 2004; Schweitzer *et al.*, 1995). The functions of these molecules are required to limit the breadth of EGFR signalling, thereby restricting the number of cells recruited to the ommatidial preclusters. Their roles will be discussed in further detail in Chapter 4.

However, the requirement for EGFR signalling is not limited to ommatidial recruitment: in the event of loss of EGFR signalling in the pre-cluster, all but the differentiating R8 cells will enter the SMW, including recruited R2-R5 cells, which results from a failure of EGFR signalling to antagonise Notch activity in these cells (Baonza and Freeman, 2005; Firth and Baker, 2005). Following this S-phase, pre-clusters again secrete the EGFR-activating ligand Spitz, which is needed for immediately adjacent cells to

overcome a G2-M checkpoint, and enter mitosis (Baker and Yu, 2001), which is mediated by the direct activation of *string* (*stg*) transcription by the EGFR target Pointed (Baonza *et al.*, 2002).

Hedgehog and Decapentaplegic

Hedgehog (Hh) and Decapentaplegic (Dpp) signalling are both required for the initiation and propogation of the morphogenetic furrow (Heberlein *et al.*, 1995; Heberlein *et al.*, 1993; Ma and Moses, 1995). Both Hh and Dpp are secreted factors that are expressed at the posterior margin of the early eye disc where they are required for the initiation of differentiation: in the absence of either, there is a complete block in furrow initiation (Chanut and Heberlein, 1997; Heberlein *et al.*, 1993). Conversely, ectopic induction of the signalling pathways associated with either molecule is also sufficient for ectopic furrow induction elsewhere in the eye disc (Chanut and Heberlein, 1995; Chanut and Heberlein, 1997; Ma and Moses, 1995; Pignoni and Zipursky, 1997). Once the MF has been initiated, they are only required somewhat redundantly for its propogation: while progression is blocked by simultaneous loss of Hh and Dpp (Curtiss and Mlodzik, 2000), loss of either alone only slows the furrow (Greenwood and Struhl, 1999).

Dpp expression at the posterior margin is dependent upon Hh (Borod and Heberlein, 1998). After initiation, Dpp is restricted to a band at the MF where it is thought to mediate progression of the furrow through inhibition of Wingless (Wg), a negative regulator of the MF (Chanut and Heberlein, 1997; Dominguez and Hafen, 1997; Pignoni and Zipursky, 1997). It is also required

for the maintenance of G1 arrest in the MF (Horsfield *et al.*, 1998; Penton *et al.*, 1997) (Figure 1.2D).

Hh is expressed first at the posterior margin at the site of furrow initiation and subsequently in all differentiating photoreceptors (Heberlein *et al.*, 1993). Secretion of Hh anteriorly triggers Dpp expression in the furrow (Borod and Heberlein, 1998; Heberlein *et al.*, 1993), which in turn initiates differentiation of naïve cells (Figure 1.2D). Hh is able to achieve this function in the absence of Dpp, albeit with lower efficiency (Dominguez and Hafen, 1997; Greenwood and Struhl, 1999).

The responses elicited by the secretion of Hedgehog have been examined in a variety of systems and contexts, and together have provided a picture of canonical Hh signalling. Binding of Hh to its receptor, Patched (Ptc), triggers the release of Ptc-dependent repression of Smoothened (Smo) (Alcedo *et al.*, 1996; Chen and Struhl, 1996; Marigo *et al.*, 1996; Murone *et al.*, 1999; Stone *et al.*, 1996). The subsequent signalling cascade results in modification of the Gli-family transcription factors from transcriptional repressors to transcriptional activators (Aza-Blanc *et al.*, 1997; Von Ohlen *et al.*, 1997). The major Gli-family molecule in *Drosophila* is Cubitus interruptus (Ci). The role of this effector will be discussed in greater detail and in the context of the results presented in Chapter 4.

Wingless

Wingless is the only signalling pathway known to negatively regulate MF progression. Wingless functions early in eye development where it is involved in defining the dorsal and ventral fields of the eye through its

activation of the Iroquois genes (Lee and Treisman, 2001; Maurel-Zaffran and Treisman, 2000). In the third instar imaginal disc, its expression is restricted to the anterior and lateral margins, regions that are ultimately fated to become head cuticle (Baker, 1988). This expression in the presumptive antenna and cuticle represses eye specific genes such as *eyes absent*, thereby refining the domain of retinal development (Baonza and Freeman, 2002). Manipulations of the domains of expression of Wg reveal that it is a potent repressor of MF progression that can act at long distances (Ma and Moses, 1995; Treisman and Rubin, 1995; Zecca *et al.*, 1996) (Figure 1.2D).

The mechanism whereby Wg acts to repress furrow progression is not fully understood. Wingless functions partly through repression of the basic-Helix-Loop-Helix transcription factor, Daughterless. Daughterless function is required for morphogenetic furrow progression, in particular the transition of cells to a proneural state. Interestingly, this repressive function of Wingless cannot be overcome by activation of Dpp and Hh signalling, indicating that it acts downstream of these pathways (Cadigan *et al.*, 2002). This observation is contrary, though not contradictory, to previous suggestions that Dpp mediates furrow progression through its repression of Wg (Pignoni and Zipursky, 1997; Royet and Finkelstein, 1997; Theisen *et al.*, 1996).

1.2.1.3 Chirality of the ommatidia is determined immediately following the passage of the MF

The chirality of the ommatidia that is apparent in the adult eye is established nearly coincidentally with the passage of the MF, immediately after the recruitment of R2-R5 that is triggered by EGFR signalling prior to the

SMW. At this point, the ommatidia in both the dorsal and ventral halves point anteriorly (Figure 1.3B). This early directionality appears to be dictated by the orientation of the MF, since the induction of ectopic furrows in inappropriate axes results in a corresponding mis-orientation of the preclusters (Ma and Moses, 1995; Reifegerste *et al.*, 1997). Initially, the cells recruited to become R3 and R4 are equivalent, but shortly thereafter, the equivalence is tipped such that the cell closest to the equator is fated to become R3 and the cell closest to the pole, either dorsal or ventral depending in the location of the pre-cluster within the eye field, is fated to become R4. This fate decision is followed by the initiation of a coordinate rotation of each pre-cluster in the direction of the R4 cell; in discs oriented such that anterior is to the left, ommatidia in the dorsal half will rotate clockwise while ommatidia in the ventral half will rotate anti-clockwise (Figure 1.3B). This rotation event continues through 90 degrees, resulting in the mirror image arrangement of the dorsal and ventral halves (Ready *et al.*, 1976; Tomlinson, 1985; Wolff and Ready, 1991a).

The phenotype that I have referred to as a rotation defect results from problems in the rotation process itself, and can range from a complete failure to rotate to over-rotation beyond the requisite 90 degrees. The phenotype that I have referred to as a D-V flip arises from incorrect specification of the R3 and R4 cells, which in turn results in ommatidial rotation in the wrong direction. One of the factors that is necessary for the correct specification of the R3 and R4 cells is the atypical cadherin Fat, the molecule that is the focus of my studies. The role of Fat in this process is discussed in greater detail, and in the context of other signalling events that are involved, later in this chapter.

1.2.2 Cell death and rearrangement in the pupal retina

Patterning in the pupal retina has traditionally received less attention, partly because of the comparatively difficult technical aspects that are involved. As such there is a less comprehensive understanding of the processes involved in the final stages of patterning. During early pupal stages, events that had been triggered during larval development are completed, namely the recruitment and differentiation of a full complement of cells to the ommatidial pre-clusters as well as the division of cells that will become the interommatidial bristles (Cagan and Ready, 1989). One of the key events of pupal retinal development is a wave of apoptosis that eliminates all supernumerary cells that were generated in the SMW, an event that follows complete ommatidial recruitment at about 20% pupal development (Cagan and Ready, 1989; Wolff and Ready, 1991b). At this stage the cells are arranged such that there are four cone cells and two primary pigment cells at the centre of each ommatidium; laser ablation experiments suggest that cell death is restricted to cells that are not in direct contact with these central cells (Miller and Cagan, 1998). This observation is supported by evidence suggesting that signalling from the primary pigment cells in the form of Spitz secretion activates the EGFR pathway in adjacent cells, offering them protection from cell death (Baker and Rubin, 1989; Miller and Cagan, 1998). Cell death itself is thought to be induced by Notch signalling (Miller and Cagan, 1998).

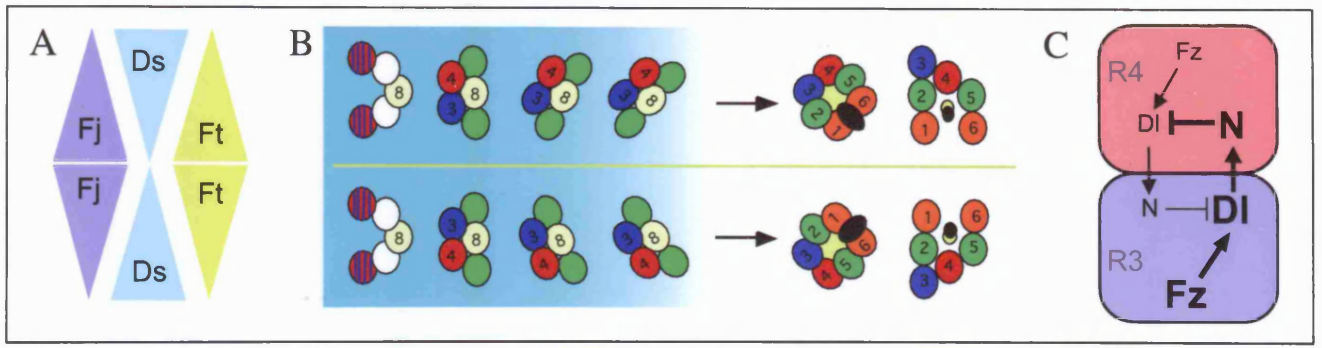

Figure 1.3 PCP of the ommatidia is established with the passage of the MF. (A) Four-jointed (Fj), Dachsous (Ds) and Ft direct the fate decisions of the presumptive R3 and R4 cells through graded expression and activity: the molecules Ds and Fj exist in gradients of opposite slope in the polar-equatorial axis; Ft activity is highest at the equator and lowest at the poles. (B) The relative levels of Fat activity determine the relative positions of R3 and R4 within the ommatidium, which in turn determine the direction of rotation and final chirality in the adult eye. (C) The R3/R4 fate decision that is directed by Fat is dependent upon relative levels of Frizzled activity, which is amplified by Delta-Notch lateral inhibition.

1.3 The role of the atypical cadherin, Fat, in eye development

As mentioned, the primary focus of the studies presented here is the role of the atypical cadherin, Fat, in the development and patterning of the *Drosophila* eye. Fat's best-characterised function is in the determination of R3/R4 fate and thus the polarity of the ommatidia. However, Fat is also classed as a tumour suppressor, since loss of Ft results in extreme hyperplastic overgrowth of all imaginal discs, and is postulated to be involved in cell adhesion, based on cell-sorting phenotypes observed in mitotic clones.

1.3.1 What is Fat?

Fat is a member of the cadherin superfamily, but is a very atypical member (Mahoney *et al.*, 1991). It, like its sister molecule Dachsous, has an extra-ordinary number of cadherin repeats: *Drosophila* Fat has 34 while Dachsous has 27 (Clark *et al.*, 1995). Four EGF domains and two Laminin-G domains have also been identified in its extracellular domain; it has a novel cytoplasmic domain (Figure 1.4A). Fat is a large protein of approximately 560kD, which makes it difficult to work with in biochemical assays.

1.3.2 Fat is necessary for PCP in the eye

The signalling events that lead to the R3/R4 fate decision that determines the direction of rotation of the ommatidia as described above have been studied extensively. Key to this decision is the activity of the seven-pass

transmembrane Wnt receptor, Frizzled (Fz): the cell with higher Fz activity will become R3. It is believed that small differences in Fz activity levels are amplified by Delta/Notch lateral inhibition resulting in repression of Fz in the R4 cell and enhanced activation in the R3 cell (Cooper and Bray, 1999; Fanto and Mlodzik, 1999; Tomlinson and Struhl, 1999) (Figure 1.3C).

The asymmetric activities of Fz at cell interfaces, either in the R3/R4 cells, or at neighbouring cell interfaces in wing imaginal disc, are linked to the recruitment of a defined complex of factors often referred to as the core PCP complex. Genetic and cell biological experiments in the wing and eye suggest that activity of Fz on one side of a cell, or indeed in one cell of a pair, triggers a redistribution of symmetrically arranged, membrane-localised factors. The result is the formation of complexes that interact across cell boundaries in a polarised way, which is the earliest visible sign of planar cell polarisation. These molecules include Dishevelled, Flamingo, Prickle, Strabismus and Frizzled itself. The importance of the formation of these complexes is reiterated by the fact that loss of one factor disrupts the localisation of all others and results in the loss of coordinated polarity of corresponding structures such as bristles (Axelrod, 2001; Das *et al.*, 2004; Jenny *et al.*, 2003; Jenny *et al.*, 2005; Rawls and Wolff, 2003; Tree *et al.*, 2002).

These experiments, however, still leave us with the question of how the initial asymmetry of Fz activity is accomplished. Early genetic experiments had led to a model whereby a gradient of activating ligand across of field of cells serves as the directional cue for PCP. The gradient of this ligand would result in very slight differences in the activity levels of the Fz receptor from one cell to the next, differences that would be recognised and amplified by

adjacent cells. The obvious candidate for this role is Wg: Fz is the receptor for Wg in many developmental contexts (Tomlinson *et al.*, 1997) and is the only known Wnt family molecule in *Drosophila* capable of triggering Fz activity. Evidence has even been presented that suggests this scenario may be possible (Povelones *et al.*, 2005; Takada *et al.*, 2005), however extensive studies have so far failed to conclusively identify any role for Wg in PCP signalling.

As mentioned, Ft is one of many molecules necessary for correct specification of the R3/R4 cell fates. It is not a member of the core PCP complex as defined above. In fact, Ft's function can be distinguished from that of the core PCP genes by its phenotype: loss of Ft results in D-V flips (Figure 1.4B; mutant tissue is marked by the absence of brown pigment granules), indicating it directs the primary decision regarding R3/R4 cell fate, whereas loss of the core molecules results in a dishevelled arrangement of ommatidia, indicating that more downstream events are compromised (Rawls *et al.*, 2002; Yang *et al.*, 2002).

Particularly revealing is the phenotype resulting from the loss of Ft in clones. Ommatidia at the equatorial margin of the clone exhibit normal and appropriate polarity, while those in the polar margin are flipped in the D-V axis. Strikingly, this reversed polarity continues non-autonomously into wild-type tissue, resulting in an ectopic equator on the polar side of the clone (Figure 1.4B,C). These observations fit with Fat's involvement in communicating a gradient of activity to Frizzled. However, Ft is membrane-bound and is uniformly distributed across the entire eye disc, so it has therefore been proposed that while it may be communicating the gradient, it is not the source. Furthermore, these results have led to the suggestion that its activity is

graded in the D-V axis, with highest activity at the equator (Rawls *et al.*, 2002; Yang *et al.*, 2002) (Figure 1.3A).

Two other molecules have been implicated in the communication of the PCP gradient based on similar phenotypes in clones: Dachsous and Four-jointed (Casal *et al.*, 2002). Dachsous is another atypical cadherin and thus membrane-bound (Clark *et al.*, 1995). It is the only known ligand for Ft and functions genetically upstream to antagonise Ft function in PCP (Matakatsu and Blair, 2004; Rawls *et al.*, 2002; Simon, 2004) (Figure 1.3A). Four-jointed has a graded distribution across the D-V axis of the eye disc, with its highest expression at the equator (Simon, 2004) (Figure 1.3A). It is a transmembrane protein capable of being secreted, but secretion is not necessary for its function, and in fact is most highly active when it is anchored in the golgi (Strutt *et al.*, 2004). Thus, like Ft, these molecules are likely to communicate the gradient of another unidentified factor required for Fz activation, often referred to as Factor-X.

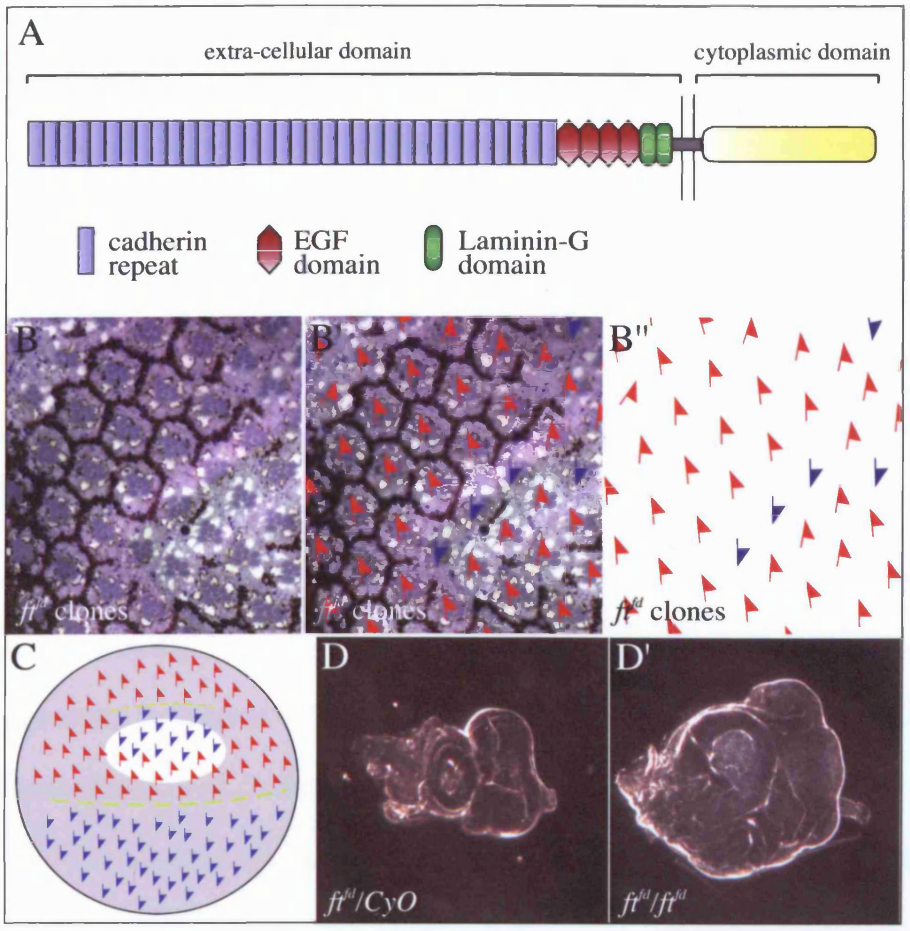

Figure 1.4 The atypical cadherin Fat directs PCP and suppresses growth. (A) Schematic of the Fat protein. (B) Sections through eyes carrying clones deficient for Fat reveal dorsal-ventral chiral flips; mutant tissue is marked by the lack of brown pigment molecules resulting from expression of the *white* transgene. (C) Schematic of the non-autonomous *ft* PCP phenotype: the dorsal-ventral flips are displaced toward the poles when compared to the clone (white), resulting in a non-autonomous phenotype and an ectopic equator. (D) *ft* heterozygous eye disc of wild-type size and morphology (D') *ft* homozygous eye discs are overgrown.

1.3.3 Fat's role in overgrowth

While Ft function is best understood in terms of its role in PCP, it was first identified genetically by its involvement in growth suppression; hypomorphic combinations are viable and result in 'fat' flies, characterised by the broadening of the thorax, abdomen and wings (Mohr, 1929). Null alleles in transheterozygous combinations result in extreme overgrowth of all imaginal discs (Figure 1.4D) and pupal lethality. This overgrowth is achieved during a greatly extended third larval instar stage that is, on average, 3.2 days longer than in heterozygous siblings (Bryant *et al.*, 1988). Interestingly, this overgrowth is hyperplastic: morphological characterisation of *ft* null discs reveals they still have a single layer epithelium with relatively normal expression patterns of Wingless, Engrailed, Apterous and Dpp (Bryant *et al.*, 1988; Garoia *et al.*, 2000).

Overgrowth of *ft* tissue is attributed solely to excess cells: loss of Ft does not alter cell size, and the cell cycle profile as revealed by fluorescent activated cell sorting (FACS) does not differ from wild-type (Garoia *et al.*, 2005). Analysis of mitotic clones revealed that the size of the clone is dependent upon its age, altogether leading to the conclusion that *ft* mutant cells cycle faster than wild-type, without any accompanying reduction in size (Garoia *et al.*, 2005).

The failure of *ft* mutant larvae to make a timely transition from larva to pupa prompted early studies to focus on a possible role for Ft in ecdysone responses. However, there could not be a simple failure of *ft* larvae to secrete or respond to hormonal signals, since transplantation of *ft* mutant discs into wild-type abdomens reveals that the overgrowth is autonomous (Bryant *et al.*,

1988). Ft-deficient discs do have decreased levels of ecdysone when compared to wild-type (Zitnan *et al.*, 1993), but this decrease is more likely to be an effect of the *fat* phenotypes rather than a cause.

Very recently there has been a resurgence of interest in the mechanisms behind the overgrowth of *ft* mutant discs. Two groups have identified roles for Fat in the repression of Wg signalling and have suggested that hyperactivity of Wingless responses contribute to *ft*-related overgrowth (Cho and Irvine, 2004; Jaiswal *et al.*, 2006). A third has found connections between EGF signalling and *ft*-deficient overgrowth (Garoia *et al.*, 2005). The crux of these data lay in genetic experiments that do not, as yet, provide mechanistic details for Ft function, and will be discussed in later chapters in the context of results presented here.

1.4 The biological question

I set out to investigate, through the course of my studies, the mechanism by which Fat is suppressing growth and whether this function is related to its role in PCP. I set about exploring these questions as described below.

1.4.1 Characterization of the *ft* overgrowth phenotype, including its effect on cell cycle molecules

As discussed above, it has been speculated that the overgrowth that is apparent in Ft-deficient clones is due to accelerated cell division cycles without an accompanying reduction in cell size. I began with an assessment of the *ft* mutant phenotype, particularly as it manifests in mitotic clones in the eye disc.

I then examined the expression patterns of a number of cell cycle markers, which revealed there is a perdurance of proliferation where cell cycle divisions should have arrested. This perdurance is apparent not only in the posterior of the disc where proliferation should give way to differentiation, but also in the failure of Ft-deficient cells to arrest in G1 at the MF. I also found there is an accumulation of *Drosophila* Inhibitor of Apoptosis 1 (Diap1), suggesting a reduction in apoptosis may also contribute to overgrowth. However, this contribution is likely to be relatively minor, since Ft-deficient cells are still capable of undergoing apoptosis during final retinal patterning at the pupal stage.

1.4.2 Fat affects the activities of a number of signalling pathways that are known to influence the dynamics of the MF

I had observed a consistent inability of Ft deficient cells to recognise cell cycle arrest signals, which was particularly evident in their delayed entry into G1 arrest at the MF. I speculated that a failure of cells to make a timely entry in the MF would result in additional cell division cycles that might account for the overgrowth of Ft-deficient clones.

I began by corroborating my earlier observations with evidence suggesting that the compromise in the ability of Ft deficient cells to enter G1 arrest is indicative of an overall delay in the execution of all events associated with MF progression. I then wanted to see if Ft could be involved in the function of any of the signalling pathways necessary for the transition from proliferation to differentiation that takes place in the morphogenetic furrow. My aim was to identify one or more pathways whose functions are

compromised in the absence of Ft and to test if this compromise is responsible for the defects in MF progression. I further hoped that I would be able to implicate these compromises in overgrowth.

Indeed, I have found that Ft influences the activities of the Epidermal Growth Factor Receptor (EGFR), Hedgehog (Hh) and Wingless (Wg) signalling pathways. However, Ft's effect in each of these pathways alone does not account for its role in growth, nor does it account for the disruption to furrow dynamics.

1.4.3 Fat functions in the Hippo signalling pathway to regulate growth

During the course of the above studies, I noticed striking similarities between *ft* mutant phenotypes and phenotypes attributed to loss of members of the Hippo signalling pathway. The Hippo signalling pathway is an emerging pathway involved in the regulation of growth and apoptosis, the details of which discussed in Chapter 5.

I have found that Ft is required for the sub-cellular localization of Expanded (Ex), the most upstream component of the pathway identified to date. In the absence of Ft, Ex is lost at the apical membrane, which ultimately results in the de-repression of the transcriptional co-activator Yorkie, the upregulation of Diap1 and the perdurance of cell cycle regulators where cell division should have arrested.

1.4.4 Fat's function in the Hippo signalling pathway may be distinct from its role in dorsal-ventral polarity

In this last chapter, I will present and discuss evidence suggesting that Fat's role in the Hippo signalling pathway, while crucial for its role in growth suppression, may be distinct from its role in dorsal-ventral planar cell polarity.

2 CHAPTER 2: MATERIALS AND METHODS

2.1 Fly stocks and genetics

2.1.1 General *Drosophila* culturing

Flies were grown on a yeast/cornmeal/molasses mixture in either bottles or vials. Unless otherwise indicated, all crosses were reared at 25^0C.

Table 2.1 Stocks used to generate clones

Chromosome 1	Chromosome 2	Chromosome 3
w[*]	FRT40A/FRT40A	
w[*]	ft[fd] FRT40A/CyO	
w[*]	ft[GRV] FRT40A/CyO	
w[*]	ft[GRV], ex[e1] FRT40A/CyO	
w[*]	ex[e1] FRT40A/CyO	
w[*]	ft[GRV] ds[UAO71] FRT40A/CyO	
w[*]	ds[UAO71] FRT40A/CyO	
w[*]	ft[fd], wg[l-12] FRT40A/CyO	
w[*]	ft[fd], wg[CX4] FRT40A/CyO	
w[*], ey-FLP	w[+mc] FRT40A/CyO	
w[*], hs-FLP	Ubi-GFP FRT40A/Ubi-GFP FRT40A	
w[*]	FRT42D hpo[42-47]/CyO	
w[*], ey-FLP	FRT42D Ubi-GFP/FRT42D Ubi-GFP	
w[*]		sty[D5] FRT80B/TM6B Tb
w[*], ey-FLP		w[+mc] FRT80B/TM3
w[*], hs-FLP		Ubi-GFP FRT80B/Ubi-GFP FRT80B

Table 2.2 Detailed genotypes used in all other assays

Chromosome 1	Chromosome 2	Chromosome 3	Chromosome 4	Experiment
Oregon-R				wild-type controls
w[*], hs-FLP	ft[fd] FRT40A, yki[B5]/Ubi-GFP FRT40A			yki genetic interaction
w[*], hs-FLP	ft[fd] FRT40A/FRT40A	PCNA-GFP		PCNA in ft clones
w[*], hs-FLP	ft[fd] FRT40A/Ubi-GFP FRT40A	dco[le88]/+		dco genetic interaction
w[*], hs-FLP	ft[fd] FRT40A/Ubi-GFP FRT40A	dco[3]/+		dco genetic interaction
w[*]	ft[1] FRT40A/ft[GRV] FRT40A	dco[le88]/+		dco genetic interaction
w[*]	ft[1] FRT40A/ft[GRV] FRT40A	dco[3]/+		dco genetic interaction
w[*], hs-FLP	ft[fd] FRT40A/Ubi-GFP FRT40A	CSN5[CX35]/+		CSN5 genetic interaction
w[*], hs-FLP	ft[fd] FRT40A/Ubi-GFP FRT40A	P{CycE16.4kb frag. lacZ}/+		CycE lacZ in ft clones
w[*], hs-FLP	ft[1] FRT40A/w[+mc] FRT40A	sty[D5] FRT80B/+		sty genetic interaction
w[*]	ft[1]/ft[GRV], ex[e1] FRT40A			ex genetic interaction
w[*]	ft[1]/ft[GRV] FRT40A			ft transheterozygotes
yw, hsflp	act>y[+]>Gal4, UAS-GFP	UAS-ft		ft O/E clones
hsflp, UAS:CD8::GFP	ft[fd] FRT40A/Gal80 FRT40A	UAS-ft	OK107y+ (ey-Gal4)	ft clones with UAS-ft
hsflp, UAS:CD8::GFP	ft[fd] FRT40A/Gal80 FRT40A	UAS-ex	OK107y+ (ey-Gal4)	ft clones with UAS-ex
yw hs-flp	P{ci-genomic rescue} FRT40A/FRT 40A		ci[D94]/ci[D94]	ci clones
yw hs-flp	P{ci-genomic rescue} FRT40A/ ft[fd] FRT 40A		ci[D94]/ci[D94]	ft, ci clones
yw hs-flp	P{ci-genomic rescue} FRT40A/ ft[fd], wg[CX4] FRT 40A		ci[D94]/ci[D94]	ft, ci, wg clones
w[*], hs-FLP	ft[fd] FRT40A/Ubi-GFP FRT40A	hh[H90]/TM3		hh lacZ in ft clones

Table 2.2 continued

Chromosome 1	Chromosome 2	Chromosome 3	Chromosome 4	Experiment
yw, mer[4]/yw, mer[4]	Ubi mer[+] GFP[nls] FRT40A/FRT40A	ey-FLP/+		mer clones
yw, mer[4]/yw, mer[4]	Ubi mer[+] GFP[nls] FRT40A/ft[fd]FRT40A	MKRS hsflp/+		mer, ft clones
w[*], hs-FLP	ft[fd] FRT40A/Ubi-GFP FRT40A		P{lacW}ci[Dplac]	ci lacZ in ft clones
w[*], hs-FLP	ft[fd] FRT40A/Ubi-GFP FRT40A	GMR-gal4, UAS-hpo/+		ft clones with GMR-hpo
		GMR-gal4, UAS-hpo/+		GMR-hpo control
		GMR-gal4/UAS-ft		GMR-ft
ms1096-Gal4/Y		UAS-ft/+		wing growth in ft O/E
ms1096-Gal4/Y				wing growth in ft O/E
		GMR-gal4/UAS-ex		Ex O/E
	GMR-p35			GMR-p35
w[*], hs-FLP	ft[1] FRT40A/Ubi-GFP FRT40A	diap1-lacZ/+		Diap1-lacZ in ft clones

2.1.2 Generation of mitotic clones

Unless otherwise indicated, Flpase was expressed from the hsp70 promotor. Progeny were reared for 60 to 70 hours before expression was induced by a single 37^0C heat-shock for two hours; while 30 minutes is normally sufficient for full expression from the hsp70 promotor, the duration was extended here to ensure thorough heating of the medium (approximately 70mL).

2.1.3 Statistical analysis of genetic interaction and clonal data

2.1.3.1 Suppression of fat^1 lethality by dco

ft^1/CyO females were crossed to either *ft^{fd}/+; dco^{le88}/TM6B, Tb* or *ft^{fd}/+; dco^3/TM6B* males in vials containing 10-12 males and 10-12 virgin females each; a total of four replicates were performed for each cross. Vials were tipped every three to four days until egg-laying was exhausted, and were kept and counted to eclosion of all progeny.

ft^1/ft^{fd} progeny were counted and scored according to whether they carried the wild-type or mutant alleles of *dco*. In the absence of genetic interaction a 1:1 ratio of wild-type to mutant would be expected from these crosses. However, it was noted that there is a non-specific genetic interaction between *ft* and the TM6B balancer: in the presence of the TM6B, Tb, there is enhanced lethality of *ft^1* transheterozygotes. In order to normalise for this effect, *ft^{fd}/+; TM6B, Tb/+* was crossed to *ft^1/CyO* as described above, and *ft^1/ft^{fd}* progeny were counted and scored according to whether they carried the

wild-type or balancer chromosome. The proportion of death caused by TM6B, Tb was calculated as follows:

$$(N)_{balancer}/(N)_{Ore\text{-}R} = 0.7612$$

This number was then used to normalise the experimental data consisting of the number of ft^{1}/ft^{fd} progeny carrying the wild-type allele of *dco*, ie. the balancer, as follows:

$$(N)_{wt}/0.7612$$

Normalised data was then subjected to Chi-squared analysis to determine if there is any significant departure from the expected ratio of 1:1. Note that normalisation of the data as described above does not err in favour of a genetic interaction.

2.1.3.2 Enhancement of fat^{1} lethality by expanded

ft^{1}/CyO was crossed to either ft^{GRV}/CyO or $ft^{GRV}ex^{e1}$/CyO in vials containing 10-12 males and 10-12 virgin females each; a total of 10 replicates were performed for each cross. Vials were tipped every three to four days until egg-laying was exhausted, and were kept and counted to eclosion of all progeny. Viability was calculated by expressing the number of ft^{1}/ft^{Grv} progeny as a percent of the total progeny in each cross. A student's T-test was performed to assess statistical significance.

2.1.3.3 Suppression or enhancement of ft^{fd} clone size

To measure growth, clones were induced at 60 to 70 hours AEL and measured as late third instars. Photoshop was used to take pixel counts of all mutant clones and all wild-type twinspots in each of at least nine discs for each genotype of interest. All discs were measured twice and an average was taken of the two measurements. This data was then presented as a ratio of mutant clone to homozygous wild-type twinspot. A student's T-test was performed to assess statistical significance. The genotypes compared were:

w[*], hs-FLP; ft[fd] FRT40A/Ubi-GFP FRT40A and
w[*], hs-FLP; ft[fd], wg[CX4] FRT40A/Ubi-GFP FRT40A and
w[*], hs-FLP; wg[CX4] FRT40A/Ubi-GFP FRT40A

or

w[*], hs-FLP; ft[fd] FRT40A, yki[B5]/Ubi-GFP FRT40A and
w[*], hs-FLP; ft[fd] FRT40A/Ubi-GFP FRT40A

2.1.4 Staging of larvae and pupae

For third instar larval discs, wandering larvae were selected. For pupal retinas, white pre-pupae were selected and aged at 20^0C for either 72 hours (40-45% pupal development) for analysis of secondary cell numbers, or for 32 hours (20% pupal development) to look at the maximal cell death phase of retinal patterning.

2.2 BrdU incorporation and Immuno-fluorescence

2.2.1 Dissecting and fixing

Wandering third instar larvae or appropriately aged pupae were dissected in phosphate buffered saline (PBS) for eye and wing imaginal discs, which

were fixed in either 4% formaldehyde or PLP (0.075M lysine, 0.037M sodium phosphate pH 7.2, 2% formaldehyde, 0.01M sodium m-periodate) for 40 minutes. Three washes of 5-10 minutes each were performed after fixation.

2.2.2 BrdU incorporation

For BrdU incorporation, discs were incubated in 75ug/mL BrdU in PBS for 40 minutes before fixation in 4% paraformaldehyde. Long BrdU incorporation assays involved a labelling pulse of 90 minutes. Following fixation, discs were incubated in 3M HCl for 30 minutes to denature the DNA, then washed three times in PBS with 0.1% Triton-X for 10 minutes each. Detection of BrdU tags by immuno-fluorescence was performed as described below.

For BrdU incorporation assays in which clones were to be marked using the immuno-fluorescence against Ci*, fixation was followed by three washes in PBS with 0.1% Triton-X. Primary antibody was added and allowed to incubate for 1.5-2 hours at room temperature, which was followed by three further washes. Discs were again fixed in 4% paraformaldehyde for 20 minutes before proceeding to the DNA denaturation step. This modification was made due to the apparent sensitivity of the Ci* antigen to HCl.

In some instances, treatment with HCl resulted in poor quality immuno-fluorescence of the antibodies used to mark clones (either Ci* or GFP); while the domains of mutant tissue could be detected under the microscope and in digital images, they did not render very well in print and thus clones are, at times, drawn in using Photoshop in some figures shown here.

2.2.3 Immuno-fluorescence

Following fixation and washing, primary antibodies were applied at dilutions listed in Table 2.3. Primary and secondary antibodies were diluted in PBS with 0.1% Triton-X and 5% normal goat serum and discs were incubated in each antibody for 90-120 minutes at room temperature or overnight at 4^0C. Secondary antibodies were from Jackson Immuno Labs and diluted at 1/200; fluorophores used were fluorescein, Cy3 and Cy5. Between antibody steps, discs were washed three times in PBS with 0.1% Triton-X. Following final washes samples were mounted in Vectashield (Vector Laboratories). Exceptions to this protocol are as follows:

2.2.3.1 Ci and dpERK antibodies

Following fixation, imaginal discs were incubated in PBS with 1.0% Triton-X for 10 minutes for permeablisation. These discs were washed a further three times in PBS with 0.1% Triton-X before exposure to antibodies.

Table 2.3 Antibodies for immuno-fluorescence

Antigen	Species	Dilution	Source
Armadillo	mouse	1/100	DSHB[1]
Atonal	rabbit	1/2000	Promega
BarH1	rat	1/100	H. McNeill
β-Gal	mouse	1/1000	ICN/Cappel
β-Gal	rabbit	1/1000	Molecular Probes
BrdU	mouse	1/20	Pharmingen
β-Tubulin	mouse	1/1000	DSHB
Caspase 3	rabbit	1/200	Cell Signalling Tech
Cubitus Interruptus	rat	1/200	T. Kornberg[2]
Cyclin A	mouse	1/20	DSHB
Cyclin B	mouse	1/100	DSHB
Cyclin D	mouse	1/20	W. Du[3]
Cyclin E	rat	1/400	see Materials and Methods
Delta	mouse	1/50	DSHB[1]
Diap1	mouse	1/250	B. Hay[4]
diphospho-ERK	mouse	1/100	Sigma
Elav	mouse	1/20	DSHB[1]
Elav	rat	1/1000	DSHB[1]
Expanded	rabbit	1/200	A. Laughon[5]
Fat	rat	1/100	H. McNeill
GFP	mouse	1/1000	Molecular Probes
GFP	rabbit	1/1000	Molecular Probes
Hippo	rabbit	1/100	N. Tapon[6]
Merlin	guinea pig	1/5000	R. Fehon[7]
Moesin	rabbit	1/1000	D. Kiehart[8]
Patched	mouse	1/50	I. Guerrero[9]
phospho-Histone H3	rabbit	1/200	Upstate
phospho-SMAD	rabbit	1/300	Cell Signalling Tech
Prospero	mouse	1/50	DSHB[1]
Senseless	guinea pig	1/5000	H.J. Bellen[10]
Wingless	mouse	1/200	DSHB[1]

1. Developmental Studies Hybridoma Bank: http://www.uiowa.edu/~dshbwww/
2. (Aza-Blanc *et al.*, 1997)
3. (Duman-Scheel *et al.*, 2002)
4. (Yoo *et al.*, 2002)
5. (Boedigheimer and Laughon, 1993)
6. (Colombani *et al.*, 2006)
7. (McCartney and Fehon, 1996)
8. (McCartney and Fehon, 1996)
9. (Capdevila *et al.*, 1994)
10. (Nolo *et al.*, 2000)

2.2.4 Generation of Cyclin E antibody

Using a Cyclin E cDNA cloned into a pET vector (kindly given to me by H. Richardson), DH5α competent cells were transformed and protein expression was induced with IPTG. Cells were resuspended in 1mL isotonic buffer (50mM Tris pH 7.5, 50mM NaCl, 5mM $MgCl_2$, protease inhibitor) and sonicated. Protein expression was checked by running a small sample on SDS-PAGE and staining with coomassie blue. 450uL of sonicated sample was combined with an equal volume of loading buffer. These samples were loaded onto a large SDS-acrylamide gel to full capacity of all wells. After electrophoresis, the gel was soaked in cold 0.2M KCl, which causes rapid precipitation of SDS in regions where the protein concentration is highest (Kosman *et al.*, 1998). These regions were taken to correspond to the Cyclin E protein and cut from the gel. Gel slices were homogenised and diluted in 25mL of PBS. The final protein concentration was determined to be approximately 100-250ng/uL. Members of the Biological Resources Unit at the London Research Institute of Cancer Research UK emulsified 10-25ug of protein with Freund's adjuvant and injected each of three rats subcutaneously. Between three and five boosts were performed prior to bleed-out. Immuno-fluorescence was performed using the resulting sera.

2.3 *In situ* hybridisation

2.3.1 Generating the probes

cDNA clones were digested using a restriction enzyme that would cut at a single site at the 5' end of the insert, then run on an agarose gel and extracted using Qiagen gel extraction kits. Labelling reactions were performed using RNA Dig Labelling Kits from Roche and were set up as follows:

5-10uL cDNA (1ug)
2uL 10X reaction buffer (SP6, T3 or T7)
2uL DIG-labelled dNTPs
1uL RNase inhibitor
1uL polymerase
RNAse-free water to 20uL

Reactions were incubated for 3-5 hours at 37^0C. The cDNA templates were removed by adding 1uL RNAse-free DNAse and incubating for 30 minutes at 37^0C. To stop the reaction 2uL 0.5M EDTA was added and incubated for 5 minutes. The probe was precipitated by using 3M NaOAC and cold ethanol and chilling at -20^0C for at least 30 minutes. After spinning and discarding the supernatent, the remaining pellet was dried and resuspended in 20uL RNAse-free water. The RNA synthesis was checked by running a small aliquot on an agarose gel (for specific information regarding each transcript, see Table 2.4).

Table 2.4 cDNAs used in *in situ* hybridisations

transcript	vector	polymerase	dilution for hybridisation	source
string	pBluescript	T7	1/500	B. Edgar
dpp	pBluescript	T3	1/200	M. Mohns
expanded	pOT2	SP6	1/1000	DGRC[1]

1. Drosophila Genome Resource Centre: http://dgrc.cgb.indiana.edu/

2.3.2 Hybridisation

Discs from wandering third larval instars were dissected in PBS and fixed in 4% paraformaldehyde in PBS for 20 minutes at room temperature. They were then washed for five minutes in PBS and fixed again in 4% paraformaldehyde in PBS containing 0.1% Triton X-100 for 20 minutes at room temperature. Discs were washed three times in PBS for 5 minutes each. For *in situ* hybridisation in combination with immuno-fluorescence against GFP, samples were, at this stage, incubated in the appropriate primary antibody for 1.5 hours at room temperature. After primary antibody binding, samples were washed three times in PBS with 0.1% Tween20, then fixed again in 4% paraformaldehyde in PBS for 20 minutes at room temperature. Samples were again washed three times for 5 minutes in PBS with 0.1% Tween20, then in a 1:1 mixture of hybridization solution (see the recipe below):PBS-Tween for 5 min. Pre-hybridization in the hybridization solution was done at 55°C for 1 hour using a thermomixer on a gentle setting. Probe was added at dilutions between 1/100 and 1/1000 (see Table 2.4 for specific dilutions for each probe) and allowed to hybridize overnight at 55^0C. Samples were washed as follows:

1X 20 minutes in hybridization buffer

1X 20 minutes in 1:1 hybridization solution :PBS-Tween

5X 20 minutes in PBS-Tween

Before detection of the DIG label, discs were blocked by incubating in PBS-Tween with 10% normal goat serum for 30 minutes at room temperature. Anti-DIG-POD antibody (Roche) was diluted to 1/100 in PBS-Tween and discs were incubated at room temp for 1.5-2 hours. Following several washes in PBS-Tween, POD was detected using a tyrimide amplification kit from Perkin-Elmer. For *in situ* hybridisation in combination with immuno-fluorescence, the secondary antibody was added following several washes in PBS-Tween and incubated for 1.5-2 hours. Following a final series of washes in PBS-Tween, discs were mounted in Vectashield (Vector Laboratories).

As with treatment with HCl for detection of BrdU, hybridisation at 55^0C resulted in poor quality immuno-fluorescence of the antibodies used to mark clones (GFP); while the domains of mutant tissue could be detected under the microscope and in digital images, they did not render very well in print and thus clones are, at times, drawn in using Photoshop in some figures shown here.

Hybridization Mix

50% formamide
5X SSC
100ug/mL sonicated herring or salmon sperm DNA
50ug/mL heparin
0.1% Tween20
100ug/mL tRNA
H_2O to 5mL

2.4 Histology

2.4.1 Fixing and embedding adult heads

Adult flies were decapitated and transferred immediately to 2% EM-grade glutaraldehyde in 0.1M $NaPO_4$, pH 7.2, on ice. An equal volume of 2% EM-grade osmium tetroxide in 0.1M $NaPO_4$ was added with a further incubation on ice for 30 minutes. Osmium/gluteraldehyde solution was replaced with fresh 2% osmium and samples were incubated for at least a further two hours on ice. Samples were then dehydrated in an ethanol series as follows:

50% ethanol for 10 minutes
70% ethanol for 10 minutes
90% ethanol for 10 minutes
100% ethanol for 10 minutes, twice

Ethanol was replaced with propylene oxide and samples were incubated for 10 minutes at room temperature. Propylene oxide washes were repeated twice. An equal volume of resin (see recipe below) was added to the last propylene oxide wash and samples were incubated overnight at room temperature. The next day, the resin/propylene mixture was replaced with resin and samples were incubated for at least 4h at room temperature. Each specimen was placed in its own mould containing resin, then baked at 70°C overnight.

Durcupan Resin (Fluka)

Resin A	54g
Hardener B	44.5g
Accelerator C	2.5g
Plasticiser D	10g

Following thorough mixing of the above components, the resin was aliquoted and stored at -20^{0}C until it was ready for use.

2.4.2 Sectioning and mounting

Using a diamond knife, 1um thick sections were made using an ultramicrotome. Sections were placed and dried onto slides, then briefly stained with Toluidine Blue for 25-35 seconds. For long-term storage, samples were mounted with DPX.

2.4.3 Preparation of samples for Scanning Electron Microscopy

Whole anaesthetised flies were immersed in 99.9% ethanol. Members of the Electron Microscopy Unit of the London Research Institute of Cancer Research UK then subjected the samples to either critical point drying or desiccation in hexamethyldisilazane (Sigma), then mounted and coated them in platinum using a Polaron SC7640 sputter coater.

2.5 Microscopy

2.5.1 Light microscopy

All bright field microscopic images, including all images of adult eye sections, were collected using either a Zeiss Axioplan microscope with OpenLab Modular Imaging software from Improvision, or a Nikon Eclipse E800 microscope with Nikon's own Act-1 Digital Imaging software. Dark

field microscopic images were collected using a Zeiss axioplan microscope with OpenLab Modular Imaging software.

2.5.2 Confocal microscopy

All confocal microscopy was performed using a Zeiss Laser Scanning Microscope with LSM 510 software. These instruments are maintained by the Light Microscopy Unit of the London Research Institute of Cancer Research UK.

2.5.3 Scanning Electron microscopy

Samples were prepared and imaged by the Electron Microscopy Unit of the London Research Institute of Cancer Research UK using a Jeol JSM 6700F Scanning electron microscope.

3 CHAPTER 3: CHARACTERISATION OF THE FAT OVERGROWTH PHENOTYPE

3.1 Overgrowth of *fat* mutant tissue is apparent at the level of whole organs as well as in clones

It has long been known that deficiencies in Fat result in overgrowth in all imaginal discs, both at the level of whole organs as well as in mitotic clones of mutant tissue in a wild-type background. In order to further examine this overgrowth phenotype, I used the yeast-derived FRT/FLP system to generate mitotic clones of *ft* in the eye (Dang and Perrimon, 1992). In this system, the enzyme Flpase binds to a pair of adjacent Flp recombination target (FRT) sites and induces mitotic recombination. In this instance, Flpase is driven by the *hsp70* promoter and binds to FRT sites that are located just distal to the centromere at cytological site 40A. Recombination of the entire 2L chromosome arm, in which one homologue carries a mutation in *ft* and the other carries a transgene in which green fluorescent protein (GFP) expressed from the ubiquitin promoter, results in mosaic tissue. Tissue that is homozygous mutant for *ft* lacks GFP, tissue that is heterozygous expresses GFP from a single copy of the transgene and thus is pale green and tissue that is homozygous wild-type expresses GFP from two copies of the transgene and is bright green. The homozygous wild-type tissue is referred to as the twinspot, since this tissue is born of the same recombination event that generates the adjacent clone.

This system has many benefits in the analysis of mutations. The obvious advantage is that it allows for analysis of phenotypes resulting from otherwise lethal mutations. In addition, there is an internal control when comparing the levels of expression of a given molecule between wild-type and mutant tissue. In the case of the eye imaginal disc, in which development progresses in a wave, one can also compare the timing of expression of a given molecule. Finally, by comparing the relative sizes of twinspot and clone, one can assess whether a mutation results in growth defects.

Mitotic clones of *ft* are extremely large: they can be up to six times the size of their adjacent twinspots (Garoia *et al.*, 2000). They also generate borders that are smooth and round, a phenotype that is usually indicative of defects in adhesion (Figure 3.1, compare A and B). Immuno-fluorescence against Elav, a marker for differentiating neurons, reveals that in *ft* clones after the morphogenetic furrow (MF) there is increased spacing between ommatidial clusters (Figure 3.1C). Since mutations in *ft* do not result in changes to cell size (Garoia *et al.*, 2005), this data implies that either there are morphological differences between *ft* mutant and wild-type interommatidial cells, or that there are more cells between clusters in *ft* mutant clones. The morphology of adult heads in which eyeless-driven Flp was used to make mitotic clones also implies that there are superfluous interommatidial cells: these eyes frequently have extra bristle cells, sometimes up to four bristles in one ommatidial junction (Figure 3.1D,E).

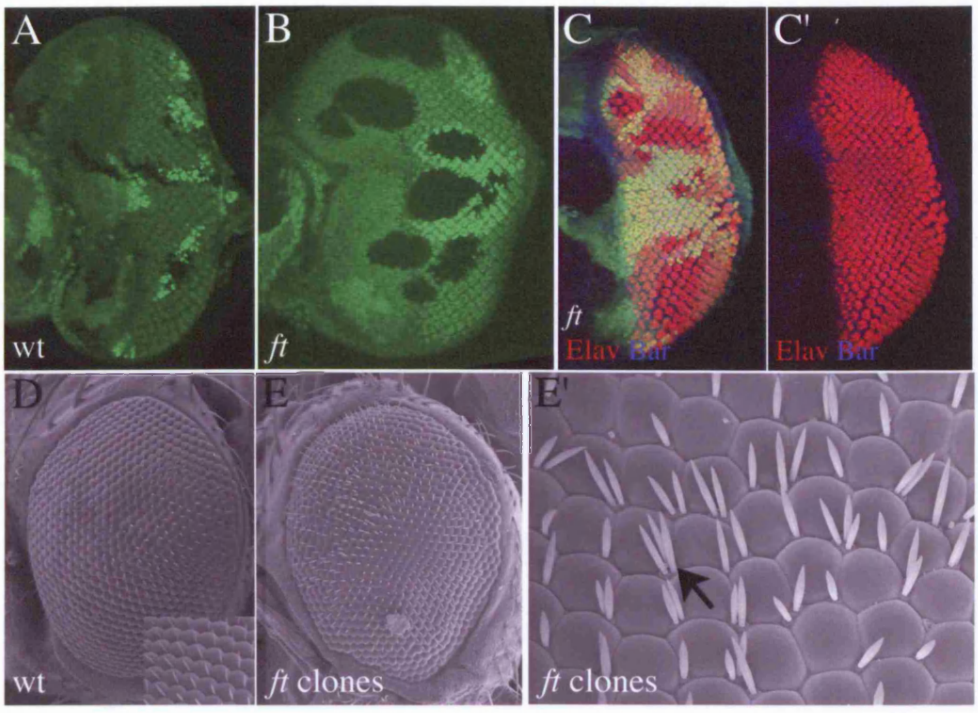

Figure 3.1 Features of the *fat* overgrowth phenotype. In clones marked with Ubi-GFP, homozygous wild-type tissue can be distinguished from heterozygous tissue by the dose-dependent intensity of the GFP signal; mutant tissue is marked by complete absence of GFP. (A) Wild-type mitotic clones, which are marked with Ubi-GFP but lack any mutation, are similar in size to their twinspots and assort freely with neighbouring cells resulting in 'wiggly' edges. (B) Clones deficient for Fat are much larger then their twinspots and have rounded edges, indicating the existence of an adhesion defect. (C) Fat deficient tissue has wider ommatidial spacing as revealed by immuno-fluorescence against Elav and Bar, which mark ommatidial clusters. Scanning electron micrographs of adult eyes: (D) wild-type and (E) *ft* clones induced by FLPase expression from the eyeless promoter. (E') Loss of Fat frequently results in duplicated bristles in the ommatidial vertices, with up to four per vertex (arrow).

3.2 Expression of cell cycle regulators in *fat* mutant clones

In order to further characterise the nature of the *ft* overgrowth phenotype, I looked at various markers of cell cycle progression. Garoia *et al.* (2005) demonstrated by FACS analysis that Fat-deficient cells do not exhibit any detectable alterations to their cell cycle profiles when compared to their neighbouring twinspot cells. However, from this experiment it is only possible to conclude that *ft* mutant cells proceed through the cell cycle with apparently normal dynamics during third larval instar and cannot be put into the context of developmentally regulated processes. Thus, I wanted to see where and when in development Fat-deficient cells could be undergoing aberrant cell divisions by examining the expression patterns of various cell cycle markers.

First I examined the pattern of S-phase cells, visualised by the incorporation of bromodeoxyuridine (BrdU). BrdU is a nucleoside analogue that incorporates into newly synthesised DNA as a substitute for thymidine. Its incorporation is detected by immuno-fluorescence, which reveals cells that were undergoing S phase during the labelling pulse. Given that the generation of extra cells requires extra cell divisions, I expected to see a higher incidence of BrdU labelled cells in *ft* mutant clones. Surprisingly, in discs labelled during a 30 to 60 minute pulse of BrdU, there was no obvious or consistent increase in S-phase observed (Figure 3.2A,A'). Instead, I observed bowing in the band of BrdU-incorporated cells that form the second mitotic wave (SMW); within *ft* mutant clones there is a delay in the progression of events that occur with the passage of the MF.

While the majority of clones did not exhibit increased numbers of S-phase cells, in one single clone (n>150) there was ectopic incorporation of BrdU posterior to the MF, a region of the disc in which proliferation should have arrested. Furthermore, this ectopic S-phase was limited to a narrow band within the clone, similar in morphology to the SMW (Figure 3.2A",A'").

The latter result suggested that *ft* mutant clones could be undergoing ectopic S phase after the furrow, but that the ectopic cycles might require a longer pulse of BrdU incorporation in order to be visualised. This suggestion was confirmed when I exposed clonal discs to a 90 minute pulse and found that the incidence of the above phenotype increased dramatically; in nearly all clones after the MF there was ectopic BrdU incorporation in a pattern resembling a "third mitotic wave".

Proliferating cell nuclear antigen (PCNA) is a cell cycle responsive protein that is required for DNA replication and repair (Jaskulski *et al.*, 1988; Mathews *et al.*, 1984; Prelich *et al.*, 1987), and thus is most highly expressed in S-phase cells. Using a transgenic line expressing GFP from a PCNA enhancer element (Thacker *et al.*, 2003), I looked at the levels of PCNA expression in *ft* clones. Once again, in *ft* clones that traverse the MF there is a bowing in the band of PCNA staining that is coincident with the BrdU incorporating region of the SMW (data not shown). Additionally, in *ft* clones that exist either behind or ahead of the furrow the levels of PCNA are elevated (Figure 3.2B). In particular, there appears to be a specific elevation of PCNA levels in interommatidial cells as well as a perdurance of expression in cells that should be arresting in G1 for entry into the MF. These observations confirm the results I obtained using long-pulse BrdU incorporation: they imply once again

that there is failure of *ft* cells to execute a timely transition from proliferation to differentiation and that after the furrow, cells that have not been recruited to the ommatidial preclusters continue to proliferate.

Next I examined the pattern of mitotic cells by immuno-fluorescence against phospho-Histone H3 (PH3). Clones mutant for *ft* did not show any obvious increase in the incidence of mitotic cells (Figure 3.2C).

Similarly, there was no increase in the incidence of *cdc25-string* (*stg*) transcribing cells (Figure 3.2D). *Cdc25-stg* transcription is indicative of cells undergoing G2-mitosis transition and is required to drive cells through one last round of mitosis before synchronisation in G1 in the MF (Edgar and O'Farrell, 1989; Mozer and Easwarachandran, 1999). This synchrony gives the appearance of a bright band of staining just ahead of the MF. As is seen in the BrdU incorporation assay, there is a bowing in the band of *stg*-transcribing cells, implying that there is a defect in the ability of *ft* cells to make a timely entry into the MF.

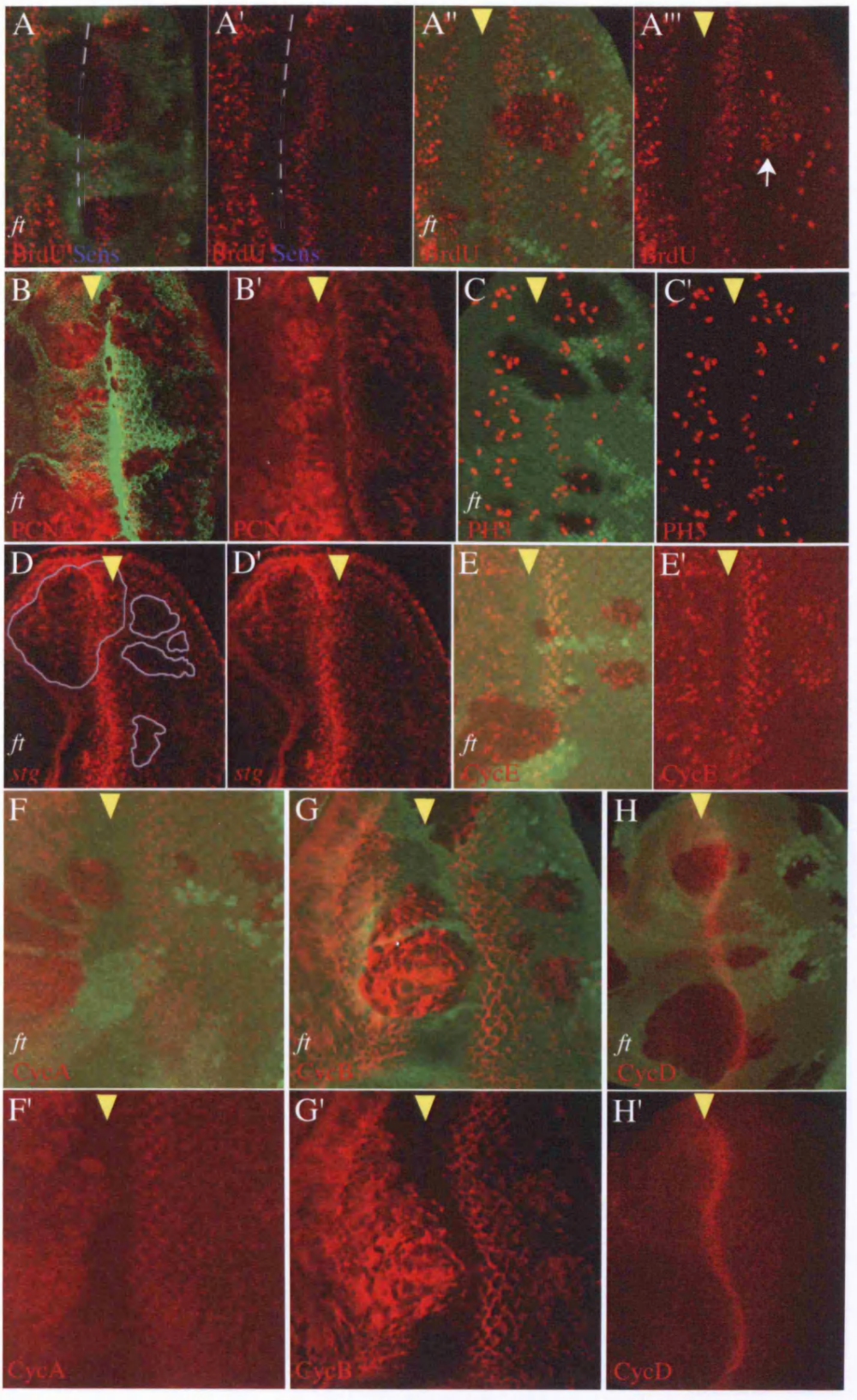

Figure 3.2 For the figure legend see the following page.

Figure 3.2 Loss of Fat results in perturbation of cell cycle markers. Yellow arrowheads indicate the positions of the MF as they are in wild-type tissue. (A, A') In Fat-deficient clones labelled with BrdU there is a delay in the SMW: the wild-type front of the SMW is marked by the dashed line. (A", A'") Longer pulses of BrdU incorporation reveal ectopic S phase posterior to the MF (white arrow). (B) Ft-deficient clones marked by immuno-fluorescence against Ft (green) in a background expressing GFP from the PCNA promoter (red). (C) Incidence of mitoses in Ft-deficient clones as revealed by PH3 expression. (D) Fluorescent *in situ* hybridisation against *stg* transcript; domains lacking Ft are drawn in grey. Expression patterns of Cyclin E (E), Cyclin A (F), Cyclin B (G) and Cyclin D (H) in Ft-deficient clones.

I next looked at the expression of three of the main Cyclins required for cell cycle progression, Cyclins A, B and E. Cyclins A and B each play a distinctive role in cell cycle progression but both are required for the transition from G2 to mitosis (Lehner and O'Farrell, 1990; Minshull *et al.*, 1990; Whitfield *et al.*, 1990). I have found that the levels of both Cyclins A and B are elevated in interommatidial cells in *ft* clones behind the MF (Figure 3.2F,G). There is also an elevation of Cyclin B levels in clones ahead of the MF; while there is no clear elevation in the levels of Cyclin A, the antibody is much less robust and may simply fail to highlight any difference between the mutant and control tissues. However, there is a consistent and strong perdurance of both Cyclins in clones that cross the MF. Cyclin E is required for G1 to S-phase transition (Dulic *et al.*, 1992; Koff *et al.*, 1991; Koff *et al.*, 1992). In *ft* deficient clones behind the MF there are strongly elevated levels of Cyclin E; in clones ahead of the MF there is a milder but consistent upregulation (Figure 3.2E).

Finally, I examined the expression pattern of Cyclin D. In *Drosophila*, Cyclin D is mainly involved in the regulation of cell growth, rather than cell division (Datar *et al.*, 2000; Meyer *et al.*, 2000). I did not expect to see any dramatic change in the levels of Cyclin D in clones deficient for Fat, since loss of Fat does not affect cell size (Garoia *et al.*, 2005). Indeed I found that there is no detectable change in the levels of Cyclin D expression in Ft-deficient clones. However, the expression of Cyclin D in the eye disc is at its highest level in the MF (Finley *et al.*, 1996), a pattern that makes it a useful indicator of MF progression, and which again reiterated that there is a failure of Ft-deficient cells to make a timely entry into the MF.

3.3 *fat* clones express increased levels of *Drosophila* Inhibitor of Apoptosis 1 (DIAP1)

Having corroborated existing evidence that implies that at least some of the overgrowth of *ft* mutant tissue is due to excessive cell division cycles, I wanted to investigate a possible role for Fat in promoting apoptosis. There is very little apoptosis in the eye imaginal disc until early pupal stages, when superfluous cells that have not been recruited to ommatidia are eliminated (Wolff and Ready, 1991b). However, mutations have been described in which this apoptosis is inhibited or eliminated (Harvey *et al.*, 2003; Kango-Singh *et al.*, 2002; Tapon *et al.*, 2002), resulting in overgrown adult tissues. To see if mutations in *ft* could result in reduced apoptosis, I looked at the expression levels of *Drosophila* Inhibitor of Apoptosis 1 (Diap1). Diap1 protects cells from apoptosis in a variety of contexts by inhibiting Caspase function (Hay *et al.*, 1995; Wang *et al.*, 1999b). I found that Diap1 is ectopically expressed in *ft* mutant clones both ahead of and behind the MF (Figure 3.3A), suggesting there could be a reduction of apoptosis that accompanies *ft*-related overproliferation and that contributes to overgrowth in mutant clones.

To see if the accumulation of Diap1 accompanies a reduction in normal apoptosis, I looked at Ft-deficient clones in retinas at 20% pupal development (32 hours APF, 20^0C), when cell death is maximal. To visualise cells undergoing apoptosis, I used an antibody against cleaved human Caspase-3, which cross-reacts with a yet unidentified *Drosophila* molecule, though likely to be an activated caspase, in a pattern identical to known patterns of apoptosis (Xu *et al.*, 2006). In this analysis, I found that despite elevated levels of

Diap1, there is no apparent reduction in the incidence of cell death in Fat-deficient clones (Figure 3.3B).

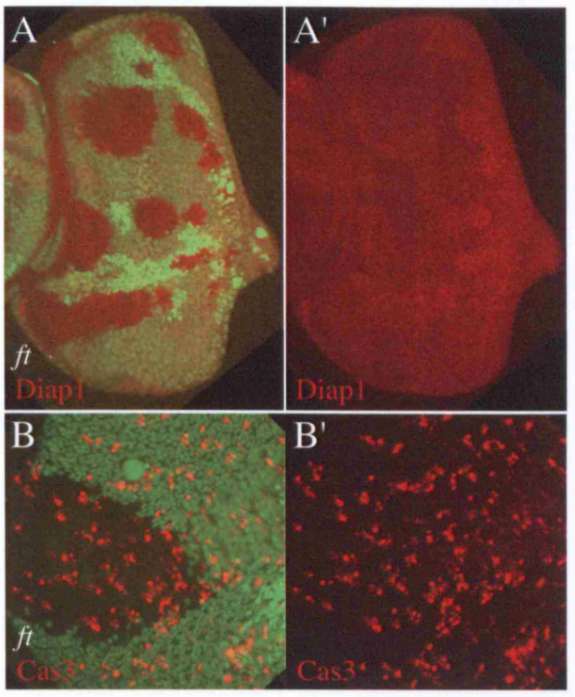

Figure 3.3 Loss of Fat results in accumulation of Diap1 but does not prevent pupal cell death. (A) Ft-deficient clones stained for Diap1. (B) Incidence of apoptosis as revealed by immuno-fluorescence against actived Caspase in Ft-deficient clones at 20% pupal development.

3.4 Discussion and Conclusions

Loss of *fat* results in dramatic overgrowth of all imaginal disc tissues: in transheterozygotes there is an extended third larval instar period lasting an additional 3.2 days, during which discs continue to proliferate generating 2.5 times the number of cells of wild-type discs (Bryant *et al.*, 1988); in mosaic eye discs, *ft* mutant clones are up to six times larger than their wild-type twinspots (Garoia *et al.*, 2000). I have found evidence that corroborates previous data demonstrating that *ft* deficient cells, as well as *ft* mutant imaginal discs, fail to respond to arrest signals and continue to proliferate, and that *ft* cells are delayed in their abilities to make a timely entry into the morphogenetic furrow. I have also presented evidence suggesting that a reduction in apoptosis may contribute to the overall overgrowth phenotype seen in adults, however any contribution is likely to minor.

Both eye imaginal discs and adult eyes appear to have superfluous interommatidial cells. These additional cells correlate with the accumulation of Cyclin A, Cyclin B and PCNA in interommatidial cells, as well as the accumulation of Cyclin E. The continued cycling of these molecules implies that *ft* cells are continuing to divide behind the furrow. However, BrdU incorporation assays and PH3 immunofluorescence experiments reveal that there is not a dramatic increase in the number of cells that are synthesising DNA or actively dividing, except in rare instances in which there appears to be BrdU incorporation in the pattern of a "third mitotic wave", or when the pulse of BrdU incorporation is greatly extended.

It is also important to note the inconsistencies observed between S-phase incidence as detected by BrdU and PCNA-GFP. The pulse of BrdU incorporation used in these experiments is 30 to 60 minutes immediately prior to fixation; this pulse was extended to 90 minutes at its most extreme. The PCNA reporter used is GFP, a molecule with a half-life of more than 24 hours (Andersen *et al.*, 1998; Chalfie *et al.*, 1994). This half-life is a great deal longer than that of PCNA itself, which degrades with every cell division cycle following the completion of S phase (Mathews *et al.*, 1984). It is therefore likely that the effects seen in PCNA-GFP transgenic animals are visible because there is an accumulation of GFP over the course of 24 hours; incorporation of BrdU will only reveal cells that are synthesising DNA during a 30 to 90 minute period.

The most intriguing, and somewhat unexpected, of the results presented here is the consistent and marked delay in the ability of *ft* cells to execute the events that accompany the passage of the morphogenetic furrow. *ft* cells do not arrest in G1 in a timely manner that this consistent with their neighbours, nor do they re-enter the cell cycle in the SMW with their neighbours. This data suggests *ft* cells are impaired in their abilities to undertake all events associated with the passage of the morphogenetic furrow, perhaps through a reduced ability to respond to the signalling cascades associated with these events. Similar to organs in many organisms, *Drosophila* imaginal disc growth can be separated into two phases: a rapid, exponential phase; followed by a slower phase just prior to reaching the final target size (Bryant and Simpson, 1984; Coelho *et al.*, 2005). It is tempting to view the delay in furrow progression as a parallel for an overall inability of *ft* mutants to make a transition from the fast

growth phase to slow growth and arrest. As such, the overgrowth phenotype of *ft* mutants would result from longer time spent proliferating before executing a differentiation program. It is unclear whether the delay experienced by *ft* cells in furrow progression is related to the failure of *ft* cells to maintain cell cycle arrest after the furrow. In the following chapter, I explore the role Fat may play in the regulation of, and response to, various signalling pathways that are known to be involved in morphogenetic furrow progression.

Finally, I have shown that *ft* clones exhibit elevated levels of Diap1, implying that overgrowth in this tissue may be due to a combination of extra cell divisions and a loss of apoptosis. Any loss of apoptosis would contribute to the overgrowth phenotype observed in the adult, particularly in the prevalence of excess interommatidial cells, since it is in the elimination of these cells that apoptosis in the *Drosophila* eye mainly functions (Wolff and Ready, 1991b). As discussed in the introduction, it is thought that all interommatidial cells that do not receive cell survival signals from the primary pigment cells will undergo apoptosis (Cagan and Ready, 1989; Miller and Cagan, 1998). Thus there is no requirement for these superfluous cells to be "tagged" for death so all extra cells should be eliminated, including those generated by over-proliferation resulting from loss of Fat. The fact that superfluous cells persist to adulthood suggests that a reduction of apoptosis makes some contribution to the *ft* overgrowth phenotype.

However, analysis of the pupal retina revealed that the accumulation of Diap1 is not sufficient to prevent the execution of normal programmed cell death as it occurs in development. Furthermore, there is very little apoptosis before 20% pupal development, so loss of apoptosis cannot contribute

significantly to the overgrowth of *ft* mutant clones as they exist in the third larval instar, particularly prior to the passage of the MF. Altogether, these data suggest that any reduction in apoptosis is a relatively minor contributing factor in *ft*-related overgrowth.

4 CHAPTER 4: FAT'S EFFECTS ON SIGNALLING PATHWAYS INVOLVED IN FURROW PROGRESSION

One of the most intriguing results to arise from the studies described in the previous chapter was a consistent tendency for various cell cycle markers to reveal a delay in the ability of *ft* cells to enter into and exit from the MF. I verified this observation by looking at the expression patterns of Atonal and Senseless, two proneural transcription factors that are expressed early in photoreceptor specification. Atonal (Ato) is a basic-helix-loop-helix transcription factor whose expression confers a 'pro-neural' status upon cells in the MF. Its expression is then restricted to a single cell per ommatidium, which is fated to become R8 (Jarman *et al.*, 1994). Senseless (Sens) is a zinc-finger transcription factor that is required for proneural gene expression (Nolo *et al.*, 2000); in the *Drosophila* eye it is expressed in cells that have been selected to become R8s. In clones that are mutant for *ft*, there is a delay in the expression of each of these transcription factors (Figure 4.1). From this data, I concluded that it is likely that in *ft* mutant cells there is a lag, but not a failure, in the execution of all events associated with MF progression and therefore in their abilities to make the transition from proliferation to differentiation in larval eye development.

I wondered if excess growth could be attributed to an impaired ability of *ft* cells to respond to differentiation signals, relegating them to continue proliferating for an extra-ordinary period of time. Excess cells would be

generated when mutant cells fail to initiate a timely arrest upon entry into the MF, as well as when mutant cells fail to respond to the signal to slow growth, which is initiated prior to differentiation. To further investigate the role for Fat in furrow dynamics, I examined the signalling pathways involved in this process.

There are four main signalling pathways involved in balancing the progression of differentiation. As described in the introduction, Notch is needed to initiate proneural gene expression in the MF (Baker and Yu, 1997; Baonza and Freeman, 2001; Li and Baker, 2001); it is needed to overcome G1 arrest as cells exit the MF (Baonza and Freeman, 2005; Firth and Baker, 2005); it is required for the selection of a single cell per ommatidium to become the founding cell, R8 (Baker *et al.*, 1990; Baker and Zitron, 1995; Jarman *et al.*, 1994), and it has a later role in the specification of R3 and R4 (Cooper and Bray, 1999; Fanto and Mlodzik, 1999), a function that is dependent upon directional cues from Ft (Rawls *et al.*, 2002; Yang *et al.*, 2002). Epidermal growth factor receptor (EGFR) signalling, in the form of Spitz secretion from R8, is needed to recruit additional cells to each ommatidium (Dominguez *et al.*, 1998; Freeman, 1994; Freeman, 1996), as well as to protect these cells from re-entering the cell cycle in the SMW (Baker and Yu, 2001; Baonza and Freeman, 2005; Firth and Baker, 2005). Hedgehog (Hh) and Decapentaplegic (Dpp) signalling drives the wave of differentiation by signalling from differentiated cells to undifferentiated cells, initiating the developmental program that is to follow (Chanut and Heberlein, 1997; Heberlein *et al.*, 1995; Heberlein *et al.*, 1993). Finally, Wingless (Wg) signalling, through a poorly understood mechanism, balances the rate of furrow progression by inhibiting its movement

anteriorly (Cadigan *et al.*, 2002; Ma and Moses, 1995; Treisman and Rubin, 1995). In the following chapter I present cell biological and genetic evidence for connections between each of these pathways and the function of Fat.

4.1 Notch signalling

Given that there is a known connection between Fat and Notch in directing PCP, I decided to see if loss of Fat affects Notch signalling in early ommatidial specification. The simplest experiment was to look at the expression pattern of Delta (Dl) in mosaic tissue. In addition to being a major ligand for Notch in the eye, Delta is regulated by Notch signalling via a feedback loop; in Notch-mediated lateral inhibition, activation of N leads to transcriptional repression of Dl in the same cell and upregulation in the neighbouring cell (Kunisch *et al.*, 1994). In the absence of *ft* there is no detectable change in Delta expression (Figure 4.2). There is a delay in the initial expression of Dl at the MF, however in the absence of any other changes to Dl's expression levels I concluded that this delay is likely to be a consequence of an earlier defect, just as it is with all other markers examined so far. This result was as expected, since I had already established that the delays that are apparent in *ft* clones originate ahead of the MF, while the earliest detectable function for Notch is in promoting proneural gene expression within the MF.

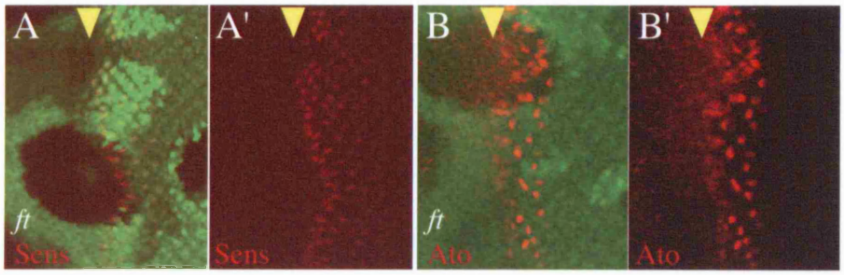

Figure 4.1 Fat-deficient clones exhibit disrupted furrow dynamics. Ft-deficient clones marked for (A) Senseless expression and (B) Atonal expression. Yellow arrowheads indicate the positions of the MF.

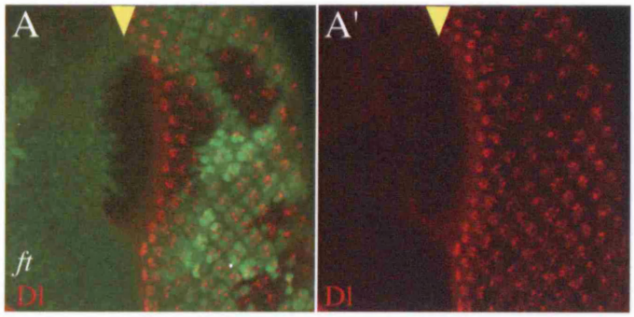

Figure 4.2 Loss of Fat does not visibly affect Notch signalling at the MF. Ft-deficient clones marked for expression of Delta. Yellow arrowheads indicate the position of the MF.

4.2 EGFR signalling

Next I examined Epidermal Growth Factor Receptor (EGFR) signalling. Previous work in the lab had identified Sprouty (Sty) in a yeast-two-hybrid assay as a putative binding partner of the intracellular domain of Ft (see Fanto et al., (2003) for details of the yeast-two-hybrid screen).

Sprouty is an antagonist of EGFR signalling through its inhibitory binding of Grb2 and Raf (Casci *et al.*, 1999; Hanafusa *et al.*, 2002; Kramer *et al.*, 1999; Reich *et al.*, 1999). In fact, Sprouty is a general inhibitor of all receptor tyrosine kinases (RTK) (Reich *et al.*, 1999), however the EGF receptor is the only identified RTK to function in early photoreceptor specification; Sevenless is also implicated in the eye but its effects are mainly exerted later, as the name implies, in R7 specification. Sprouty can also act as an agonist through sequestration of c-Cbl, a molecule that binds phosphorylated RTKs, triggering their ubiquitination and degradation; its ability to propagate the signal in this way is transient, however, since binding to c-Cbl triggers its own degradation (Egan *et al.*, 2002; Rubin *et al.*, 2003; Wong *et al.*, 2002). As an antagonist of EGFR signalling, mutations in *sprouty* are known to result in the recruitment of additional photoreceptors to each ommatidium (Casci *et al.*, 1999).

I began by assessing whether Sprouty could play a role in planar cell polarity, the best documented of Fat's functions. Using the FLP-FRT system, I generated mitotic clones of *sty* that are marked by the absence of *white* gene expression (visible as brown pigment in adult eye sections). Sections of these eyes revealed a recapitulation of the documented *sty* phenotype: wholly mutant

ommatidia frequently exhibit supernumerary photoreceptors previously identified as R7s (Casci *et al.*, 1999). Additionally, I was able to identify ommatidia that had failed to execute a precise 90° rotation. These ommatidia tended to lie on the periphery of the mutant clone and consisted either wholly or partially of wild-type cells (Figure 4.3A).

Planar cell polarity defects can only be assessed when there is a full complement of photoreceptors arranged as the characteristically wild-type trapezoid. The supernumerary R7 cells in ommatidia that are entirely mutant for *sty* therefore preclude any analysis of their PCP phenotypes. To determine the full extent of potential PCP defects in *sty* clones, I used the FLP-FRT system with chromosomes marked with ubiquitin-GFP and looked in late larval eye discs. At the wandering third instar larval stage, the arrangements of R1 and R6, as visualised by immunofluorescence against BarH1, are apparent as diagonal rows of cells (Figure 4.3B) (Higashijima *et al.*, 1992); defects in PCP result in disruption to this characteristic pattern. Clones of *sty* exhibit defective planar cell polarity both within and outside the clones (Figure 4.3C). These defects occur with greater frequency than is implied by examining adult eye sections, and they reveal that the origins of the PCP defect in *sty* mutants lie in larval development.

I then tested to see if there is a genetic interaction between *sty* and *fat* with respect to PCP. To do this, I generated clones of *fat* in a background that is heterozygous for *sty*. ft^1 is a hypomorphic allele: homozygous flies are viable and clones in the adult eye rarely result in the characteristic dorsal-ventral flips of stronger *fat* alleles (Figure 4.3E). However, when these clones

are haplo-insufficient for *sty* there is a high incidence of these flips, even in small clones (Figure 4.3F).

Knowing that *sprouty*, a documented antagonist of EGFR signalling in the eye, interacts genetically with *fat*, and that clones for *sty* result in PCP defects, I then looked at the effect of loss of Fat on the EGFR signalling cascade itself. To do this, I used an antibody against the active, dual phosphorylated form of mitogen-activated protein kinase (dpERK). The phosphorylation of MAPK is a readout for activation of RTK signalling (Gabay *et al.*, 1997b; Gomez and Cohen, 1991), and in the *Drosophila* eye disc dpERK is found at its highest levels at the MF where secretion of Spitz from each R8 triggers the cascade in its nearest neighbouring cells, recruiting them as photoreceptors (Gabay *et al.*, 1997a). I found that *ft* mutant clones exhibit no overall change in the levels of dpERK (Figure 4.3D). However, I did note that there was, as with most other markers examined, a delay in the expression pattern.

Figure 4.3 *fat* genetically interacts with *sty*, but does not affect EGFR signalling.

(A) Sections of Sty-deficient clones in the adult eye reveal polarity defects; loss of Sty is marked by the lack of brown pigment granules indicating the absence of expression from the *white* transgene; the endogenous equator is marked in yellow. (B) Expression of BarH1 in R1 and R6 of each ommatidium in wild-type imaginal discs reveal the opposite chirality of the dorsal and ventral halves, resulting in the appearance of diagonal lines of staining. (C) Sty-deficient clones have polarity defects both autonomously (arrowhead) and non-autonomously (arrow) as revealed by BarH1 expression. Co-immunofluorescence against Elav assists in assigning pairs of cells to particular ommatidia (C). (D) Ft-deficient clones marked for dpERK expression. Yellow arrowhead marks the position of the MF. Clones homozygous for the hypomorphic allele, ft^{1}, in wild-type (E) and *sty* heterozygous (F) backgrounds.

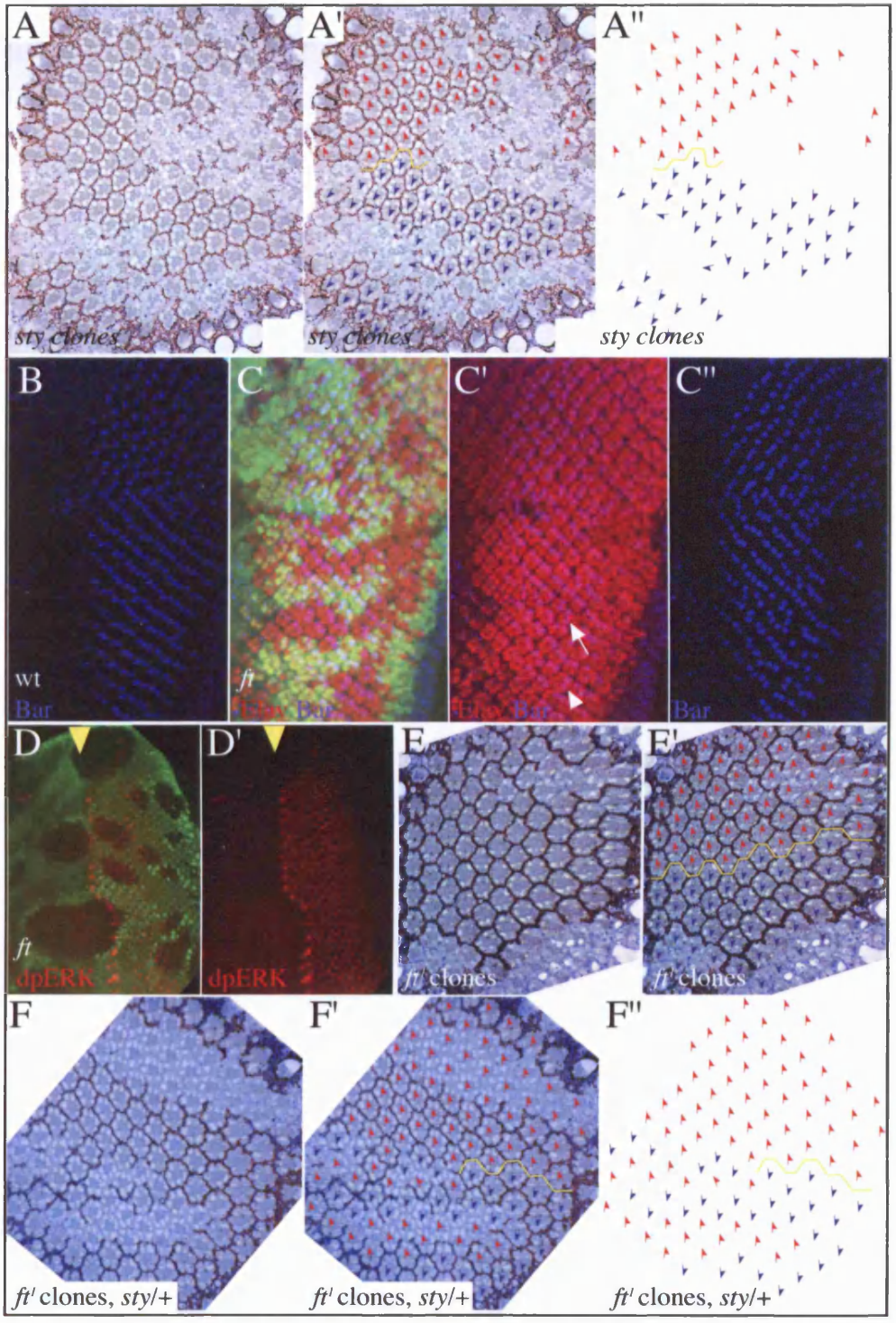

Figure 4.3 For the figure legend see the previous page.

From the data presented here, I had concluded there is a possible role for EGFR signalling in the phenotypes resulting from loss of Fat, but the evidence collected indicated this role might lie principally in Ft's function in PCP. While I did not directly test the possibility of a role for EGFR signalling in Ft-related overgrowth, I could see no detectable change in the levels of mitogen activated protein kinase (MAPK) signalling in the absence of Ft, nor any aberration in the pattern that might indicate a primary role for EGFR signalling in the retardation of MF progression.

4.3 Dpp and Hedgehog signalling

Differentiation in the eye is initiated at the posterior midline by a combination of activated Notch, and Hedgehog (Hh) and Decapentaplegic (Dpp) signalling. Once initiated, however, the maintenance of MF progression relies on Hh and Dpp in a somewhat redundant manner: the loss of either cascade alone only slows furrow progression, however in the absence of both the MF completely arrests (Strutt and Mlodzik, 1997).

4.3.1 Dpp signalling

I began by looking at Dpp expression in *ft* mutant clones. Since I was unable to obtain a suitable antibody, I decided to perform this analysis by fluorescent *in situ* hybridisation. These experiments revealed that there is no clear disruption to the pattern of *dpp* expression, other than the ubiquitous delay of markers of the MF (Figure 4.4A).

While the expression of Dpp itself appears to be unaffected, it was still possible there is some deficiency in Dpp signalling that could account for the delayed-furrow phenotype, either through defects in Dpp processing and trafficking or in the reception of the signal. Active BMP/Dpp signalling results in the activation of Mothers Against Dpp (Mad) related proteins, which then function as transcriptional co-activators (Kim *et al.*, 1997; Liu *et al.*, 1996; Wiersdorff *et al.*, 1996; Zhang *et al.*, 1996). I used an antibody raised against the phosphorylated isoform of mammalian Smad to look at the pattern of active Dpp signalling (Teleman and Cohen, 2000) in the absence of Ft. I found that these results reflected those seen in *dpp* expression: there is a delay in furrow progression but no other obvious disruption to the pattern (Figure 4.4B).

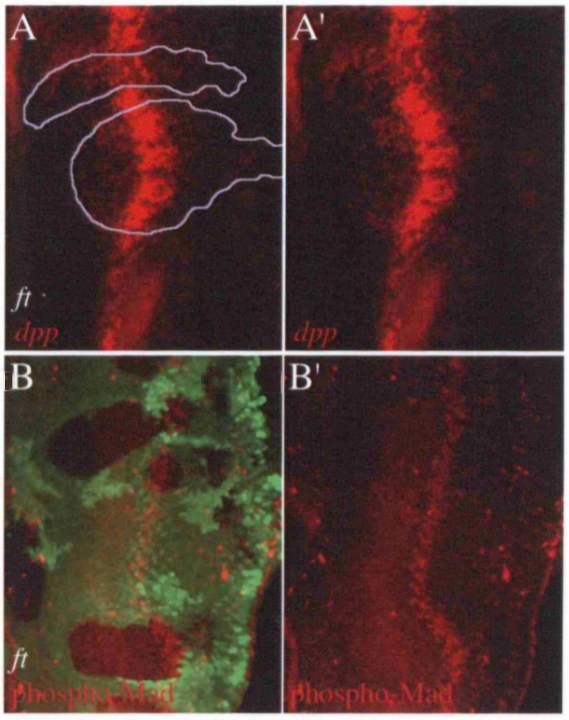

Figure 4.4 Loss of Fat does not affect Dpp signalling. (A) Fluorescent *in situ* hybridisation against the *dpp* transcript. Domains lacking Fat are drawn in grey. (B) Ft-deficient clones marked for expression of phosphorylated-MAD.

4.3.2 Hedgehog signalling

I next turned my attention to Hedgehog signalling. Deficiencies in Hh signalling resulting from loss of the positive regulator, Smoothened (Smo), are known to inhibit but not block the progression of the MF (Dominguez, 1999; Greenwood and Struhl, 1999); activation of Hh signalling triggered by loss of Patched, an Hh receptor and antagonist of Smoothened, or by overexpressing Hh itself, results in induction of ectopic furrows.

4.3.2.1 Ft deficient clones show no changes to Hedgehog and Patched expression, but accumulate active Ci at the MF by a post-transcriptional mechanism

As with Dpp, I could find no antibody suitable for examining the Hh expression pattern *in vivo*. However, there is a transgenic reporter line in which β-galactosidase (β-gal) is expressed from the Hh promoter and that can be expressed in a background suitable for generating Ft-deficient clones. In the absence of Ft there are no observable disruptions to the expression of Hh as detected by immuno-fluorescence against β-gal (Figure 4.5A).

As with Dpp, while the Hh protein may be expressed normally, I cannot eliminate the possibility that Hh signalling overall is affected. Since there is a readily available antibody suitable for immuno-fluorescence, I decided to look at the expression of the Hh signalling antagonist, Patched (Ptc), in the absence of Ft. As mentioned, binding of Hh to Ptc releases it from its repression of Smoothened (Smo); Smo is then free to activate Hh signalling responses. I found that there is no consistent change in the levels of Ptc expession in the absence of Ft (Figure 4.5B).

While the expression of ligand and receptor appeared to be unaffected in Ft-deficient clones, there still could be modulation of Hh signalling more downstream in the cascade. The best indicator for assessing Hh pathway activation is accumulation of full-length Cubitus Interruptus (Ci), a Gli family transcription factor. The Gli family proteins are thought to mediate the majority of Hh responses; in the *Drosophila* eye Ci is stably maintained at its full length primarily at the furrow, where Hh signalling is at its highest. Thus, using an antibody specifically raised against 'active' Ci, which does not detect the smaller repressor form (Aza-Blanc *et al.*, 1997), I could determine if loss of Ft results in an overall modulation of Hh signalling. I found that in the absence of Ft, there is an accumulation of active Ci at the MF, which appears to initiate normally but persists inappropriately for several cell rows to the posterior (Figure 4.5C), indicating there is a possible elevation in Hh signalling in *ft* cells.

I next wanted to know if this accumulation of Ci^{155} is post-transcriptional. Full-length, 'active' Ci is uniformly expressed throughout the eye disc but is post-translationally modified by two distinct mechanisms (Ou *et al.*, 2002). In the anterior of the eye disc, Ci is proteolytically cleaved from its full-length form, which measures 155kD (Ci^{155} or Ci*), to its repressor form, which measures 75kD (Ci^{75}), in a Protein Kinase A (PKA) -dependent manner; in the posterior eye disc, Ci is degraded in a PKA-independent manner. Thus, I wanted to know whether the accumulation that I see in the absence of Ft is due to changes in its post-translational modification or to transcriptional upregulation. To find out, I generated Ft deficient clones in a background in which β-Gal is expressed from the *ci* locus. In these clones, I could find no

disruption to the pattern of β-Gal, indicating that *ci* transcription is unaffected and thus the accumulation is post-transcriptional (Figure 4.5D).

4.3.2.2 ft genetically interacts with genes involved in Ci processing and degradation

Loss of Ft results in an accumulation of full-length Ci by a post-transcriptional mechanism. This accumulation would normally be indicative of an elevation of Hh signalling, which would result in an acceleration of MF progression, contrary to the phenotype documented in *ft* mutants: I would have predicted that if there is a role for modulated Hh signalling in the *ft* furrow phenotype, it would be a loss, rather than a gain, of signalling that would be responsible. Therefore I wondered if the delay was not due to a problem with Hh signalling itself, but in the regulation of Ci processing.

The function of Ci at the MF is still unclear: it was previously presumed, as in other models, that Ci^{155} is responsible for transcribing Hh response genes (Methot and Basler, 2001). More recent data indicated that Ci^{155} is not at all required for MF progression and that it is only release from repressive effects of Ci^{75} that is important for Hh signalling responses in the MF (Pappu *et al.*, 2003). However this conclusion is contested by Fu and Baker (2003) who propose that active Ci does have a role in promoting proneural gene expression in a manner redundant to other signalling pathways. Furthermore, the observation that the region of highest Ci^{155} accumulation is not directly adjacent to the source of the Hh signal has also led to the proposal that high levels of Hh lead to the loss of active Ci, rather than its strong accumulation (Dominguez, 1999). It is clear that the role of Ci as an Hh signal effector in the

context of MF progression is not fully understood. Thus, I wondered if there is a previously unidentified requirement for the down-regulation of Ci^{155} in this process. In other words, could the perdurance of Ci^{155} be preventing a transition from a proliferative to a neural state?

I began testing this possibility by looking for genetic interaction between *ft* and genes involved in Ci processing and degradation. Ci^{155} processing requires permissive phosphorylations that not only tag it for cleavage but also limit its activity (Methot and Basler, 2001; Wang *et al.*, 1999a). Protein Kinase A (PKA) is responsible for the first set of phosphorylation events (Price and Kalderon, 1999; Wang *et al.*, 1999a), which prime Ci^{155} for subsequent phosphorylation at adjacent sites by Glycogen Synthase Kinase 3 (GSK3, or Shaggy) and Casein Kinase I (CKI); without these phosphorylation events, Ci remains uncleaved and active, even in the absence of Hh (Jia *et al.*, 2002; Price and Kalderon, 2002). Cleavage is then executed by Cullin 1 and the associated SCF complex (Cul1/Skp1/F-box) (Ou *et al.*, 2002). There is some data suggesting that the proteolytic cleavage of Ci as described here occurs only in the anterior eye disc. In the posterior, Ci^{155} is lost in a smoothened dependent manner that does not require PKA phosphorylation, and is mediated by Cullin3, rather than Cullin1 (Ou *et al.*, 2002). However Ci^{155} in the posterior does still require CKI activity, since clones deficient for *discs overgrown* (*dco*), the *Drosophila* homologue of Casein kinase Iε (CKIε) (Jia *et al.*, 2005; Price and Kalderon, 2002; Zilian *et al.*, 1999), accumulate Ci^{155} both before and after the MF in a cell-autonomous manner (Joseph Bateman, personal communication).

dco is so named because transheterozygous combinations that include the allele dco^3 result in hyperplastic overgrowth of all imaginal discs in a fashion reminiscent of mutations in *ft*. Given the similarities in phenotype, I wondered if I could see a genetic interaction between *ft* and *dco*. I used the hypomorphic allele, ft^1, which is viable in transheterozygous combination with null alleles, albeit in reduced numbers. I generated crosses in which I could compare the viability of ft^1/ft^{fd} progeny with wild-type and *dco* heterozygous backgrounds. I found that in a background that is heterozygous for a null allele, dco^{le88}, there is a decrease in the lethality of ft^1/ft^{fd} transheterozygotes. This interaction was highly significant in Chi-squared analysis ($p > 0.0001$). Interestingly, in a background heterozygous for the hypomorphic allele, dco^3, there was no genetic interaction ($p = 0.95$) (Figure 4.5E, Table 4.1).

I next wanted to see if I could see a genetic interaction specifically in the context of the phenotype in which I was interested: the accumulation of Ci^{155}. To do this, I generated clones deficient for Ft, and compared the accumulation of Ci^{155} in wild-type versus *dco* heterozygous backgrounds. Again, I found that haploinsufficiency of *dco* results in suppression of the *ft* mutant phenotype (Figure 4.5F): in the majority of clones examined, there is little, if any, accumulation of active Ci.

Table 4.1 Loss of Dco suppresses *ft* lethality

allele of *dco*	ft/ft (N)	ft/ft; dco/+ (N)	χ squared value	P value
3	283.26*	284	0.00385	0.951
le88	173.65*	275	0.9505	1.71E-06

* values have been normalised for deleterious effect of the balancer; see Materials and Methods.

The suppression of *ft* mutant phenotypes by loss of *dco* was somewhat unexpected: the preliminary indication was that Dco and Ft would act in the same direction, since they appeared to phenocopy one another, resulting in enhancement of *ft*-associated phenotypes. Thus I wanted to look for interaction between *ft* and another molecule required for the regulation of Ci processing. Regulation of the activities of both Cullins relies on the function of the COP9 signalosome, a relative of the 26S proteosome complex: COP9-mediated deneddylation of the Cullins results in their inactivation (Lyapina *et al.*, 2001; Wu *et al.*, 2005). Interestingly, the COP9 signallosome has also been shown to promote the degradation of Cyclin E (Doronkin *et al.*, 2003).

To see if *ft* genetically interacts with components of the COP9 signalosome, I generated clones in a background that is haplo-insufficient for CSN5, one of the eight subunits of the COP9 complex (Freilich *et al.*, 1999). I found that these clones show an enhanced accumulation of Ci^{155} compared to loss of *ft* alone (Figure 4.5G). Once again, this data seems to contradict the prediction: loss of COP9 complex function would result in increased activity of the Cullins and increased degradation of Ci^{155}, which should manifest as a suppression of the *ft* mutant phenotype. This data, though somewhat unexpected, indicates that Ft function is required for appropriate regulation of the processing or degradation of Ci.

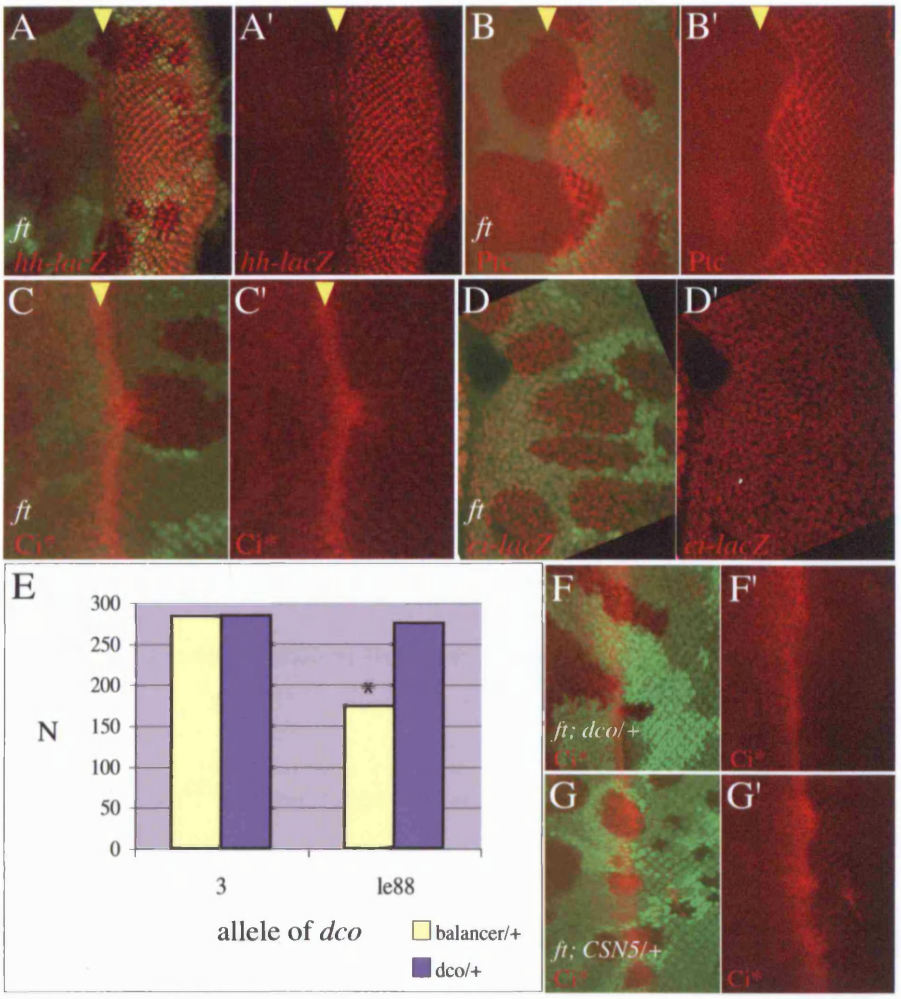

Figure 4.5 Loss of Fat affects the levels of active Ci. Yellow arrowheads indicate the positions of the MF as they are in wild-type tissue. (A) Ft-deficient clones generated in a background expressing β-Gal from the *hedgehog* promoter. (B) Ft-deficient clones marked for expression of Ptc. (C) Ft-deficient clones show an accumulation of full-length Ci. This accumulation is post-transcriptional, since (D) loss of Fat does not affect expression of β-Gal from the *ci* promoter. (E) *fat* viability is suppressed by haploinsufficiency of the null allele, dco^{le88}, but not dco^{3}. On the Y-axis is the number of progeny of each genotype; the asterisk indicates statistical significance as determined by Chi-squared analysis. (F) Ft-related accumulation of full-length Ci is suppressed by haploinsufficiency of the null allele, dco^{le88}. (G) Ft-related accumulation of full-length Ci is enhanced by haploinsufficiency of the COP9 signalosome subunit, *CSN5*.

4.3.2.3 Accumulation of Ci^{155} is not responsible for fat mutant phenotypes

While the investigation of a possible role for Fat in the regulation of Ci processing is most certainly an intriguing line of enquiry, my primary interest still lay in the mechanism behind the delay in MF progression observed in *ft* mutant clones. As discussed earlier, Ci^{75} must be eliminated to relieve repression of a number of Hh target genes, a mode of regulation that is distinct from the activation of transcription of genes in response to Ci^{155}. Regardless of the underlying mechanism for the accumulation of Ci^{155}, I wondered if there could be, in a manner analogous to Ci^{75}, a requirement for the loss of full-length Ci in order for transition from proliferation to differentiation to take place.

To see if Ci^{155} accumulation is responsible for the delayed furrow phenotype, I wanted to generate clones deficient for Ft and Ci^{155} together. Previous reports had indicated that Ci expression is wholly unnecessary for the progression of the MF (Fu and Baker, 2003; Pappu *et al.*, 2003), so I decided to remove Ci altogether.

First, I wanted to confirm previous data demonstrating that Ci expression is dispensable for events associated with the progression of the MF. The *ci* locus is on the fourth chromosome, a notoriously difficult chromosome to work with, mainly because it is entirely heterochromatic and resistant to recombination. To generate clones deficient for Ci, I used a transgenic line in which a genomic rescue construct for Ci on the left arm of the second chromosome is subject to mitotic recombination in a background that is wholly mutant for *ci* at the endogenous locus (Methot and Basler, 1999); clones were then visualised by immuno-fluorescence against Ci^{155}. As has been described

previously (Fu and Baker, 2003; Pappu *et al.*, 2003), I found that in the absence of Ci, there is no disruption to events associated with the progression of the MF with respect to expression of the neural markers Sens and Ato (Figure 4.6A).

Confident that loss of Ci alone does not result in deleterious effects to MF progression, I generated clones deficient for both Ci and Ft. I found that removal of Ci, both its repressor and activator forms, does not rescue delays in the MF resulting from loss of Ft: immuno-fluorescence against Ato and Sens reveals disruption to neurogenesis still exists; BrdU incorporation assays reveal there is still a delay in the initiation of the SMW; immuno-fluorescence against Cyclins B and E reveal there is still ectopic cell cycling posterior to the furrow and that there is still a delay in the ability of Ft deficient cells to enter G1 arrest (Figure 4.6B-E). These results indicate that it is highly unlikely that the accumulation of full-length Ci in the absence of Ft is causing a delay in the progression of the MF.

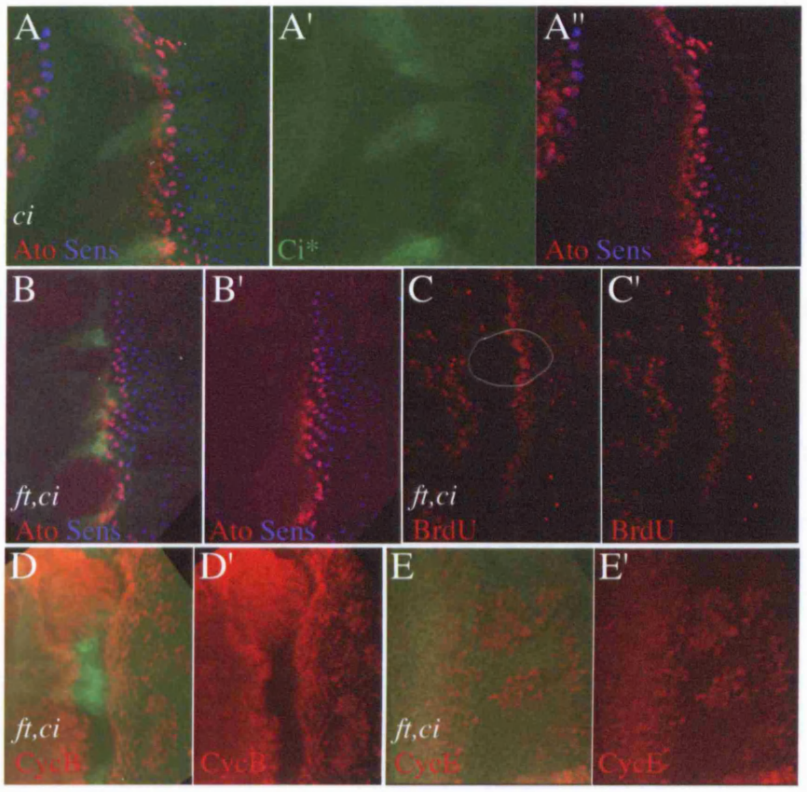

Figure 4.6 Accumulation of Ci* is not responsible for *fat* mutant phenotypes. In all images, Ci- and Ft/Ci-deficient tissue is marked by the lack of Ci*. (A) Loss of Ci in clones does not affect furrow dynamics with respect to expression of Atonal and Senseless. (B) Loss of Fat and Ci together result in delayed expression Atonal and Senseless. (C) Loss of Fat and Ci together result in delays to the SMW as visualised by BrdU incorporation; the domain of Ft/Ci-deficient tissue is drawn in grey. (D) Loss of Fat and Ci together result in delayed entry into G1 arrest in the MF, as well as perdurance of proliferation posterior to the furrow as visualised by expression of Cyclin B. (E) Loss of Fat and Ci together results in the accumulation of Cyclin E posterior to the MF.

4.4 Wingless signalling

Wingless signalling serves three main functions in the patterning of the eye. It first functions early in eye imaginal disc development where it is required for defining the dorsal-ventral boundary. Wg is expressed in the dorsal margin and signals for activation of the Iroquois complex genes in the dorsal half of the eye (Cavodeassi *et al.*, 1999; Heberlein *et al.*, 1998; McNeill *et al.*, 1997), which ultimately results in Notch activation in a narrow band that will become the dorsal-ventral midline. Wg is also required to restrict the expression of eye specification genes to the retinal field by inhibiting their transcription in the presumptive cuticle and antenna (Baonza and Freeman, 2002). Finally, Wg negatively regulates the progression of the MF (Ma and Moses, 1995; Treisman and Rubin, 1995).

Previous analysis of the function of Fat in the wing had revealed that loss of Fat leads to an accumulation of Wg (Cho and Irvine, 2004). Since Wg is known to negatively regulate furrow progression, I speculated that an accumulation of Wg could account for the delayed furrow phenotype in Fat clones.

4.4.1 Wingless is ectopically elevated in *fat* clones

To see if Fat function affects Wingless expression, I generated *ft* loss of function clones and performed immuno-fluorescence against Wg. In wild-type third instar eye discs, Wg expression is normally restricted to the antero-polar margins (Figure 4.7A). In clones deficient for Ft, I found that there is a subtle

but reproducible increase in Wg: this protein is ectopic, since in wild-type discs there is no detectable protein in the centre of third instar discs; it is also non-autonomous, as would be expected for a diffusible morphogen such as Wg; and it only occurs in clones ahead of the MF (Figure 4.7B). In the example shown here, the domains of endogenous Wg expression are largely out of the plane of focus.

One of the key mediators of Wg signalling is Armadillo (Arm), the *Drosophila* homologue of β-catenin (Sanson *et al.*, 1996). Activation of Wingless signalling can result in an accumulation of Arm at the apical membrane (Riggleman *et al.*, 1990), and data from the analysis in the wing has shown that accumulation of Wg resulting from loss of Fat also leads to increased Arm (Jaiswal *et al.*, 2006). However, I found that in the eye, accumulation of Wg resulting from loss of Fat is not accompanied by an accumulation of Arm (Figure 4.7C).

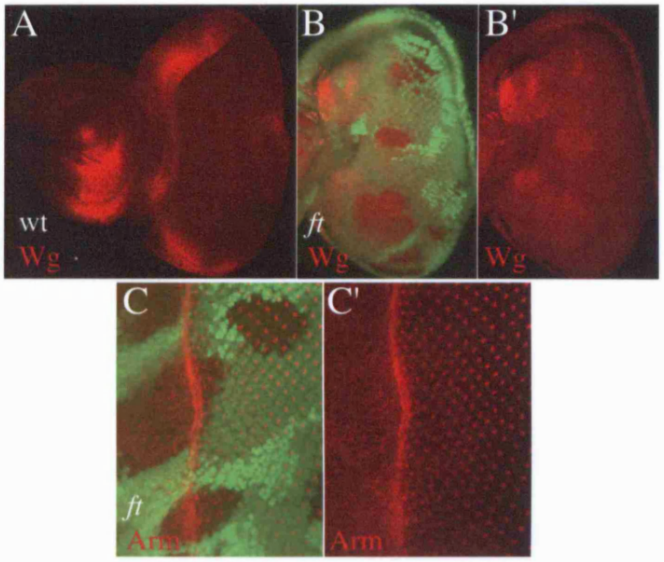

Figure 4.7 Loss of Fat results in an accumulation of Wg. (A) Wild-type eye disc expressing Wg in the antennal disc, and in the antero-polar margins. (B) Loss of Ft results in an ectopic accumulation of Wg in centre of the disc. (C) Loss of Ft does not result in accumulation of Armadillo.

4.4.2 Accumulation of Wingless is not responsible for *fat* mutant phenotypes

The phenotype of *ft* in which I was primarily interested was the delay in furrow progression. The accumulation of Wg, particularly since it is strongest anterior to the MF, provided a simple and plausible explanation for this retardation, since Wg is known to fulfil this function in normal eye development.

To see if the ectopic Wingless could be responsible for the delay in furrow progression, I generated recombinant flies to make clones that were doubly deficient for both Fat and Wg. By this method, clones would lack ectopic Wg that accompanies loss of Fat, but I was concerned that they would also lack endogenous Wg expression. Any phenotypes resulting from loss of Wg alone would not confuse my analysis since I was only interested in clones that did not lie in endogenous Wg-expressing domains, however Wingless signalling is crucial to all stages of *Drosophila* development and, as such, I was concerned that complete loss of Wg, even in clones, would result in early lethality. To overcome any potential difficulties in rearing these larvae, I began by using a temperature sensitive allele, $wg^{l\text{-}12}$; in the context of embryonic development, this allele has been demonstrated to result in non-functional protein at 25^0C (Bejsovec and Martinez Arias, 1991). Should larvae grown at the restrictive temperature fail to complete third instar development, I could overcome the lethality by initially rearing them at the permissive temperature then transferring them to the restrictive temperature prior to analysis.

In order to be sure there are no deleterious effects caused by the loss of Wg itself, I began by looking at larvae carrying clones of the wg^{l-12} allele alone, to see what phenotypes might be affected. Surprisingly, I found that larvae carrying clones that are homozygous for the wg^{l-12} allele are not only viable, but they also do not appear to exhibit any visible defects in gross morphology. This was true when the larvae were reared at either 25°C or 29°C. Analysis of third instar eye discs revealed there is no disruption to the patterns of BrdU incorporation, nor to the expression of Cyclin B and activated Ci (Figure 4.8A,B).

These unexpected results indicated there is no compromise associated with loss-of-function Wg clones. As such, I wanted to be sure that this allele was truly non-functional at the restrictive temperature. In other circumstances I would assess the loss of function by immuno-fluorescence against the protein of interest. However, as a temperature-sensitive allele, the *wg* locus produces a protein that, though non-functional, still presents an epitope recognised by the antibody (Figure 4.8C). Thus, to see how I was affecting Wg function, I looked at clones deficient for Wg in the wing imaginal disc to see if, at 25°C, there is a compromise to the expression of the Wg target, Sens, along the dorsal-ventral margin. In these clones there is a reduction of Sens expression (Figure 4.8D).

Confident that the allele wg^{l-12} produces a non-functional protein, I looked at clones deficient for Ft and Wg for various *ft*-associated phenotypes that I have described. I found that removal of ectopic Wg in clones deficient for Fat does not rescue the accumulation of Cyclins B or E, nor does it rescue the delay in furrow progression as visualised by BrdU incorporation in the

SMW (Figure 4.8E-G). These clones still exhibit increased levels of Diap1 (Figure 4.8H), still have widely spaced ommatidia suggesting the existence of superfluous interommatidial cells and still have non-autonomous PCP defects as revealed by immuno-fluorescence against Bar and Prospero (Figure 4.8I). Non-autonomous dorsal-ventral flips are also prevalent in the adult eye (Figure 4.8K, compare to loss of Wg alone in Figure 4.8J). These results were highly unexpected, however they were confirmed by repeating the analysis using an unconditional null allele, wg^{CX4}. Thus, the accumulation of ectopic Wg resulting from loss of Fat is not responsible for any of the phenotypes tested, including delay in morphogenetic furrow progression.

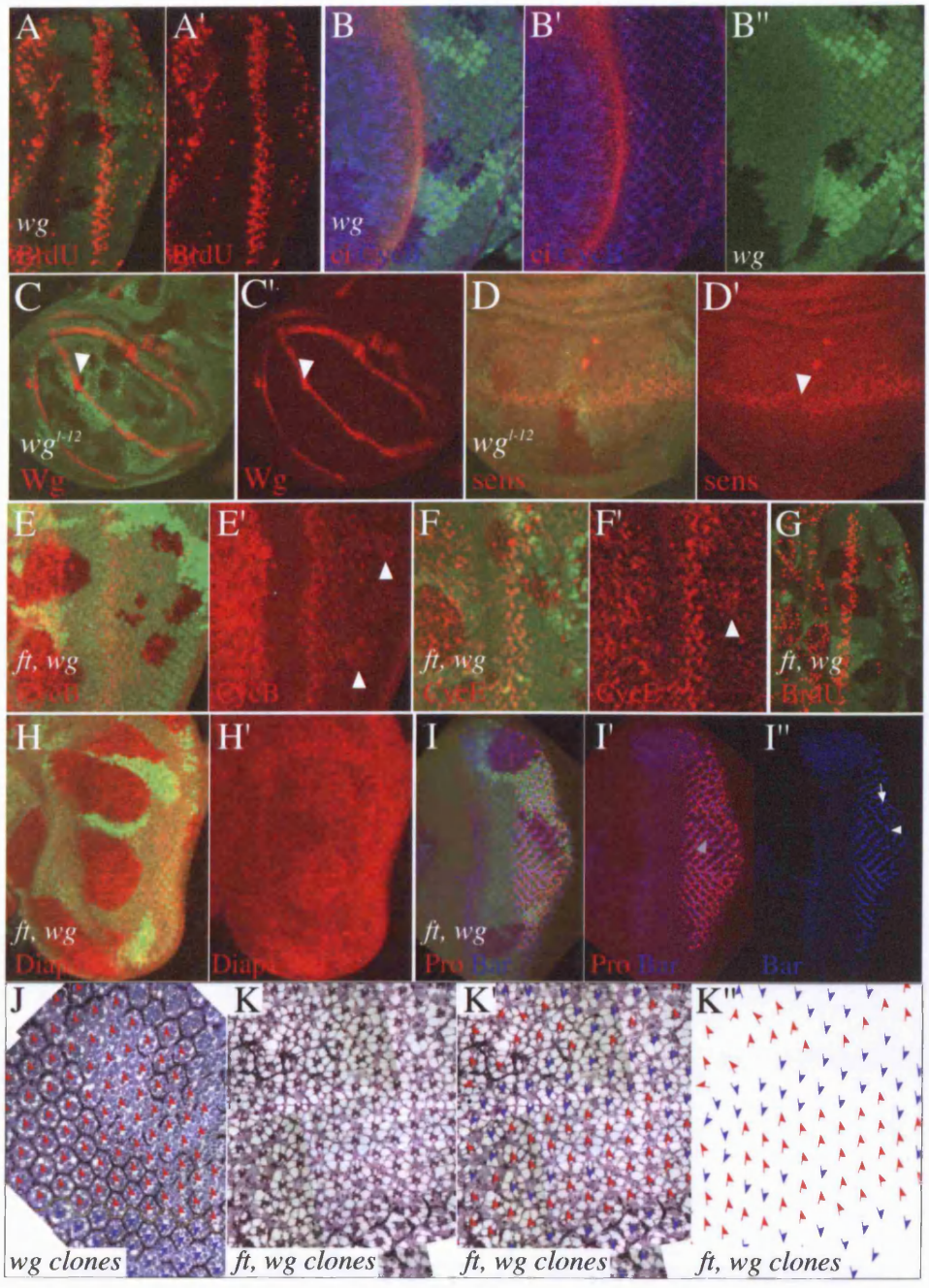

Figure 4.8 Accumulation of Wg is not responsible for *fat*-related phenotypes. BrdU incorporation (A), and Cyclin B and Ci* expression (B) are not affected in Wg-deficient clones. In discs grown at 25°C, clones of the allele wg^{l-12} still accumulate Wg (C, arrowhead), but lose Wg-dependent Sens expression (arrowhead, D). (E-K) Clones deficient for Ft and Wg together exhibit Ft-related phenotypes. In clones deficient for Ft and Wg, there is over-expression of Cyclin B (arrowheads) (E), Cyclin E (arrowhead) (F), and Diap1 (H); there is delayed entry into the SMW as revealed by BrdU incorporation (G). (I) There is increased ommatidial spacing as revealed by Bar and Prospero expression (grey arrowhead). There are autonomous (white arrowhead) and non-autonomous (white arrow) rotation defects in the larva, as revealed by BarH1 expression (I), and in the adult (K). Loss of Wg alone does not result in PCP defects (J).

4.4.3 Removal of Wg enhances the *fat* overgrowth phenotype

In the above experiments, I generated clones deficient for Fat and Wg together under the assumption that the accumulated Wg that I observed in fat clones before the passage of the MF was entirely ectopic. According to published data there is little, if any, detectable expression of Wingless outside the polar-anterior margins, and my data has shown that there is no detectable accumulation of Wg in Ft-deficient clones that lie posterior to the MF. Thus, I was very surprised to observe what appeared to be an increase in proliferation in clones deficient for both Wg and Ft: within clones located in the posterior eye disc, there is a dramatic increase in the incidence of BrdU incorporating cells. Interestingly, this phenotype is only apparent in cells that are situated approximately 4-6 ommatidial rows behind the MF, which is particularly striking when the clone spans a region that extends either further anteriorly or posteriorly (Figure 4.9A), giving it the appearance of a 'third mitotic wave'. I had previously noted the existence of this phenotype in clones deficient for Ft alone, but only when cells are exposed to greatly extended pulses of BrdU incorporation. In clones lacking Ft and Wg together, this phenotype was apparent when clones were exposed to pulses of just 30 to 40 minutes.

These results led me to look at the incidence of mitoses in clones deficient for both Fat and Wg. Immuno-fluorescence against phospho-Histone H3 (PH3) to visualise mitotic cells revealed that there is not an obvious increase in the incidence of cell division within the clones; there is no clustering of PH3 positive cells (Figure 4.9B).

However, knowing that *ft, wg* mutant cells undergo ectopic S-phase, and that it is likely that this S-phase would be followed by ectopic mitosis, I wanted to see if there is an overall effect on growth, when compared to loss of Fat alone. To do this, I took advantage of the dose-sensitive expression of the ubiquitin-driven GFP transgene to compare the sizes of mutants clones, which completely lack GFP, with homozygous wild-type tissue, which is bright green. Using Photoshop, I took pixel counts of each tissue type in several discs, then calculated the ratio of mutant to wild-type tissue to quantify the degree of overgrowth associated with each of three genotypes: *ft*, *wg*, and *ft* and *wg*. In this assay, I found that there is a significant increase in the size of clones deficient for Ft and Wg together (Figure 4.9C, Table 4.2). On average, clones deficient for Ft alone are 1.9 times the size of their twinspots (1.88±0.64). Clones deficient for Ft and Wg together are 4.9 times the size of their twinspots (4.93±2.6). The large standard deviation that is apparent in the latter genotype reveals that the sizes of these clones are very variable, but the difference between the two genotypes is statistically significant ($p = 0.00066$). Note that these results cannot be due to a cumulative effect of loss of Ft and Wg together, since loss of Wg alone has no apparent effect on growth (ratio of clone to twinspot = 1.05±0.22).

Table 4.2 Loss of Wingless enhances growth in the absence of Fat

genotype	mean ratio clone : twinspot	standard deviation	P value (against *ft* alone)
wg	1.05	0.22	0.00075
ft	1.88	0.64	N/A
ft,wg	4.93	2.6	0.00066

4.5 Wingless and Hedgehog

I had found that *ft* mutant clones exhibit an accumulation of Wg and of activated Ci anterior to and at the MF, respectively. However, the accumulation of neither molecule alone appeared to be responsible for the delay in entry into the MF that is apparent in *ft* mutant cells. I therefore wondered if accumulation of both signalling molecules together could account for this phenotype.

To test this possibility, I generated clones deficient for Fat, Wingless and Cubitus interruptus together. I found that within these clones, the accumulation of Cyclin E and the incidence of ectopic S phase clearly persist, and do not appear to be any more or less severe than loss of Ft and Wg together (Figure 4.10A,B).

Loss of Wg and Ci in *ft* clones also fails to rescue the ectopic accumulation of Cyclin B posterior to the furrow. Where there are clones that traverse the furrow, it appears that there may be some rescue of the perdurance of Cyclin B seen in *ft* tissue, which would indicate that these cells are able to make a timely transition into G1 arrest (Figure 4.10C). However, this rescue is not consistent: in the BrdU labelled disc shown here there appears to be a perdurance of S-phase in clones that lie ahead of and cross the MF (Figure 4.10A). Unfortunately it is not possible to assess any degree of rescue of the overgrowth phenotype by analysis of clone size: as with the generation of clones deficient for Ft and Ci together, clonal tissue is identified using an antibody against activated Ci, which means homozygous wild-type tissue cannot be distinguish from heterozygous. However, the persistence of cell

cycle markers both ahead of and behind the MF indicate that there is still a failure to execute timely G1 arrest, which is accompanied by ectopic cycling of interommatidial cells.

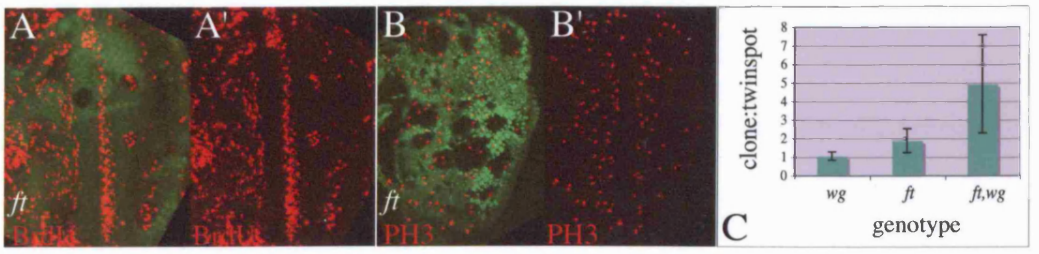

Figure 4.9 Loss of Wingless enhances Fat-related overgrowth. (A) Clones deficient for Ft and Wg, and located after the MF, strongly incorporate BrdU after just 30-40 minutes. (B) There is no obvious increase in the incidence of mitosis in these clones, as visualised by phospho-Histone H3 expression. (C) Clones deficient for Ft and Wg together grow much larger than clones deficient for Ft alone, when compared to wild-type twinspot. Values in the Y-axis are the average ratios of clone size to twinspot size of each of three different genotypes, plus or minus the standard deviation. Difference between *ft* and *wg*, and *ft* and *ft/wg* are statistically significant in a student's T-test.

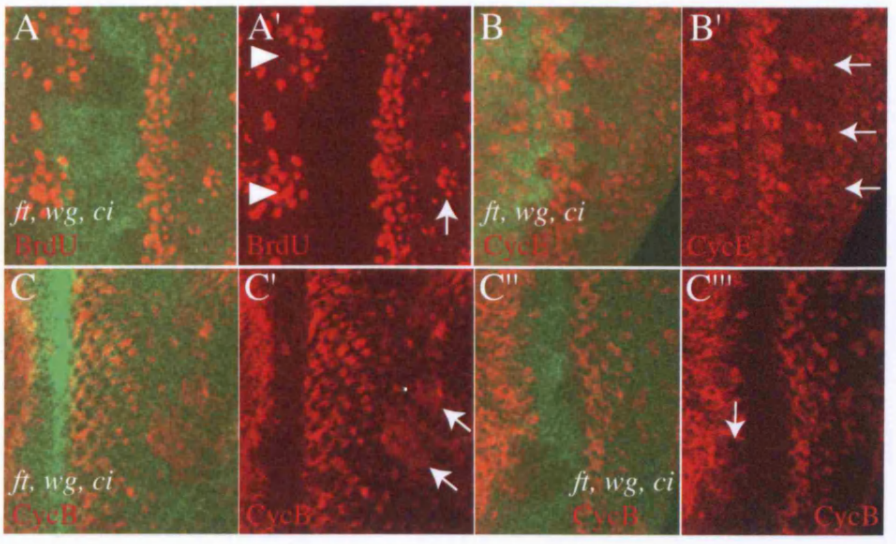

Figure 4.10 Accumulation of Wingless and Ci together is not responsible for Fat-related phenotypes. In all panels, clones deficient for Ft, Wg and Ci together are marked by the lack of Ci*. (A) Clones deficient for Wg, Ci and Ft incorporate ectopic BrdU in a fashion similar to loss of Wg and Ft. Arrow indicates BrdU incorporation in a post-mitotic clone, arrowheads indicate perduring S-phase in the MF. These clones also accumulate Cyclin E (B) and Cyclin B (C, C'), indicated by arrows. There appears to be some rescue of the perdurance of Cyclin B in clones that traverse the MF (arrow), but this rescue is not consistent (C'', C''').

4.6 Discussion and Conclusions

I examined the states of various signalling pathways that are known to be involved in the regulation of MF movement in the hopes of identifying any or all that might be affected in *ft* mutant cells. I had hypothesised that if Ft is required for cells to efficiently recognise or respond to one of these signals, mutant cells would remain in the proliferative state longer, thus producing more cells. While I was able to identify several signalling pathways that are connected to Fat function, including the EGFR, Hedgehog and Wingless pathways, I was unable to attribute the delay in MF progression to any of these effects, and therefore unable to test this hypothesis. Furthermore, where possible I demonstrated that the accumulations of active Ci and of Wingless are not responsible for the *ft*-associated overgrowth; on the contrary, I demonstrated that loss of Wg enhances the overgrowth defect.

4.6.1 EGFR signalling and Fat

Building on data gathered from a yeast-two-hybrid assay performed in the lab, I investigated a role for Ft in receptor tyrosine kinase signalling, specifically EGFR. This interaction seemed particularly intriguing because Ft possesses four extracellular EGF-like domains (Mahoney *et al.*, 1991). I demonstrated that *sty* mutant clones exhibit defects in ommatidial rotation that originate in the third instar imaginal disc and that *sty* genetically interacts with *ft* to enhance its PCP defects. However, I found no detectable disruption to EGFR signalling as visualised by dpERK immuno-fluorescence in the third

instar eye imaginal disc in the absence of Ft. Taken together, these data seemed to indicate that any connection between Ft and EGFR signalling lies principally in Ft's role in PCP.

In support of this conclusion, simultaneous work from three labs demonstrated that EGFR signalling is involved in PCP. The principle finding that triggered this flurry of data was that the PCP gene *roulette* is in fact an allele of *argos* that appears to specifically affect ommatidial rotation. Argos is a secreted inhibitor of EGFR signalling that operates in a negative feedback loop to limit the breadth of signalling (Klein *et al.*, 2004; Wasserman and Freeman, 1998). While all three groups agreed that the primary role for EGFR signalling in PCP lay in ommatidial rotation rather than chirality, the mechanism behind this role is unclear. Strutt and Strutt (2003) found that misregulation in the form of increased EGFR signalling appears to result in transformation of the mystery cells into superfluous neuronal cells, which 'confuses' the PCP complexes into mislocalising. However, they also observe PCP defects in the absence of mystery cell transformation, particularly when EGFR signalling is artificially decreased. Interestingly, these authors confirmed my own observations, noting that loss of Sty results in defects originating in the larval disc. Brown and Freeman (2003) concluded that EGFR signalling is not required for initial polarisation, but is needed to 'lock' the ommatidia in place, possibly via cadherin-mediated cell-cell interactions. Their results suggest that EGFR signalling is required later than is implied by Strutt and Strutt, as well as by own data. However these findings could account for the incidence of PCP defects in the absence of mystery cell transformation. Indeed, Gaengel and Mlodzik (2003) find evidence for the

induction of two distinct sets of effectors of Ras pathway activation in PCP. Similar to Brown and Freeman, they postulate that the role of EGFR signalling lay in cell-cell adhesion and interaction, as well as in cell motility, two phenomena that would logically be required for coordinated physical movement of a cluster of cells. Given that I have shown that *ft* genetically interacts with *sty*, and that the corresponding proteins may also physically interact, it is likely that any connection between Ft and EGFR signalling in PCP would lie predominantly in the earlier of the two mechanisms proposed above. This prediction would fit with Ft's function in directing the polarisation of the core PCP molecules, which results in dorsal-ventral flips rather than rotation defects.

Although I had concluded that any connections between Fat and EGFR signalling most likely lay in PCP, more recent work has found that *ft*-associated overgrowth is exacerbated by induction of the EGFR pathway (Garoia *et al.*, 2005). This same work demonstrated by RT-PCR that loss of Ft results in transcriptional upregulation of *yan* and *myc in vivo*, but confirmed that loss of Ft does not affect signalling as visualised by immuno-fluorescence against dpERK, placing Ft's function in this pathway downstream of MAPK activation.

Yan is a transcriptional repressor of EGFR target genes that is itself repressed in the presence of EGFR signalling (Gabay *et al.*, 1996; Rohrbaugh *et al.*, 2002). Recent work has identified Atrophin (Atro) as a negative regulator of EGFR signalling through genetic cooperation with Yan (Charroux *et al.*, 2006). Interestingly, Atro was identified in the same yeast-two-hybrid assay that recovered Sty. Work by several members of our lab and in

collaboration with others demonstrated that Atro physically interacts with Ft and presented evidence that suggests that Ft's function in the regulation of *four-jointed* and PCP is accomplished through Atro (Fanto *et al.*, 2003). Together this would suggest that Ft's ability to modulate *yan* transcription could be mediated through Atro and that this modulation could account, at least in part, for Ft's effects on both growth and PCP. It is clear that more work will be required to reconcile all aspects of Ft function in EGFR signalling.

4.6.2 Hedgehog signalling and Fat

The data I collected regarding a possible role for Ft in modulating Hedgehog signalling output were very intriguing. I demonstrated that there is an accumulation of full-length 'active' Ci, which I argue is unlikely to be the result of an increase in Hh signalling. First, an upregulation of Hh signalling would be expected to result in acceleration, not deceleration, of the MF, as implied by work demonstrating that ectopic activation of Hh signalling either by removing Ptc or expressing Hh results in ectopic furrows. Second, I demonstrated that *ft* genetically interacts with molecules that have been implicated in the processing and degradation of Ci, implying that Ft's requirement lies here, rather than in signal induction.

The directionality of the genetic interactions described above was particularly interesting. I had expected that the accumulation of Ci^{155} would be enhanced by loss of Dco, since they seem to phenocopy one another in three respects. First, there is accumulation of Ci^{155} that is apparent in both *ft* and *dco* loss of function alleles. Second, *dco* and *ft* mutations both result in hyperplastic overgrowth, which I had initially suspected to result from

hypomorphic conditions: dco^3 is a documented hypomorphic allele (Zilian *et al.*, 1999), and the alleles of ft^{GRV} and ft^{fd} had yet to be molecularly characterised and therefore could have been either complete loss-of-function alleles or strong hypomorphs. Third, our lab had isolated an additional allele of *ft*, ft^{X13}, a deletion mutant that was determined to be missing a large portion of the 5' region, including the promoter; clones of this mutation are severely growth compromised, a phenotype that is common to loss-of-function alleles of *dco*. The strength of the phenocopy was such that I had initially suspected there could be a direct role for Ft in the phosphorylation process that tags Ci for proteolytic cleavage. However, I have since reconsidered this opinion for two reasons. First, I now believe that the deletion in ft^{X13} also affects the neighbouring gene, and that it is the disruption of this gene that compromises the viability of these clones, since I was unable to rescue this phenotype using a transgenic Ft construct. Additionally, ft^{fd} and ft^{GRV} have since been shown to be null alleles (Matakatsu and Blair, 2006), altogether revealing that overgrowth is the true condition resulting from complete loss of Fat. Second, the implication of Dco in growth suppression is based solely on the phenotype arising from the allele dco^3. There are several other alleles of *dco*, none of which result in overgrowth unless they are put in transheterozygous combination with dco^3. All other trans-heterozygous combinations result in growth inhibition. This data suggests that there could be an aberration associated with dco^3 that is not related to its endogenous function.

However, the genetic interaction data is still compelling, and of particular note is that it indicates Ft's *in vivo* function might be in promoting Ci processing, rather than inhibiting it as would be inferred from the clonal data:

loss of Dco suppressed both the clonal phenotype and lethality, and loss of COP9 complex function enhances the phenotype. Dco is responsible for a subset of the phosphorylations that tag Ci^{155} for proteolytic cleavage. Tagged Ci^{155} is then processed by the Cullins, whose functions require a post-translational modification referred to as neddylation, whereby it is tagged with a Nedd8 group. The COP9 signalosome regulates Cullin function by deneddylation, which renders it inactive. Interestingly, Casein Kinase I has also been implicated in positive regulation of Hh signalling: activation of Smoothened, the Hh signalling effector, requires PKA– and CKI–dependent phosphorylation (Apionishev *et al.*, 2005; Jia *et al.*, 2004; Zhang *et al.*, 2004). Also contrary to its established function, the COP9 signalosome is capable of attenuating, as well as stimulating, Hh signalling: the neddylated Cullins are unstable, leading to the conclusion that the COP9 signalosome does not simply function in the negative regulation of the Cullins by deneddylation, but promotes E3 ligase activity through its role in recycling the Cullins for further activity (Wu *et al.*, 2005). Thus these genetic interactions may not be as contradictory as they first appeared: by removing Dco, I am limiting the activity of Smo as well as the ability of Ci to be proteolytically cleaved; by impairing CSN5 function, and thereby COP9 signalosome function, I am impairing the recycling of the Cullins, as well as promoting their activation.

Interestingly, recent studies in the wing have shown that Dco is necessary for phosphorylation of Dishevelled, one of the core PCP molecules. In the absence of Dco-mediated phosphorylation, Dsh fails to localise appropriately resulting in mis-orientation of the bristles (Strutt *et al.*, 2006), implicating Dco as a regulator of PCP.

I made numerous attempts clarify the nature of these genetic interactions by biochemical means. I have attempted western blot analysis of Cullin 1 and Cullin 3, the two Cullins that have been implicated in Ci processing in the eye imaginal disc, to see if there is any compromise in the neddylation state in the absence of Fat, but I was not able to reproduce published data that demonstrated neddylation of the Cullins in a wild-type background.

I have also looked more closely at Ci subcellular localisation in Ft deficient clones. Ci must be sequestered in the cytoplasm for proteolytic cleavage to take place (Aza-Blanc *et al.*, 1997; Monnier *et al.*, 1998; Robbins *et al.*, 1997). In the absence of sequestration, Ci^{155} moves to the nucleus where it is protected from cleavage and therefore accumulates. This accumulation in the absence of sequestration can be artificially enhanced by treatment with leptomycin-B (LMB), a Streptomyces metabolite that impairs nuclear export (Wolff *et al.*, 1997). Thus, if Ft affects Ci processing through an involvement in sequestration, I expected that in tissue treated with LMB, I would see an enhancement of Ci^{155} accumulation in the nuclei of Ft deficient cells compared to wild-type. However, I found no difference between *ft* and wild-type tissue.

Regardless of the mechanism behind the accumulation of full-length Ci, the question I was most interested in was whether this accumulation could be responsible for the delay in MF progression that I see in the absence of Ft. I believe I have conclusively demonstrated that it cannot be the culprit. In the absence of Ci altogether, including any accumulated full-length Ci arising from the loss of Ft, there is no modulation of any of several phenotypes tested, including disrupted furrow dynamics, adhesion defects and ectopic cell cycling in the posterior disc. Thus accumulated Ci^{155} is not the causative factor in the

generation of *ft*-associated phenotypes. However, it is important to note that I have not addressed the possibility of a role for Ci^{75} in the manifestation of these phenotypes.

4.6.3 Wingless signalling and Fat

The observation that there is an accumulation of Wg protein in Ft clones in the eye was not particularly surprising, since previous data had already revealed the existence of this phenotype in the wing (Cho and Irvine, 2004). However, I have found a key difference in the nature of this accumulation. In the wing, elevated Wg is limited to the proximal wing where there is also endogenous expression; in the eye the accumulation of Wg is entirely ectopic. This data suggests Wg is accumulating by two different mechanisms in each of the two different systems. This difference is substantiated by data demonstrating that in the eye, unlike in the wing, there is no accompanying accumulation of Armadillo (Jaiswal *et al.*, 2006), suggesting that accumulated Wg in *ft* clones in the eye is not inducing canonical Wingless signalling, at least not to the same extent as in the wing. There is precedent for distinct modes of regulation of Wingless signalling, even in a single tissue: a positive auto-regulatory loop is used in the distal, but not proximal, wing (Rodriguez *et al.*, 2002).

Since Wg is a known antagonist of MF progression, accumulated Wg in clones ahead of the furrow would be a natural suspect as the source of delays in MF progression seen in Fat-deficient clones. However, my genetic experiments seem to indicate that ectopic Wg is not the culprit.

Wingless is, in many contexts, an oncogene: activation of Wg signalling has been implicated in number of tumour types, and can directly result in tumour formation in mice (reviewed in Akiyama (2000); Nusse (1990)). Thus I would have predicted that even if the delay in furrow progression is not rescued in *ft,wg* loss of function tissue, then perhaps overgrowth would be. This prediction was also made by Cho and Irvine (2004), who were the first to publish the finding that Wg accumulates in *ft* clones. Since they had observed an accumulation of Wg only in the proximal wing, they reasoned that it is over-proliferation caused by Wg signalling that is responsible for the broadening of the proximal adult wing that is apparent in *ft* hypomorphs. In support of this hypothesis, disproportionate overgrowth of the proximal wing in Ft-deficient discs is rescued by a reduction in Wg expression (Cho and Irvine, 2004). However, overall wing size appears to be unaffected.

The role for Fat in the repression of Wg signalling was emphasised by later work that demonstrated that loss of Fat results in modulation of Wg signalling targets and their associated phenotypes even when there is no apparent accumulation of Wg itself (Jaiswal *et al.*, 2006). These authors placed Ft function downstream of Wg, and in parallel to or upstream of the Wnt receptors Frizzled and Frizzled2. Furthermore, Dachsous, an antagonist of and the only known ligand for Fat, has been implicated in Wg-dependent pattern formation in the wing (Rodriguez, 2004). These observations led to the conclusion that there are moderate increases in Wg signalling wherever there is loss of Fat, and the speculation that since moderate increases in Wg signalling lead to overgrowth, repression of Wg signalling might be the mechanism underlying Ft-related growth suppression.

However, more recent work found that Ft-dependent overgrowth does not necessarily correlate with changes to Wg transcription or signalling. Matakatsu and Blair (2006) found that in Ft deficient clones there is no change to the levels of Vestigal and Distalless, two molecules that are expressed in response to low and moderate levels of Wg signalling, respectively. Furthermore, the expression of a truncated Fat transgene that acts as a dominant negative allele with respect to growth suppression does not affect the expression of any of Dll, Vg or Wg.

The nature of the accumulation of Wg in the eye provided an altogether new way for testing the effect of Wg signalling in *ft* clones. Here I could remove ectopic Wg without affecting endogenous signalling and see if there is any rescue of *ft*-dependent overgrowth. However, this method had other caveats: Jaiswal *et al.* (2006) had demonstrated that Ft represses Wg signalling downstream of the ligand. If there was no modulation to the overgrowth phenotype in *ft/wg* double mutants, I could not eliminate the possibility that ectopic Wg signalling is still active and resulting in overgrowth even though I was removing Wg itself. In fact, the existence of ectopic Wg signalling despite the absence of Wg itself could explain why there is no rescue of the furrow-delay phenotype in *ft/wg* double mutant clones.

Surprisingly, loss of Wg in conjunction with Ft exacerbated the phenotype, which was particularly apparent in clones in the posterior where there was a dramatic increase in BrdU-labelled cells. I have already shown that cells lacking Ft are cycling ectopically after the furrow, but in the absence of Wg this cycling seems to take place faster or in more cells (or both); visualisation of ectopic S phase did not require the used of a long-lived GFP

expressed from the PCNA promoter, nor did it require an extended pulse of BrdU incorporation.

This result is surprising for two reasons. First, as mentioned, Wg signalling normally functions to promote growth, rather than inhibit it. However, Wg has been shown to function in growth suppression in some contexts: more specifically, it is required for growth arrest at the dorsal-ventral boundary of the wing disc (Johnston and Edgar, 1998). Second, there is no documented expression of Wg posterior to the furrow; its classic pattern of expression is restricted, in the eye disc, to the antero-distal margins where it represses furrow movement. Thus I did not expect to see any phenotype associated with clones situated in the posterior, with the possible exception of rescue of *ft* phenotype resulting from undetected Wg accumulation.

The characteristic that was most intriguing about this phenotype was the pattern of incorporation in these clones: BrdU incorporation appears to be restricted to a narrow band in the disc, approximately two to three ommatidial rows posterior to the MF. While I have not gathered sufficient data to speculate on the mechanism behind Wg's ability to suppress Ft-related overgrowth, this striking phenotype will be discussed in more detail in the next chapter.

5 CHAPTER 5: OVERGROWTH OF *FAT* CLONES CAN BE ATTRIBUTED TO ITS FUNCTION IN THE HIPPO SIGNALLING PATHWAY

Many of the phenotypes I have described are reminiscent of those seen in flies mutant for either of the tumour suppressor genes *hippo* (*hpo*) or *salvador* (*sav*). For example, clones mutant for either *hpo* or *sav* exhibit transcriptionally elevated levels of Cyclin E and Diap1 (Harvey *et al.*, 2003; Kango-Singh *et al.*, 2002; Pantalacci *et al.*, 2003; Tapon *et al.*, 2002; Udan *et al.*, 2003; Wu *et al.*, 2003), which lead to continued proliferation and inhibition of apoptosis resulting in an excess of interommatidial cells (Harvey *et al.*, 2003; Kango-Singh *et al.*, 2002; Tapon *et al.*, 2002; Udan *et al.*, 2003; Wu *et al.*, 2003). They also have large, round clones as well as cell cycle profiles indistinguishable from neighbouring wild-type cells(Harvey *et al.*, 2003; Kango-Singh *et al.*, 2002; Tapon *et al.*, 2002). One further phenotype that *ft* shares with *hpo* and *sav*, which is more readily apparent when *ft* mutant clones are induced in the absence of Wingless, is the incidence of a "third mitotic wave", visible as a band of BrdU incorporating cells posterior to the second mitotic wave (Harvey *et al.*, 2003; Kango-Singh *et al.*, 2002; Pantalacci *et al.*, 2003; Tapon *et al.*, 2002; Udan *et al.*, 2003; Wu *et al.*, 2003).

Hippo and Salvador are the founding members of a conserved pathway that functions to both promote apoptosis and inhibit proliferation. Hpo is a Ste-20 kinase with high homology to mammalian sterile twenty kinase (Mst1) (Harvey *et al.*, 2003; Pantalacci *et al.*, 2003; Wu *et al.*, 2003) and Sav is a

WW-domain protein (Kango-Singh *et al.*, 2002; Tapon *et al.*, 2002). In the current model, Hpo binds to and phosphorylates Sav, which in turn brings Warts (Wts), a protein kinase of the NDR family, in proximity to Hpo. Hpo can then phosphorylate and activate Wts (Harvey *et al.*, 2003; Udan *et al.*, 2003; Wu *et al.*, 2003). Warts, in the presence of mobs as tumour suppressor (MATS), its activating subunit, can then bind and inhibit the transcriptional coactivator, Yorkie (Yki) (Huang *et al.*, 2005; Lai *et al.*, 2005). In the absence of this inhibitory phosphorylation, Yki is responsible for transcription of *cyclin E* and *diap1*; normal expression of Diap1, in particular, requires Yki function (Huang *et al.*, 2005).

Despite the wealth of biochemical data available from detailed analysis of this emerging pathway, little is known about the input mechanism for its stimulation. However, a recent paper has brought things one step closer. Merlin (Mer) and Expanded (Ex) are members of the protein 4.1 superfamily (Boedigheimer *et al.*, 1993; Boedigheimer and Laughon, 1993; Rouleau *et al.*, 1993). These two molecules physically interact at apical membranes (Boedigheimer *et al.*, 1997; McCartney and Fehon, 1996) and, individually, have relatively mild effects on growth and apoptosis (Blaumueller and Mlodzik, 2000; Boedigheimer *et al.*, 1997; LaJeunesse *et al.*, 1998). Interestingly, coincidental removal of both together results in phenotypes that fully recapitulate those of mutations in *hippo* or *salvador* (Hamaratoglu *et al.*, 2006; McCartney *et al.*, 2000). In both genetic and biochemical assays they can be placed, together, upstream of all known components of the Hippo pathway (Hamaratoglu *et al.*, 2006). However, while both of these molecules are found at the membrane, neither traverses it, implying that there are yet to

be identified molecules that receive the extracellular cues that regulate this pathway (Edgar, 2006). In this chapter I present evidence that implicates Ft as a possible candidate for this role.

5.1 Further similarities between mutations in *fat* and members of the Hippo pathway

I wanted to see if there are further phenotypic similarities between mutations in *ft* and mutations in components of the Hippo pathway. I have already demonstrated that *ft* mutant cells, as with *hpo* and *sav* mutant cells, accumulate Cyclin E and Diap1. I wanted to know if this accumulation is due to transcriptional upregulation, since decreased Hippo signalling leads to a derepression of Yki, which acts a transcriptional coactivator for the expression of these molecules. To test for transcriptional upregulation of *diap1*, I used an allele of *diap1* containing an enhancer trap element that results in beta-galactosidase (β-Gal) expression in a *diap1*-specific pattern. When I induced *ft* mutant clones in this background and performed immuno-fluorescence against the β-Gal molecule, I confirmed that the accumulation of Diap1 protein originates at transcription (Figure 5.1A). I wanted to perform an analogous experiment to look at *cyclin E* transcription. However, while an enhancer-trap allele of *cyclin E* does exist, both it and *ft* are on the left arm of chromosome two. As a consequence, the induction of site-specific recombination of chromosome 2L would result in clones of both *ft* and the *cyclin E* enhancer trap; the wild-type tissue would lack β-Gal expression and thus could not be compared to the mutant tissue. To overcome this problem, I used a transgenic

line expressing β-Gal from a 16.4kb region of the *Cyclin E* promoter. This 16.4kb region has previously been demonstrated to recapitulate all endogenous Cyclin E expression in the embryo (Jones *et al.*, 2000). In the eye its expression is very weak: in domains of endogenous Cyclin E expression, β-Gal is barely detectable. However this transgene can and has been used to identify contexts in which the endogenous locus is likely to upregulated (Hamaratoglu *et al.*, 2006). When I generate *ft* clones in the presence of this transgene, I see an upregulation of β-Gal expression in the clones, suggesting that the accumulation of Cyclin E, as with Diap1, originates at transcription (Figure 5.1B)

I have presented data demonstrating that *ft* phenocopies nearly all cell biological and genetic characteristics that have previously been documented for Hippo pathway components. I next wanted to see if there were any *ft* phenotypes that exist, but have been hitherto unknown, in Hippo pathway mutants. For example, do mutations in either of *hpo* or *ex* affect the expression of Cyclins A and B? If they do, it would be further evidence of a role for Fat in this pathway. To answer this question, I looked at the expression patterns of each of these two cyclins in clones deficient for Hpo or Ex. I found that a compromise in the function of either of these two molecules results in a strong derepression of both Cyclins A and B after the furrow, and that this derepression is particularly evident in interommatidial cells (Figure 5.1C-E). In clones that are deficient for *hpo* there is also a consistent perdurance of Cyclin A in cells that should have arrested in G1 for entry into the MF (Figure 5.1C, arrowheads). Clones deficient for *ex* also show a perdurance of both

Cyclins A and B, but to a lesser degree than either *ft* or *hpo* mutant tissue (Figure 5.1D,E).

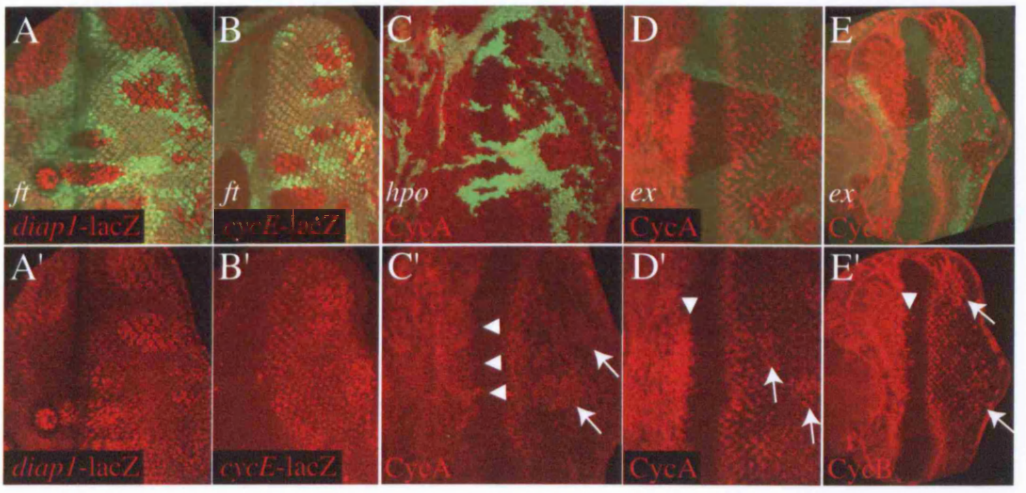

Figure 5.1 Phenotypes arising from mutations in *fat* resemble those of mutations in Hippo pathway components. (A) Ft-deficient clones generated in a background expressing β-Gal from the endogenous *diap1* promoter. (B) Ft-deficient clones generated in a background expressing β-Gal from a transgene carrying a 16.4kb region of the *cyclin E* promoter. (C) Hippo-deficient clones accumulate Cyclin A expression after the MF (arrows) and show some perdurance of Cyclin A into the MF (arrowheads). Ex- deficient clones accumulate Cyclin A (D) and Cyclin B (E), both in clones after the MF (arrows) and, more mildly, in clones that traverse the MF (arrowheads).

5.2 *fat* genetically interacts with members of the Hippo pathway

Next I looked for genetic interaction between *ft* and members of the Hippo pathway. In the first experiment I took advantage of the viability of the hypomorphic allele ft^{1}. I had previously used this allele in transheterozygous combination with ft^{fd} to demonstrate genetic interaction with *discs overgrown*. In this assay I put ft^{1} in combination with the null allele, ft^{GRV}, in either a wild-type or *ex* heterozygous background. In an *ex* haploinsufficient background, there is a small but statistically significant decrease in the viability of ft^{1} transheterozygotes (Figure 5.2A): in a wild-type background, 31.6% of the progeny are ft^{1} transheterozygotes compared with 27.0% in an ex^{e1} heterozygous background. In a student's T-test these results yielded a P value of 0.0031 (Table 5.1).

Table 5.1 *fat* genetically interacts with *expanded*

allele of *ex*	mean proportion	standard deviation	p value (t test)
wt	0.316	0.037	0.0031
e1	0.270	0.029	

While dominant enhancement of a phenotype is an excellent indication of a genetic interaction, I wanted to see if I could suppress any of the *ft* phenotypes through similar means. Yki is the only member of the pathway

known to act as an inhibitor of apoptosis and promoter of proliferation, and previous work has shown that *yki* interacts with other members of the pathway in a dose sensitive manner (Huang *et al.*, 2005). In this instance I wanted to test for genetic interaction in the context of growth. To do so, I made *ft* mutant clones that are induced by expressing FLP from the *eyeless* promoter. The expression of *eyeless* begins in the embryonic eye primordium and can be detected not only in the eye but also in the optic lobes as well as in the brain and ventral nerve cord (Quiring *et al.*, 1994), ultimately resulting in a broad domain of clonal tissue and phenotypes that are much more severe than those observed in the presence of *hs*-Flp mediated clones. The result is adult heads that are generally much larger than wild-type and frequently exhibit large cuticular overgrowths around the antennae (Figure 5.2D, compare to C). When I induced these clones in a *yki* heterozygous background, the resulting heads were smaller and the cuticular overgrowths were reduced (Figure 5.2E, compare to D). Thus, reductions in the level of Yki suppress *ft*-related overgrowth.

In order to quantitate suppression of the overgrowth phenotype, I again generated ft mutant clones in a background that is either wild-type or heterozygous for *yki* but used Ubi-GFP as a marker and analysed the resulting clones in the third larval instar. As in the analysis of the effect of Wg on *ft* mutant clones, I took pixel counts using Photoshop, then calculated the ratio of mutant tissue to wild-type twinspot and compared the two genotypes. To ensure that the measurements were accurate, I took two counts of each sample then took the average of those measurements. In this assay, I found that *fat* mutant clones in a wild-type background are 1.6 times larger than those in a *yki*

heterozygous background (Figure 5.2B). A student's T-test yields a P-value of 0.0036 (Table 5.2), indicating the difference is statistically significant.

Table 5.2 *fat* genetically interacts with *yorkie*

allele of *yki*	mean ratio	standard deviation	p value (t test)
wt	1.88	0.64	0.0036
B5	1.21	0.31	

The final phenotype for which I tested *yki* suppression was in the ectopic expression of Cyclin E that is visible in *ft* clones. Once again I generated clones of *ft* mutant tissue in a background that is heterozygous for *yki*. In these discs I frequently found no detectable expression of ectopic Cyclin E (Figure 5.2F).

These genetic interactions, in the form of both suppression and enhancement, provide evidence for a role for Fat in the Hippo pathway.

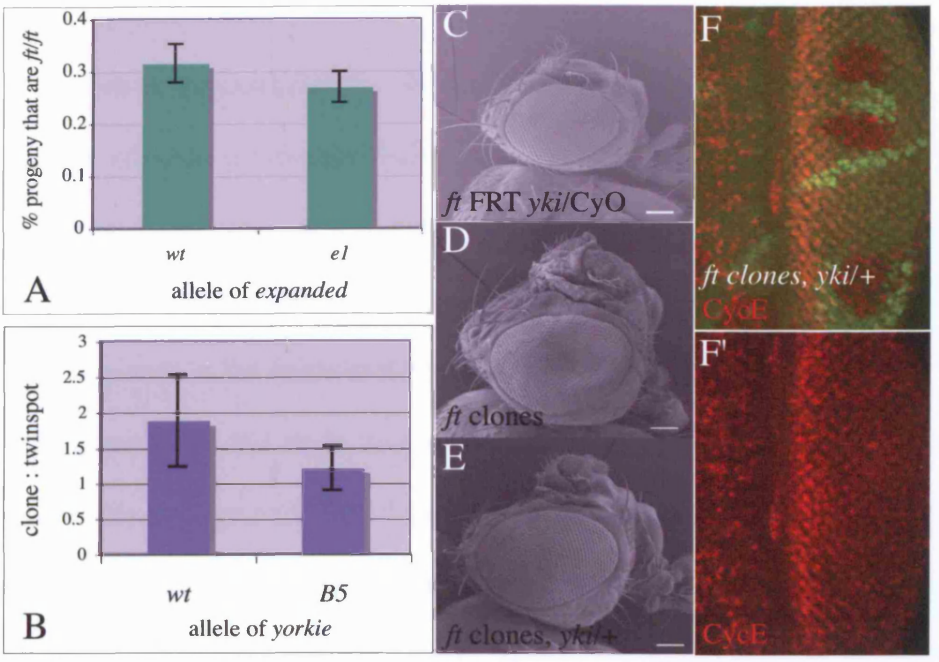

Figure 5.2 *fat* genetically interacts with members of the Hippo pathway. Haploinsufficiency of *ex* enhances the lethality of ft^{l}/ft^{grv} transheterozygotes. *ft* progeny are expressed as a percentage of the total progeny in each of two separate crossing schemes, one with a wild-type and the other with a heterozygous *ex* background; shown here is the average calculated from several crosses of each scheme, plus or minus the standard deviation. (B) Haploinsufficiency of *yki* suppresses the overgrowth of *ft* mutant clones. Clones deficient for Ft in background that is haploinsufficient for *yki* overgrow less than clones deficient for Ft alone, when compared to wild-type twinspot. Values in the Y-axis are the average ratios of clone size to twinspot size of each of two different genotypes, plus or minus the standard deviation. Scanning electron micrographs of heads that are (C) heterozygous for *ft* and *yki*, which is generally of wild-type size, (D) carrying *ey*-FLP induced clones that are deficient for Ft, and (E) carrying *ey*-FLP induced clones that are deficient for Ft in a background that is heterozygous for *yki*. Bar = 100um. (F) Ft-deficient clones generated in a *yki* haploinsufficient background do not accumulate ectopic Cyclin E.

5.3 Fat functions with Expanded in parallel to Merlin

5.3.1 *fat* mutant clones have excess interommatidial cells in the pupal retina

One of the characteristic phenotypes of Hippo pathway mutants is a specific effect in interommatidial cells: the ectopic expression of cell cycle promoters in the larva, as well as the inhibition of apoptosis in the pupa, results in an extraordinary number of supporting cells in the adult eye. This effect is most apparent in the retina as it exists at approximately 45% pupal development. At this stage, all growth and cell death is complete and ommatidia are organized into their final, hexagonal array (Cagan and Ready, 1989). In each wild-type ommatidium there are 11 supporting cells, all of which are visible in a distal or "apical" section through the retina. In the centre are four cone cells, surrounded by two primary pigment cells, which are in turn surrounded by six secondary pigment cells, three tertiary pigment cells and three bristle cells; the secondary and tertiary pigment cells and the bristle cells are shared with neighbouring ommatidia (Figure 5.3A,B). Inhibition of apoptosis by over-expression of the baculovirus apoptotic inhibitor p35 results in the accumulation of excess cells, mainly secondary and tertiary pigment cells (Figure 5.3C). Here, p35 is over-expressed using the eye-specific driver GMR: a transgenic reporter carrying a multimer of Glass protein binding domains, which drives strong ectopic expression in all cells posterior to the MF (Hay *et al.*, 1997).

In *hpo* or *sav* mutant ommatidia there are often normal numbers of cone cells and primary pigment cells but three to four times the number of bristle

cells, as well as secondary and tertiary pigment cells (Harvey *et al.*, 2003; Pantalacci *et al.*, 2003; Tapon *et al.*, 2002; Wu *et al.*, 2003).

Scanning electron micrographs of eyes containing large *ft* mutant clones had already revealed the existence of duplicated bristles, and detection of Elav expression in third instar larval discs revealed increased interommatidial spacing. I reasoned that if mutations in *fat* do, indeed, result in supernumerary supporting cells, this phenotype could be used to quantitatively analyse the *ft* mutant phenotype, allowing for comparison with other Hippo pathway mutants and, through epistasis, possible insights into Ft's position within the pathway.

I looked at *ft* mutant clones in retinas at 45% pupal development, visualised by immuno-fluorescence against Armadillo (Arm). I found that *ft* mutant ommatidia, on average, have just over nine secondary cells (9.35 ± 1.14; measured by H. McNeill) (Figure 5.3D,H). While this phenotype appears to be far weaker than that of *hpo* mutant ommatidia, it is very comparable to that of ommatidia lacking *ex* expression (8.08 ± 0.24; measured by H. McNeill) (Figure 5.3E,H); they also frequently have duplicated bristles, a phenotype that I had observed in the adult (Figure 5.3D, inset). Ommitidia lacking *mer* expression exhibit an even milder phenotype (Figure 5.3F).

5.3.2 Fat acts in conjunction with Expanded and redundantly to Merlin

Recent studies, as mentioned above, had implicated Expanded and Merlin as the most upstream components of the Hippo pathway identified to date. These studies also revealed that they work somewhat redundantly: each alone has a mild phenotype, but *mer/ex* double mutants greatly resemble

mutations in either *hpo* or *sav* (Hamaratoglu *et al.*, 2006). With this data in mind, I then asked whether Ft could be acting redundantly with either Mer or Ex. I began by inducing clones that were doubly mutant for *ex* and *ft*. In retinas at 45% pupal development, I found that ommatidia lacking both Ft and Ex have, on average, 9.55 ± 1.67 secondary cells (measured by H. McNeill) (Figure 5.3G,H). This figure does not differ significantly from that of ommatidia deficient for Ft alone (Table 5.3). Next I generated clones that were deficient for both *mer* and *ft*. In these retinas, I found that there is a dramatic increase in the number of interommatidial cells (Figure 5.3I). This phenotype is much more comparable to mutations in *hpo* or *sav*, and is of sufficient severity that it is not possible to define secondary and tertiary cells nor, therefore, to quantify the phenotype.

Table 5.3 Loss of Fat is indistinguishable from loss of Fat and Expanded together

genotype	average number secondary cells	standard deviation	p value (t test)
wt	6.04	0.20	
ft	9.35	1.1	0.66
ex	8.08	1.2	0.0022
ft,ex	9.55	1.7	

This data suggests that Fat acts in parallel to Mer, in conjunction with Ex: the phenotypes of the *mer/ft* double mutants are similar to those of *mer/ex* double mutants and the phenotypes of *ex/ft* double mutants are indistinguishable from those of *ft* mutants. If Ft acts in the pathway in a manner that is linear to Ex, then loss of both will have no further effect on

other phenotypes than the loss of each molecule alone. I looked at the upregulation of Cyclin E and Diap1 in clones deficient for each of Ex, and Ex and Ft together, and compared them to the upregulation seen in clones deficient for Ft alone (Figure 5.4, compare A and C to B and D). These results confirm that there is comparable upregulation in all three genotypes. While this data is not quantitative, it further supports the above hypothesis that Ft and Ex function together in the pathway.

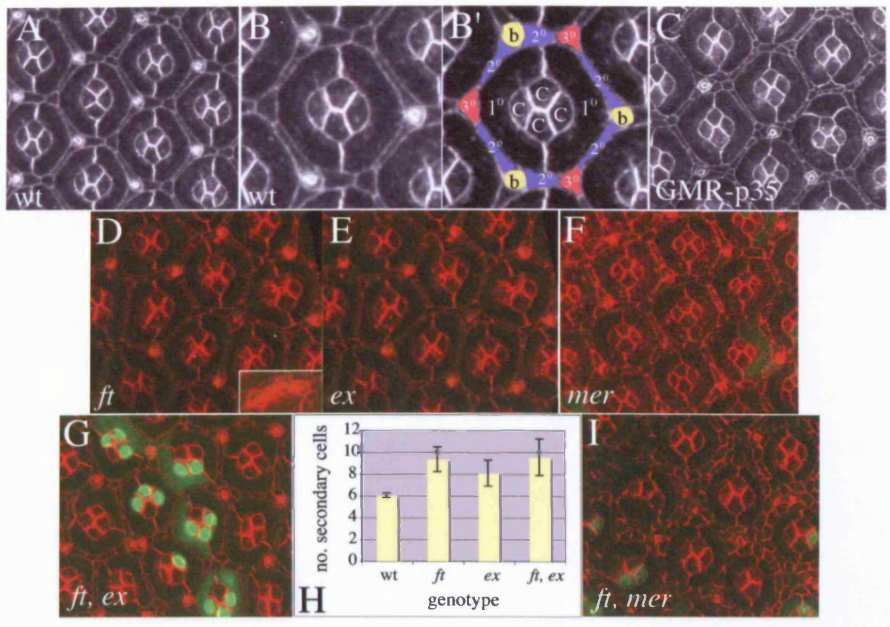

Figure 5.3 Fat functions with Expanded in parallel to Merlin. Confocal images are of retinas at 45% pupal development labelled with Armadillo to reveal cell outlines. (A) Crystalline arrangement of wild-type pupal retina. (B, B') Enlargement of a single, wild-type ommatidium reveals four cone cells (labelled C), two primary pigment cells (1°), six secondary pigment cells (blue, 2°), three tertiary pigment cells (pink, 3°) and three bristle cells (yellow, b). (C) Inhibition of apoptosis by expression of p35 results in excess cells, primarily secondary and tertiary pigment cells. (D) Loss of Ft results in excess interommatidial cells; often there are duplicated bristle cells (inset). Loss of Ex (E) or Mer (F) results in a excess interommatidial cells. (G) Loss of Ex and Ft together resemble loss of either alone. (H) Loss of Ex and Ft together results in a phenotype statistically indistinguishable from loss of Ft alone. On the Y-axis is the average number of secondary cells for each of four genotypes, plus or minus the standard deviation. (I) Loss of Ft and Mer together result in a dramatic increase in the number of interommatidial cells.

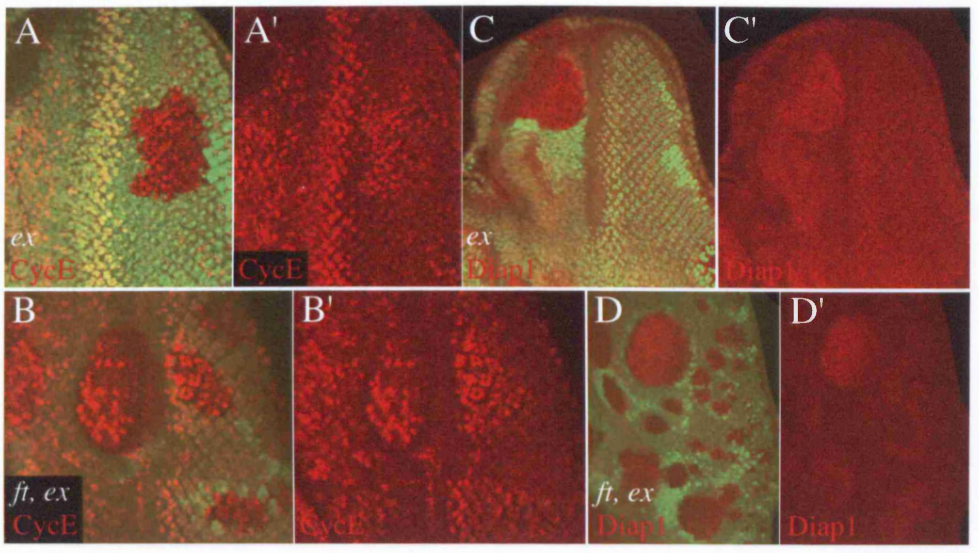

Figure 5.4 Loss of Fat and Expanded together resembles loss of Expanded alone. Clones deficient for Ex accumulate Cyclin E (A) and Diap1 (C) to similar extents as loss of Ft and Ex together (compare to B and D).

5.4 Fat is required for localisation and function of Expanded in Hippo signalling

5.4.1 Fat is necessary for Expanded localisation

With the hypothesis that Ft and Ex function together upstream of Hpo, I began to look at the effect of loss of Ft on Ex expression and function. Both Ft and Ex are known to localize to the apical membrane (Boedigheimer and Laughon, 1993; Ma *et al.*, 2003). This presents an attractive model in which Ft, as a transmembrane protein, recruits and possibly activates Ex at the membrane. Co-immunofluorescence confirms that these two molecules co-localise at the level of confocal analysis (Figure 5.5A,B); this co-localisation is apparent in the apical/basal axis where both molecules exist above the adherens junctions, marked here by expression of Armadillo/β-catenin (Figure 5.5C).

To see if Ex localization requires Ft function, I looked at the pattern of Ex protein in clones deficient for *ft*. In these clones, I find that there is strong reduction in the levels of Ex protein. Images of these clones taken in cross-section confirm the loss of Ex at the apical membrane (Figure 5.5D). This loss is post-transcriptional, since fluorescent *in situ* hybridisation using a ribo-probe directed against the *ex* transcript reveals there is no change in *ex* gene expression (Figure 5.5E).

The above data implies that in the absence of Ft, there is a loss of either stability or localisation of Expanded protein. To distinguish between these two possibilities, a technician in the lab, Yonit Tsatkis, kindly performed a western blot against Ex on protein extracted from each of wild-type and *ft* mutant

imaginal discs. In this assay there was no detectable reduction in the overall levels of Ex in the absence of Ft (Figure 5.5F). This data led me to conclude that Ex localisation, but not stability, is compromised in the absence of Ft.

5.4.2 Expanded is not necessary for Fat localisation

Next I checked to see if Fat protein localisation or stability is affected in the absence of Ex. In clones deficient for Ex, there is no detectable change in the levels of Ft (Figure 5.5G). Thus Ex localisation requires Ft function, but Ft localisation does not require Ex function.

5.4.3 Fat's requirement for Ex localisation is specific to Ex

While the above data is compelling, it does not preclude the possibility that Ft is required for general membrane integrity or morphology. As a protocadherin whose loss results in adhesion defects, it is possible that the loss of Ex is indicative of an overall disruption to junctional complexes or the general stability of membrane-localised proteins. I did not believe this scenario to be likely, since I had already demonstrated that there is no change in the expression patterns of Armadillo, a component of apical junctions, or Patched, a membrane localised receptor, in the absence of Ft. In addition, previous work had demonstrated that apico-lateral junctions are not affected by loss of Fat (Woods *et al.*, 1997). However, to test the specificity of the Ex's requirement for Ft function, I performed immuno-fluorescence against each of Hippo, Merlin and Moesin (Moe) in the absence of Ft. Moe and Mer, like Ex, are both FERM domain proteins, and Moe has been identified through yeast-

two-hybrid assays as a putative binding partner to Ft (Formstecher *et al.*, 2005). These experiments reveal that there is no detectable change in the localisation or expression of any of these molecules (Figure 5.5H-J). Finally, I tested to see if the effect in Ex could be a general one elicited by the loss of any tumour suppressor. To do this, I generated clones deficient for Tuberous Sclerosis 1 (Tsc1) and looked at the localisation of Ex. There was no detectable change in the distribution of Ex protein in these clones (Figure 5.5K). All of these data together imply that the requirement for Ft function is specific to Ex.

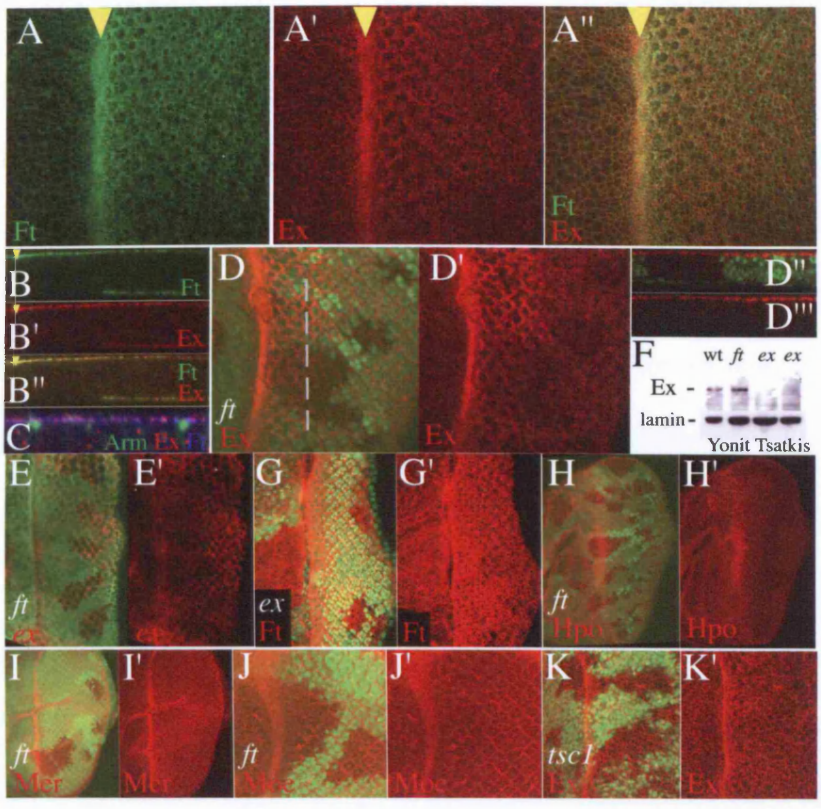

Figure 5.5 Fat is specifically required for localisation of Expanded at the apical membrane. Ex and Ft co-localise (A-C). (A) Expression patterns of Ft and Ex in wild-type discs; (B) co-localisation is also apparent in Z section: there is some Ex visible in the cytoplasm that does not co-localise with Ft, but the majority of Ft and Ex is at the apical membrane (C, compare to localisation of Armadillo; concentrated foci of Armadillo expression correspond to ommatidal preclusters). Yellow arrowheads indicate the positions of the MF, where the pattern of expression is at its most intense. Loss of Ft results in loss of Ex at the membrane (D-F). (D) Loss of Ft results in a dramatic reduction of Ex at the apical membrane; the Z section shown here (D", D"') is taken at the position of the dashed line in D. The loss of Ex resulting from loss of Ft is posttranscriptional and is due to loss of localisation rather than protein stability (E, F). (E) Fluorescent *in situ* hybridisation against the *ex* transcript in Ft-deficient clones. (F) Western blot of total protein from eye imaginal discs from wt, *ft* and *ex* larvae, and wing discs from *ex* larvae: Ex protein is lost in *ex* mutants, but not in *ft* mutants; loading was controlled by detection of Lamin. (G) Loss of Ex does not affect the levels of Ft. Loss of Ft does not affect the levels of Hpo (H), Mer (I) or Moe (J). Loss of Tsc1 does not affect the levels of Ex (K).

5.4.4 Apical localisation of Expanded is necessary for its function

The data I have presented regarding the phenotypes in the pupal retina suggest that either Ft requires Ex function or Ex requires Ft function, since the loss of *ft* and *mer* together phenocopies the loss of *ex* and *mer* together. I have further demonstrated that the localisation of Ex at the apical membrane specifically requires Ft function, however Ex is not needed for Ft localisation. Taken together, I hypothesised that Ft is needed for Ex localisation and that this localisation is needed for Ex function. To test this hypothesis, I generated clones that are simultaneously deficient for *ft* and over-expressing Ex, using mosaic analysis with a repressible marker (MARCM) (Lee and Luo, 2001). This technique combines Flp/Frt site-specific recombination with the Gal4/UAS expression system, as well as repression of UAS-mediated expression by Gal80. The result is the induction of mutant clones with simultaneous repression of the expression of the transgene in all heterozygous and wild-type tissue.

Over-expression of Ex has previously been shown to induce apoptosis (Blaumueller and Mlodzik, 2000; Hamaratoglu *et al.*, 2006), which can be visualised by immuno-fluorescence against activated Caspase (Figure 5.6A). When this over-expression is induced in the absence of *ft*, there is no increase in the incidence of apoptotic cells (Figure 5.6C). Similarly, the over-expression of Ex is not able to rescue the ectopic upregulation of Cyclin E that is apparent in the absence of *ft* (Figure 5.6B).

It is possible that the inability of Ex to induce apoptosis in the absence of Fat is the result of increased levels of Diap1, which could lead to a general

reduction of apoptosis that is not necessarily specific to Ex function. In order to see if there is a general reduction in apoptosis in the absence of Ft, I performed a similar experiment, this time inducing apoptosis by over-expressing Hpo. In this instance, I used the eye-specific driver, GMR, to over-express Hpo after the MF. In clones deficient for Ft there is no compromise to the ability of Hpo to induce apoptosis as visualised by immuno-fluorescence against Caspase 3 (Figure 5.6D). These results suggest that Ft is specifically required for Ex function, as well as provide evidence that any function for Ft in the Hippo signalling pathway would be upstream of Hpo, and thus Sav, Wts, Mats and Yki.

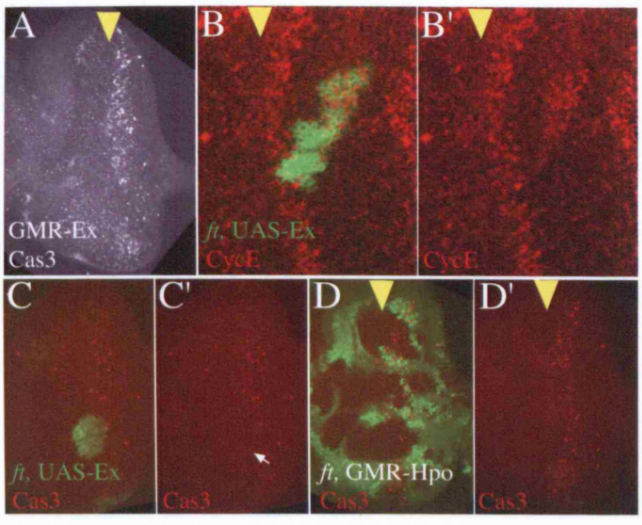

Figure 5.6 Fat is necessary for Expanded function. Yellow arrowheads correspond to the position of the MF. (A) Over-expression of Ex using the GMR-driver results in apoptosis as revealed by Caspase activation. Clones deficient for Ft and over-expressing Ex (green) exhibit accumulation of Cyclin E (B), and do not have increased incidence of apoptosis (C, arrow). Loss of Ft does not affect apoptosis induced by over-expressing Hpo (D).

5.5 Fat is not limiting in the function of the Hippo pathway but can induce its activation

I have demonstrated that Ft is required for Ex localisation and that Ex localisation is required for Ex's ability to induce apoptosis. I have also presented data suggesting that the functions of Ex that are compromised in the absence of Ft are necessary for full activation of the Hippo pathway; these data include genetic interactions in the form of both enhancement and suppression, as well as epistasis. However, I wanted to further substantiate the hypothesis that the compromise to Ex function that results from loss of Fat is specifically relevant to Ex's role in Hpo signalling. Over-expression of all positive regulators of the Hippo pathway results in growth arrest and induction of apoptosis and I wanted to see if the same is true for Fat.

5.5.1 Over-expressed transgenic Fat is functional

I used a transgenic *Drosophila* line carrying a full-length *fat* cDNA under the control of the upstream activating sequence (UAS) that our lab had previously acquired from S. Blair (Matakatsu and Blair, 2006). However, before using this construct in an experimental context, I wanted to be sure that it was fully functional. I began by using the "flip-on" method for inducing clones that over-express *ft* transcript from a UAS promoter. According to this method, an actin promoter is separated from the GAL4-encoding sequence by a stop signal, which is in turn flanked by FRT sequences. Expression of Flpase results in selective excision of the stop signal and thus allows for GAL4

expression from the actin promoter, resulting in clones of tissue that are over-expressing Fat (Pignoni and Zipursky, 1997). Fat over-expression clones generated in this manner result in the characteristic dorsal-ventral PCP phenotype that is consistent with the gradient model for Fat function. In the adult eye, although the clones are not marked due to the nature of the genotype, D-V polarity defects are clearly visible. Note that the reversal of polarity in this section cannot be the endogenous equator, since in this instance the dorsal ommatidia lie below the ventral field. The endogenous equator is out of the field of view (Figure 5.7A). Furthermore, these D-V flips occur non-autonomously, as is revealed by Bar expression in the third instar larva (Figure 5.7B).

I had not yet found any strong connections between Ft's roles in dorsal-ventral polarity and overgrowth; it is possible that Fat function in PCP is separate from its function in proliferation and apoptosis. Thus, I wanted to test this construct in a context more relevant to overgrowth. The most convincing way to test whether it is functional is to see if it would rescue any of the overgrowth phenotypes, which can be achieved by using the MARCM system to overexpress Ft in *ft* deficient clones. Unfortunately, the nature of the MARCM system, in which mutant clones are positively marked with GFP, precludes analysis of clone size. While I had a general impression that these clones were smaller than those deficient for *ft* alone, I could not quantitate and therefore confirm this observation, since there is no way to determine the size of the twinspot. However, I have demonstrated that cells deficient for any of *ft, ex* or *hpo* have elevated levels of Cyclins A and B, a phenotype that likely correlates to ectopic proliferation in the interommatidial cells posterior to the

MF. Therefore I decided to see if this phenotype is rescued in clones that are both deficient for and overexpressing Ft. In this assay, I was able to successfully rescue the accumulation of Cyclin B (Figure 5.7C), indicating that the expression of transgenic Fat is likely capable of suppressing overgrowth resulting from loss of endogenous Fat.

As one last test of the function of transgenic Ft, I tested its ability to rescue the accumulation of full-length Ci, one of the other phenotypes that I had examined. As with Cyclin B, expression of transgenic Ft rescues this accumulation (Figure 5.7D).

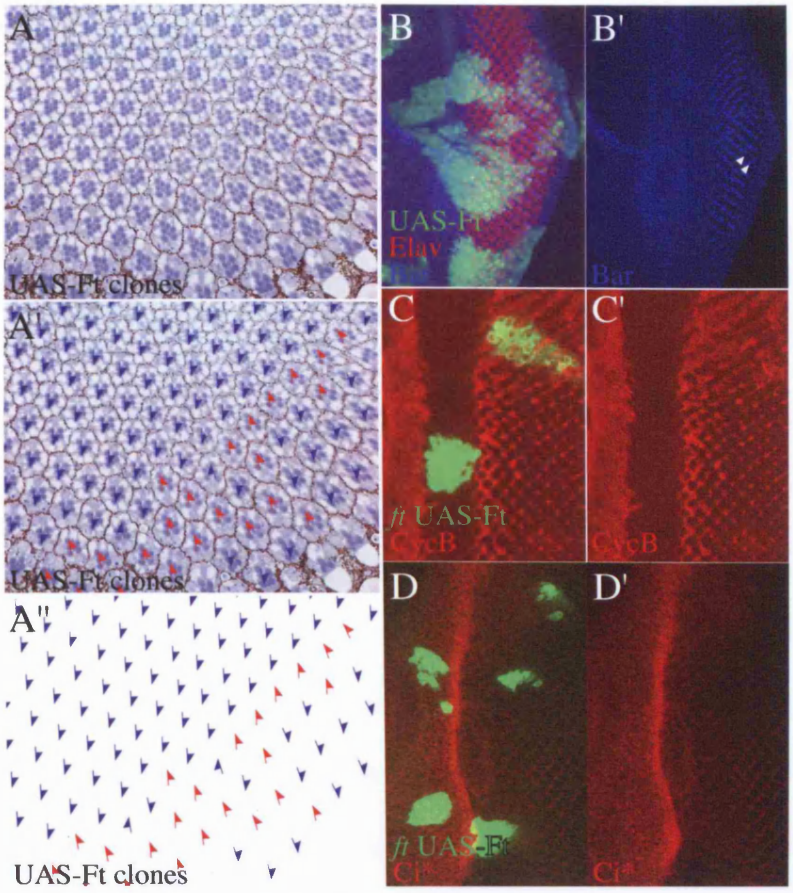

Figure 5.7 Full-length transgenic Fat is functional. (A) Over-expression of transgenic Ft in clones, in a background expressing wild-type endogenous Ft, results in polarity defects in the adult; domains of over-expression are not marked. (B) These polarity defects are non-autonomous as revealed by expression of BarH1 and Elav in the larva (arrowheads). Expression of transgenic Ft in clones deficient for endogenous Ft have normal patterns of expression of Cyclin B (C) and Ci* (D).

5.5.2 Expression of Fat is not limiting for suppression of growth *in vivo*

Having determined that UAS-Ft is functional *in vivo*, I then looked to see if over-expression of Fat could suppress growth or enhance apoptosis in a way that is similar to Ex and Hpo. Similarly to the MARCM system, the flip-on system results in clones that are positively marked with GFP, precluding analysis of clone size. In fact, since flp-on clones are generated by induction of recombination between sites on the same chromosome, rather than between homologues, there is no twinspot with which the mutant clone size can be compared. So I decided to examine Fat over-expression clones for possible repression of Cyclins B and E. I found that in the presence of elevated levels of Ft, there is no disruption to the expression patterns of each of these Cyclins (Figure 5.8A,B). Indirectly, this would indicate that Ft activity that is in excess of endogenous levels does not result in further growth suppression. However, while over-expression of each of Hpo and Ex is known to reduce growth, there is no published data demonstrating a suppression of Cyclin expression *in vivo*.

Over-expression of Hpo in the wing using a strong, wing-specific driver results in near-complete loss of wing tissue (Wu *et al.*, 2003). I decided to test the ability of over-expressed Ft to suppress growth in this more direct assay. Using the MS1096 driver, the same that was used in analysis of Hpo function, I drove strong over-expression of Ft in the wing. I found that this over-expression resulted in consistent patterning defects, including a shortening and broadening of the wing and a partial to full loss of the proximal crossvein (Figure 5.8C'). However, measurements of these wings revealed there is no

statistically significant difference in size between Ft-overexpressing wings and those expressing Gal4 alone (Figure 5.8C,D). From this data I concluded that over-expression of Ft beyond endogenous levels does not repress growth.

5.5.3 Expression of Fat is not limiting for induction of apoptosis *in vivo*

I then asked whether over-expression of Fat could induce apoptosis. It seemed unlikely that this would be true: induction of apoptosis would likely have resulted in a reduced wing size in the above assay. However, to test this possibility more directly, I examined discs in which Ft expression is driven by the eye-specific GMR driver. Expression of either Ex or Hpo in this way results in a strong induction of apoptosis as revealed by activated Caspase expression (Blaumueller and Mlodzik, 2000; Pantalacci *et al.*, 2003; Udan *et al.*, 2003; Wu *et al.*, 2003) (Figure 5.8E'; Figure 5.6A). However, I saw no such induction resulting from GMR-driven Ft expression (Figure 5.8E"); here the incidence of apoptotic cells is comparable to wild-type (Figure 5.8E). From these data I concluded that, *in vivo*, expression of Fat beyond endogenous levels is unable to further limit proliferation and induce apoptosis.

5.5.4 Expression of Fat is not limiting in the recruitment of Expanded to the membrane *in vivo*

The failure of Ft over-expression to restrict cell growth or induce apoptosis could indicate that Ft is not a limiting factor in the activation of Ex: if Ft, in its role in recruiting Ex to the apical membrane, already exists in

excess, further expression would not result in further activation of the Hippo pathway. This scenario is similar to that of Sav over-expression, which leads to only a very weak induction of apoptosis (N. Tapon, personal communication); as a molecule whose main function seems to be the mediation of interaction between Hpo and Wts, Sav likely exists in sufficient quantities for the available pool of these other molecules.

Again, using the flip-on system, I over-expressed Ft in clones. Immuno-fluorescence against Ex reveals that there is no detectable accumulation of Ex above wild-type levels in the presence of excess Ft (Figure 5.8F). Since Ft appears to function in the recruitment of Ex to the membrane, and this recruitment appears to be necessary for Ex's function in activating the Hpo pathway, the failure of Ft over-expression to suppress growth and induce apoptosis is likely because Ft is not a limiting factor in this recruitment.

5.5.5 Fat expression can induce activating phosphorylation of Hippo in cell culture

These experiments still left the question of whether Ft is able to induce activation of the Hpo pathway. In order to substantiate the hypothesis that Ft can induce activation of the Hippo signalling pathway, Nic Tapon, a colleague and collaborator in this project, performed experiments in *Drosophila* Kc cells in which he attempted to detect activating phosphorylation of Hpo using a phospho-specific antibody against its human homologue, MST-1. This antibody has previously been shown to cross-react with *Drosophila* Hippo specifically in its phosphorylated, and thus active, form (Colombani *et al.*, 2006). There is no detectable expression of endogenous Fat in Kc cells, so the

experiment was performed using transiently transfected cells. In these experiments he was able to detect, by western blot, activating phosphorylation of Hpo in response to transfection with either Fat or Ex. Furthermore, this phosphorylation is stronger when the cells are transfected with Ft and Ex together (Figure 5.8G).

Taken together, these experiments suggest three conclusions. First, localisation of Ex at the apical membrane requires Ft function. Second, Ex function requires apical localisation. Third, the compromise to Ex function that results from Ex's delocalisation equates to a compromise in the activity of the Hippo pathway.

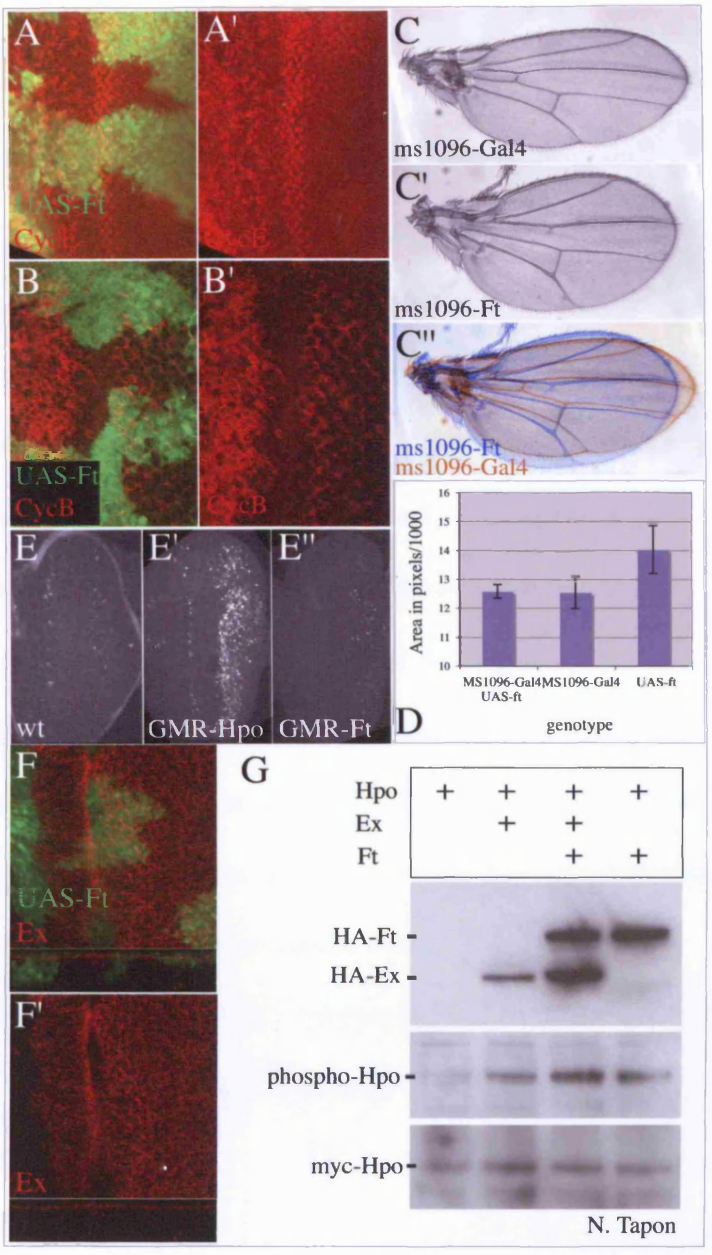

Figure 5.8 Over-expression of Fat does not affect growth or apoptosis. Over-expression of Ft beyond endogenous levels does not suppress growth (A-D); domains of Ft over-expression are in green. Over-expression clones of Ft do not show altered levels of Cyclin E (A) or Cyclin B (B). Over-expression of UAS-Ft in the wing using the ms1096-Gal4 driver results in short, broad wings (C') that do not differ in size from ms1096-Gal4 (C); overlay of wings of the two genotypes (C''). Measurements of these wings in number of pixels reveal there is no statistically significant difference between ms1096-Gal4 and ms1096-Gal4/UAS-Ft; wings carrying, but not expressing, the UAS-Ft transgene are larger than the other genotypes (D). Over-expression of Fat beyond endogenous levels does not induce apoptosis: wild-type (E) and GMR-Ft (E'') eye discs show comparable levels of apoptosis as revealed by activated caspase, while expression of Hpo from the GMR driver induces extensive cell death (E'). (F) Over-expression of Fat does not recruit additional Ex to the membrane: the levels of Ex as visualised in the X-Y axis, as well as in Z-section, are comparable in wild-type and Ft over-expressing tissue. (G) Fat is able to induce activated phosphorylation of Hpo: total protein from Kc cells co-transfected with Myc-Hpo and each of HA-Ft, HA-Ex and HA-Ft/HA-Ex and probed for phosphorylated Hippo; levels of total Hippo protein are the same in all lanes as revealed by detection of the Myc-tag.

5.6 Discussion and Conclusions

In this chapter I have presented genetic, cell biological and biochemical evidence that Fat is a positive regulator of the Hippo pathway. In the absence of Fat, Expanded localisation at the apical membrane is reduced, resulting in a compromise to Expanded's function in the suppression of growth and promotion of apoptosis. I have shown that *in vivo* overexpression of Fat cannot induce ectopic activation of the Hippo pathway, but loss of Fat recapitulates phenotypes resulting from loss of Expanded and that in cell culture models Fat is able to induce Hippo pathway activation.

This relationship between Fat and the Hippo signalling pathway first became clear with the observation that mutations in *fat* phenocopy those in *salvador* and *hippo*. Of particular note, to my eye, were the wide ommatidial spacing in the larval eye disc, the accumulation of Cyclin E and the characteristic and unique pattern of BrdU incorporation that seems to occur in a band resembling a 'third mitotic wave'. However, this last phenotype was only noticeable in the absence of Wg. The fact that loss of Wg is capable of exacerbating a phenotype of Fat that is particularly characteristic of its function in the Hippo pathway is intriguing. As discussed in the previous chapter, this function would be an unusual, though not unprecedented, one for Wg, since the majority of published data has it acting as a promoter, rather than inhibitor, of growth (Nusse, 1990; Vincan, 2004).

The pattern of BrdU is particularly interesting. I had initially taken it to imply that there is perhaps a 'zone of competency' in which Hippo-compromised cells are insensitive to regulation. However, it is equally

possible that this pattern is simply the result of earlier synchronisation of all cells in G1 arrest and the SMW. Following this synchronisation cells would require a minimum amount of time to proceed through the intervening mitosis before reaching the next round of S-phase in the 'third mitotic wave'. Interestingly, this model would imply that the loss of Ft or Hippo function does not render cells insensitive to basic cell cycle regulation and thus is corroborated by the observation that these cells do not have altered cell cycle profiles (Garoia *et al.*, 2005; Harvey *et al.*, 2003; Tapon *et al.*, 2002). It also predicts that there would be analogous gaps in Cyclin E and Cyclin B expression between the endogenous domains just after the furrow and the ectopic domains that arise later. These gaps do exist, and thus the prediction holds true. However, I still cannot exclude the former possibility of a 'zone of competency'.

The relationship between Fat and Hippo was further strengthened by the apparent accumulation of the G2 cyclins, A and B, in clones deficient for either Ex or Sav. This result is not surprising, since the ectopic expression of Cyclin E and the apparent existence of superfluous cells in both the retina and adult had already suggested a perdurance of cell divisions posterior to the MF. These cell divisions would require expression of all three cyclins for complete rounds of mitoses. Mutations in either *ex* or *sav* also result in the accumulation of these Cyclins ahead of the MF. Interestingly, there is also a bowing in the MF as visualised by BrdU in clones deficient for both Mer and Ex; this phenotype is not alluded to in the text but is clearly visible in published images (Hamaratoglu *et al.*, 2006). In Chapter 3, I presented evidence that indicated the accumulation of the Cyclins anterior to the MF and the delay in the SMW

might be connected, and suggested that a delay in the timely transition from proliferation to differentiation might account for the overgrowth of *ft* mutant clones compared to their twinspots. Since these phenotypes are also common to Ex and Sav deficient clones, it is possible that they are related to Fat's function in Hippo signalling. There were, however, discrepancies with respect to the accumulation and perdurance of Cyclins A and B anterior to the MF. Mutations in *ft* result in a very strong accumulation of these cyclins, which is somewhat comparable to accumulation resulting from mutations in *sav* but is much stronger than in Ex deficient clones. This discrepancy in its simplest interpretation could be attributed to a function for Fat, possibly in Hippo signalling, that does not require Ex. This function may also account for the additional 1.27 cells per ommatidium that are, on average, generated in the absence of Fat compared to Ex.

The majority of published data regarding the overproliferation of Hippo pathway mutants has focussed on the phenotypes as they impact growth after the MF. However, from images of clonal discs it is clear that there is a growth phenotype that pre-exists the passage of the MF. Strikingly, as with mutations in *ft*, loss of Ex results in a greatly extended third larval instar stage during which cells of all imaginal discs continue to proliferate (Boedigheimer and Laughon, 1993), indicating that here, too, there could be a general extension of the proliferative state that is contributing to overall hyperplasticity. This phenotype is not common to larvae lacking *mer* alone (McCartney *et al.*, 2000) but comparable analysis has not been performed in whole larvae deficient for other Hippo pathway members. However, as I have already discussed in Chapter 3, the delay in the transition from proliferation to differentiation, as

visualised by detection of Cyclins A and B and that is apparent in mutations for *ft*, *sav*, *ex* and *mer/ex*, could be indicative of an overall failure to recognise signals to slow and stop growth. This explanation might resolve the issue of the source of overgrowth that is apparent in *hpo* and *sav* clones anterior to the MF.

Genetic interaction assays between *fat* and each of *ex* and *yki* provided further confirmation of a role for Ft in the Hippo pathway. Loss of Ex exacerbates Ft loss of function phenotypes, while manipulating the levels of Yki, a transcriptional co-activator that is negatively regulated by the Hippo pathway, suppresses these phenotypes. These interactions were not particularly strong, but statistical analysis of quantifiable phenotypes such as clone size revealed that they are significant. While enhancement of a phenotype, particularly lethality, could be attributed to an overall compromise in the health of an organism, suppression of a phenotype is a striking indication of a genuine relationship between two molecules.

Satisfied that there is a role for Fat in the activation of Hippo signalling, I then set out to determine where in the pathway it might function. Analysis of the phenotypes as they exist in the pupal retina is a particularly sensitive way of doing so, since the phenotypes can be quantified and range from mild, as seen in *mer* clones, to extreme, as seen in *hippo* clones. Analysis of retinas of various genotypes indicated that Fat could be functioning in conjunction with Ex: mutations in *ft* resulted in phenotypes of a severity similar to mutations in *ex* and loss of both together was not significantly different from loss of *ft* alone. However, the result that was most striking was the phenotype resulting from loss of *mer* and *ft* together. Previous work had established that Mer and Ex

function redundantly in the control of proliferation and apoptosis, resulting in a far stronger phenotype than is seen in the absence of either molecule alone (Hamaratoglu *et al.*, 2006; Maitra *et al.*, 2006); if Fat does, indeed, fit into the pathway with Ex, I expected that it would also function redundantly to Mer. In agreement with this prediction, loss of Fat and Mer together resulted in a greatly enhanced phenotype similar to loss of Ex and Mer together (Hamaratoglu *et al.*, 2006).

How do Ft and Ex function together? My genetic analysis, coupled with biochemical data, demonstrate that Ft is required for Ex localisation at the apical membrane, and suggest that this localisation is necessary for Ex function in Hippo signalling. However, there is a caveat associated with the latter statement. I had demonstrated that over-expression of Ex using the UAS-Gal4 system driven by GMR is capable of inducing apoptosis as visualised by active caspase staining. However, in testing for caspase activation in the absence of Ft, Ex expression was driven by the *eyeless* promoter in the MARCM system. Ideally I would have liked to generate Ft-deficient clones in a background expressing Ex from the same GMR-driver used above, but found I had insufficient time to complete the necessary genetics. However, previous work has demonstrated that *eyeless*-Gal4 driven expression of Ex is sufficient to induce cell death as visualised by acridine orange, resulting in greatly reduced eye discs (Blaumueller and Mlodzik, 2000). This data suggests that loss of Fat is, indeed, preventing Ex from inducing apoptosis.

In the absence of Ft, Ex is not completely lost at the apical membrane, suggesting that Fat functions somewhat redundantly in this respect. Previous work using *Drosophila* cell culture found that co-transfection with Mer is

sufficient for the redistribution of Ex from the cytoplasm to the membrane (McCartney *et al.*, 2000), suggesting that Mer may be tethering or recruiting the residual Ex seen in *ft* deficient cells. However, loss of Mer and Fat together result in a phenotype that appears to be slightly less severe than loss of Mer and Ex together (Hamaratoglu *et al.*, 2006), and one explanation for this discrepancy could be that residual Expanded is sufficient to execute some growth and apoptotic control. This conclusion would suggest there is another, yet to be identified, molecule capable of this function.

Recent work has demonstrated that Hippo exists at the membrane, at least in part (Colombani *et al.*, 2006). This work, coupled with the data I have presented here, suggests an attractive model in which Ft recruits Ex to the apical membrane where it is then in proximity to, and thereby capable of activating, Hpo. Direct interaction has not been shown to exist between Ex and Hpo, however this model does not rule out the possible involvement of an intermediary that is also apically localised.

I have repeatedly attempted, with the help of colleagues and collaborators, to demonstrate the existence of a physical interaction between Ex and Ft. Together, we have performed pull-downs, co-immunoprecipitation experiments and luciferase reporter assays, *in vivo* and in cell culture models, all without success. There are a number of reasons this may be so. Fat is more than 560kD in size and primarily insoluble, making extraction and co-immunoprecipitation difficult. In cell culture models it is possible that there is poor or incorrect presentation of Fat. On speculation that there could be an intermediary involved in this interaction, I looked at the localisation of Moesin in the absence of Fat. I reasoned that if the loss of Expanded at the membrane

was due to loss of an intermediary, there could also be a loss of that intermediary in the absence of Fat. As mentioned previously, Moe was identified in a yeast-two-hybrid assay as a potential binding partner of Fat (Formstecher *et al.*, 2005) and thus seemed a reasonable candidate for this role. I did not find any evidence to support this hypothesis, but I also cannot eliminate it: it is possible that, as the intermediary, Moesin could properly localise but could lack some activity that is dependent on Fat and that is needed for Ex localisation. Additionally, there still may be as yet unidentified candidates to act as adapters between Ft and Ex.

Recent data have implicated Mer and Ex in endocytosis (Maitra *et al.*, 2006). Experiments here suggest that, in addition to, or perhaps as an explanation for, their role in transducing apoptotic and growth signals to the Hippo pathway, Mer and Ex together function to endocytose a variety of receptor signalling molecules, including Patched, Smoothened, Notch, EGFR and Fat. I could find no evidence to indicate that Fat's requirement for Hippo signalling lies in a compromise in endocytosis, since in the absence of Ft I can detect no change in the localizations of Patched, Delta or Armadillo.

While I have demonstrated that Fat functions through the Hippo pathway to restrict growth, I cannot eliminate the possibility that it also acts through other pathways in growth regulation: while there is suppression of *ft*-related overgrowth in a *yki* haplo-insufficient background, time and genetics have limited any attempts to show complete rescue via modulation of the pathway. In fact, as discussed in Chapter 4, recent data has demonstrated genetic interaction between Ft and components of the EGFR signalling pathway with respect to growth: misregulation of EGFR pathway components resulting in

minor effects on growth are strongly exacerbated by loss of Ft. This work also identified *yan* and *myc* as transcriptional targets of Ft (Garoia *et al.*, 2005). However there is, as yet, no mechanistic explanation for this connection, nor is there evidence to indicate whether this function is related to, or completely independent from, Hippo signalling.

Earlier I had presented evidence that loss of Fat results in the accumulation of Diap1, and here demonstrated that this accumulation is due to increased transcription. However, this increase is not sufficient to abolish apoptosis that is involved in patterning of the pupal retina. Recent work has found that the Hippo signalling pathway is required for full induction of p53-mediated apoptosis in response to DNA damage caused by exposure to ionizing radiation (Colombani *et al.*, 2006). It would be interesting to test whether there is a role for Ft in mediating this response in the larval eye disc, where I have shown that Diap1 accumulates in the absence of Ft.

Interestingly, Expanded has previously been noted to have a role in PCP: *expanded* loss of function clones result in polarity defects in the eye, including dorsal-ventral flips (Blaumueller and Mlodzik, 2000). Knowing that Fat and Ex function together in control of proliferation through the Hippo signalling pathway, and that loss of Fat and Ex both result in dorsal-ventral flips, it is tempting to conclude that they could also be working together in PCP. However, although haploinsufficiency of *ex* is capable of dominantly enhancing polarity defects caused by over-expressing Dsh from the Sevenless promoter, this enhancement occurs mainly in the form of an increase in the incidence of ommatidia that are 'unscoreable' due to an abnormal number of

photoreceptors. This data suggests that while there is a clear role for Ex in PCP, this role may lie outside the canonical PCP pathways.

Furthermore, there is no detectable polarity phenotype in clones deficient for Ex's partner, Mer (McCartney *et al.*, 2000). In the absence of *hpo* or *sav* there are clearly visible PCP defects that have not been acknowledged in publication (Kango-Singh *et al.*, 2002; Udan *et al.*, 2003; Wu *et al.*, 2003), but these mainly consist of defects in rotation, and thus could be the result of problems caused by excess cells that either interfere with the physical processes involved in rotation or confuse the signals directing it. Thus, with the exception of Ex and Ft, there is as yet no evidence for roles for the Hippo signalling pathway in canonical PCP signalling. In the following chapter I present evidence that suggests Fat's function in PCP is distinct from its function in the activation of the Hippo signalling pathway.

6 CHAPTER 6: FAT'S FUNCTION IN THE HIPPO PATHWAY DOES NOT AFFECT DORSAL-VENTRAL CHIRAL FLIPS

I have presented data demonstrating that Fat functions in proliferation control through its regulation of the Hippo signalling pathway. In this chapter I will present evidence suggesting that this role is independent of its function in PCP.

6.1 Over-expression of Fat has no detectable affect on growth but does affect dorsal-ventral polarity

I presented data in the previous chapter demonstrating that the over-expression of Ft beyond endogenous levels does not affect growth or apoptosis: over-expression of Ft in clones does not disrupt the expression patterns of Cyclin E or Cyclin B; over-expression of Ft using a strong eye-specific driver does not result in increased incidence of active-caspase positive cells, indicating there is no induction of apoptosis; over-expression of Ft using a strong wing-specific driver did not result in a statistically significant reduction in wing size, indicating there is no effect on either growth or apoptosis (Figure 5.8). However, over-expression of Ft in clones does result in a PCP phenotype consisting of dorsal-ventral chiral flips that are clearly visible in the adult eye (Figure 5.7A,B). Due to genetic limitations clones over-expressing Ft in the

adult eye are unmarked, but from data in the larval eye disc, it is clear that these PCP defects can occur non-autonomously.

Furthermore, work from another lab has demonstrated that in adult eyes in which Fat over-expression clones are marked using a *white* transgene, non-autonomous chiral flips occur in exactly the manner as would be predicted from the gradient model for Ft's role in PCP. In each ommatidium the cell with higher Ft activity, usually that which is closer to the equator, is fated to become R3. A 90 degree rotation in the direction of the R4 cell results in dorsal and ventral chirality. Thus in Ft loss of function clones non-autonomous D-V flips occur on the polar side of the clone. In Ft over-expression clones non-autonomous D-V flips occur on the equatorial side of the clone (D. Strutt, personal communication).

Taken together this data suggests that Ft induces the activities of at least two separate pathways. The first is involved in growth control and is not affected by increased expression, either because Fat is not active in this context or is not the limiting factor in the execution of this pathway. The second is involved in dorsal-ventral polarity cues and does respond to increased Ft expression.

6.2 Loss of Dachsous does not result in phenotypes associated with defects in Hippo signalling

As a transmembrane protein, Ft could be one of the molecules responsible for receiving extracellular cues for activition of the Hippo pathway. I wondered if these cues could be the same as those that are received by Ft for

planar cell polarity. Dachsous (Ds) is the only confirmed ligand for Fat. It functions as a directional cue for PCP and it is suggested to preferentially interact with Fat intercellularly in a heterophilic manner (Matakatsu and Blair, 2004).

I tested to see if loss of Ds function results in any of the same defects that are associated with the loss of Hippo signalling. By immuno-fluorescence against Cyclins B and E, I found there is no evidence to suggest that proliferation is continuing ectopically: there is no disruption to the expression patterns of these molecules (Figure 6.1B,C). This conclusion was corroborated by BrdU incorporation assays in which I saw no ectopic S phase in clones posterior to the furrow (Figure 6.1A). Furthermore, there is no evidence that Ds-deficient cells are delayed in their abilities to enter the SMW. Finally, I examined Ex expression in Ds-deficient clones and found no disruption to its localisation (Figure 6.1D).

Since Ds is a known ligand for Ft in PCP, and since loss of Dachsous does not appear to have any effect on growth-associated phenotypes, these results suggest that Ft's function in receiving directional cues for PCP may be independent of its function in receiving cues for activation of the Hippo signalling pathway.

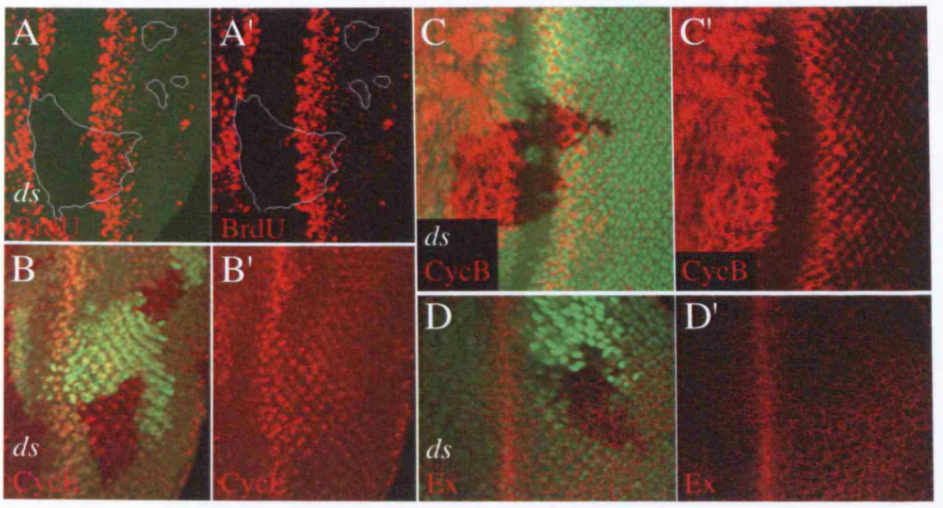

Figure 6.1 Mutations in *dachsous* do not exhibit Hpo-associated phenotypes. Clones deficient for Ds do not accumulate BrdU posterior to the MF, nor do they have delayed entry into the SMW (A); they do not accumulate Cyclin E (B) and they do not exhibit a perdurance of Cyclin B anterior to the MF (C). Loss of Ds does not affect the pattern of expression of Ex (D).

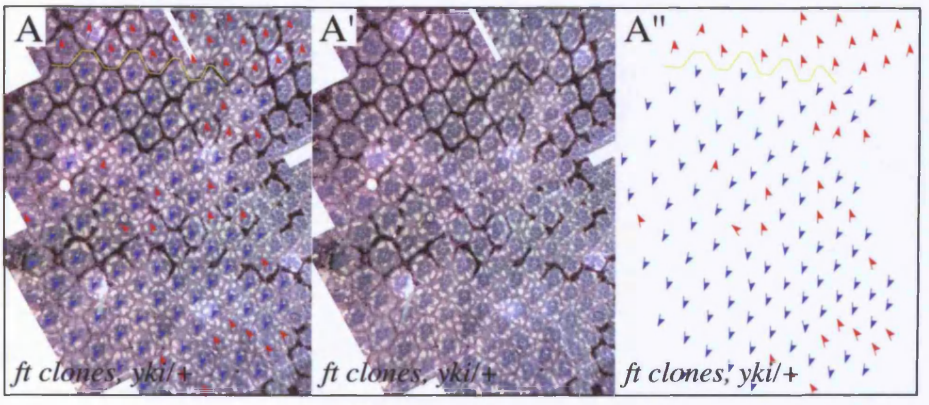

Figure 6.2 Clones deficient for Fat in a background haploinsufficient for Yki still exhibit PCP defects. (A) Sections through eyes carrying Ft-deficient clones in a background that is heterozygous for *yki* exhibit PCP defects. The endogenous equator is marked in yellow.

6.3 PCP defects persist when overgrowth is genetically suppressed

As one last test for a connection between Ft's role in overgrowth and Ft's role in PCP, I examined sections of adult heads in which the overgrowth that results from large mitotic clones is suppressed by haploinsufficiency of *yorkie*. It is clear that dorsal-ventral polarity defects are still prevalent when overgrowth is suppressed (Figure 6.2).

6.4 Discussion and Conclusions

Here I have presented evidence suggesting that Fat's function in the control of proliferation and apoptosis through the Hippo signalling pathway may be independent of its role in dorsal-ventral planar cell polarity. This postulation arises from three main lines of evidence. First, over-expression of Ft beyond endogenous levels is able induce responses in PCP, but has no affect on Hippo-associated growth phenotypes. Second, Ds is the only known ligand for Fat: in numerous *in vivo* and *in vitro* assays they have been demonstrated to form stable, heterophilic interactions between cell membranes in a calcium-dependent fashion (Ma *et al.*, 2003; Matakatsu and Blair, 2004; Strutt and Strutt, 2002). Ds is capable of directing PCP along axes that are parallel with its expression but seems to have only a small role in growth repression (Clark *et al.*, 1995), and loss of Dachsous does not result in Hippo-associated phenotypes (Figure 6.1). Finally, I have shown that dorsal-ventral flips are still

prevalent when the *ft* overgrowth phenotype is suppressed through reduction in the levels of Yorkie.

While these results are consistent with a role for Ft in PCP that is distinct from its role in growth suppression, they are far from conclusive. One of the key limitations to the experiments I have presented here is the lack of quantification of the polarity phenotype as it manifests in wild-type versus Yki-haploinsufficient backgrounds. Thus I cannot rule out the existence of an undetected suppression of the incidence of D-V flips, which would link Fat's roles in PCP and Hippo-mediated growth regulation.

Further complications to the interpretation presented here arise from its inconsistencies with data from other groups. I had initially favoured a model in which the intracellular domain of Ft is necessary for the localisation of Expanded and thus growth regulation through Hpo signalling, while the extracellular domain functions in PCP through its interaction with Ds. Previous work had shown that heterophilic interactions between Ds and Ft could be crucial for their roles in PCP: these interactions would facilitate the intercellular coordination of the core PCP molecules such as Frizzled (Ma *et al.*, 2003; Strutt and Strutt, 2002; Yang *et al.*, 2002). However, in testing this model, basic predictions have not held true. First, it has become apparent that while Ds is instructional in directing PCP there is no requirement for its expression in a gradient along the naturally occurring axis. Furthermore, Ft is capable of directing PCP in the absence of Ds (Matakatsu and Blair, 2004). Thus, it is possible that Ft's function in the Hippo signalling pathway could be connected to its role in PCP via a mechanism that is independent of the function of Ds.

Furthermore, very recent work on both Fat and Dachsous has attempted to elucidate the domains of each molecule that are important for their functions in different contexts. Using transgenes that are missing either the cytoplasmic or extracellular domains, they have found that the extra-cellular domain of Ft is largely dispensable for its function in growth suppression and PCP, despite the fact that loss of the extra-cellular domain results in the loss of intercellular heterophilic interactions with Ds (Matakatsu and Blair, 2006), further corroborating earlier data demonstrating that Ft can function in PCP independently of Ds. However, interpretations of these results are themselves complicated by the observation that extracellular Ft stabilises Ft and Ds at the membrane while acting as a dominant-negative regulator of growth: expression of the extra-cellular domain in the absence of Fat results in greatly overgrown discs that are much larger than those lacking Ft alone (Matakatsu and Blair, 2006). These results imply that the extra-cellular domain is binding and blocking the functions of Ft and Ds and that both are involved in growth suppression, perhaps redundantly. Indeed, while loss of Ds alone results in little or no compromise to growth suppression, it does strongly exacerbate Ft-related overgrowth (Matakatsu and Blair, 2006). Although the evidence I have presented here so far suggests that Ds functions outside the Hippo signalling pathway, it is clear that Ds functions in Ft-mediated growth suppression. Thus, contrary to my initial hypothesis, the function of Ft in the localisation of Expanded could require modulation of its activity through its extracellular domain, which could in turn be affected by modulation of Ds.

One other molecule that has been implicated in mediating Ft-dependent growth suppression is Dachs. Dachs was recently identified as a non-

conventional myosin that appears to be expressed in all imaginal discs (Mao *et al.*, 2006). Of particular significance for the work presented here is the observation that loss of Dachs results in what appears to be full-suppression of nearly all Fat-associated phenotypes. In particular, there is full suppression of whole organ overgrowth as well as clonal overgrowth. There is also suppression of adhesion defects in the form of round clones and accumulation of Wg and Serrate in the proximal wing.

However, the one notable exception to the rescue of Ft-related phenotypes is the persistence of PCP defects. From this data, (Mao *et al.*, 2006) speculate that there are at least two signalling pathways functioning downstream of Fat, one in Dachs-mediated growth suppression and the other in directing PCP. This data would fit nicely with the results I have presented here, and thus could implicate Dachs, which is genetically down-stream of Fat, in the mediation of Ft's function in Hippo signalling regulation. These authors are currently testing this possibility (K. Irvine, personal communication).

7 CHAPTER 7: CONCLUSIONS AND FUTURE WORK

The primary goal of this work was to explore the nature of the overgrowth phenotype associated with the loss of Ft function in the *Drosophila* eye. I have presented results indicating that in the absence of Ft, cells are compromised in their abilities to recognise or respond to signals that trigger the transition from proliferation to differentiation. This compromise leads to a delay in G1 arrest at the morphogenetic furrow that in turn leads to delays in subsequent differentiation events as well as ectopic perdurance of cell division in uncommitted interommatidial cells posterior to the furrow.

I reasoned that a delay in the ability of the Ft-deficient cells to enter the MF could be due to a failure to respond to any of a number of signals that are responsible for initiating and propagating various events associated with the MF. Thus, I attempted to identify a signalling pathway whose function is affected in the absence of Ft. I found that Ft function can be linked to EGFR, Wingless and Hedgehog signalling, but that the accumulation of Wg and of active Ci does not account for the delay in furrow progression, nor for overgrowth of Ft-deficient clones. On the contrary, I found that loss of Wg enhances overgrowth resulting from loss of Ft.

However, I did find that Ft functions upstream of the Hippo signalling pathway to regulate proliferation and that it does so through stabilisation of Ex at the apical membrane. Reduction in Hippo signalling results in de-repression of the transcriptional co-activator, Yorkie, and transcription of *cyclin E* and

diap1. Reduced Hippo signalling also accounts for the increased incidence of BrdU-labelled cells, and likely accounts for the perduring expression of Cyclins A and B in clones posterior to the MF.

Finally, I have presented evidence suggesting that Ft's role in the Hippo signalling pathway is distinct from its role in mediating PCP. However, this evidence is not conclusive, and when examined in the context of published data it is clear that there will be no simple resolution to attempts to reconcile these roles for Ft.

There is no obvious direction for the future of this work, but there are a number of unresolved issues that merit further exploration. In my view, the impaired ability of Fat deficient cells to enter G1 arrest in the MF is of particular interest, especially when contemplated in the context of Ft's role in the localisation of Ex. As discussed, this phenotype exists in clones deficient for Mer and Ex together (Hamaratoglu *et al.*, 2006), but has so far gone unremarked in published work. Could this delay in MF progression contribute to the overgrowth observed in clones deficient for other Hippo pathway components?

I had also suggested that this impaired transition from proliferation to differentiation could be indicative of a more wide-spread impairment in the ability of Ft cells to recognise signals to slow and arrest growth at the end of third instar larval development, as the larva prepares for metamorphosis. Interestingly, this model would make a simple prediction: Ft-deficient clones and their twinspots would proliferate at equal rates until the 'stop' signal is initiated. Thus, it would be interesting to see if Ft-deficient clones as they exist in the second instar larvae are of a size equal to their twinspots.

Finally, further work is being carried out to determine the mechanisms of function for Ft in EGFR signalling. I had concluded that any role for Fat in this pathway lay in its function in PCP, however more recent data has demonstrated otherwise: Fat appears to impinge upon EGFR targets downstream of MAPK. However, Sprouty had been identified as a binding partner for Ft in yeast-two-hybrid assays and if this interaction holds true, it would put Ft either upstream or in parallel to MAPK activation. Work is underway to confirm this interaction *in vivo*, as well as to examine it in the context of Hippo-mediated growth suppression.

References

Akiyama, T. (2000). Wnt/beta-catenin signaling. *Cytokine Growth Factor Rev* **11,** 273-82.

Alcedo, J., Ayzenzon, M., Von Ohlen, T., Noll, M., and Hooper, J. E. (1996). The Drosophila smoothened gene encodes a seven-pass membrane protein, a putative receptor for the hedgehog signal. *Cell* **86,** 221-32.

Andersen, J. B., Sternberg, C., Poulsen, L. K., Bjorn, S. P., Givskov, M., and Molin, S. (1998). New unstable variants of green fluorescent protein for studies of transient gene expression in bacteria. *Appl Environ Microbiol* **64,** 2240-6.

Apionishev, S., Katanayeva, N. M., Marks, S. A., Kalderon, D., and Tomlinson, A. (2005). Drosophila Smoothened phosphorylation sites essential for Hedgehog signal transduction. *Nat Cell Biol* **7,** 86-92.

Axelrod, J. D. (2001). Unipolar membrane association of Dishevelled mediates Frizzled planar cell polarity signaling. *Genes Dev* **15,** 1182-7.

Aza-Blanc, P., Ramirez-Weber, F. A., Laget, M. P., Schwartz, C., and Kornberg, T. B. (1997). Proteolysis that is inhibited by hedgehog targets Cubitus interruptus protein to the nucleus and converts it to a repressor. *Cell* **89,** 1043-53.

Baena-Lopez, L. A., Baonza, A., and Garcia-Bellido, A. (2005). The orientation of cell divisions determines the shape of Drosophila organs. *Curr Biol* **15,** 1640-4.

Baker, N. E. (1988). Transcription of the segment-polarity gene wingless in the imaginal discs of Drosophila, and the phenotype of a pupal-lethal wg mutation. *Development* **102,** 489-97.

Baker, N. E., Mlodzik, M., and Rubin, G. M. (1990). Spacing differentiation in the developing Drosophila eye: a fibrinogen-related lateral inhibitor encoded by scabrous. *Science* **250,** 1370-7.

Baker, N. E., and Rubin, G. M. (1989). Effect on eye development of dominant mutations in Drosophila homologue of the EGF receptor. *Nature* **340,** 150-3.

Baker, N. E., and Yu, S. Y. (1997). Proneural function of neurogenic genes in the developing Drosophila eye. *Curr Biol* **7,** 122-32.

Baker, N. E., and Yu, S. Y. (2001). The EGF receptor defines domains of cell cycle progression and survival to regulate cell number in the developing Drosophila eye. *Cell* **104,** 699-708.

Baker, N. E., and Zitron, A. E. (1995). Drosophila eye development: Notch and Delta amplify a neurogenic pattern conferred on the morphogenetic furrow by scabrous. *Mech Dev* **49,** 173-89.

Baonza, A., and Freeman, M. (2001). Notch signalling and the initiation of neural development in the Drosophila eye. *Development* **128,** 3889-98.

Baonza, A., and Freeman, M. (2002). Control of Drosophila eye specification by Wingless signalling. *Development* **129,** 5313-22.

Baonza, A., and Freeman, M. (2005). Control of cell proliferation in the Drosophila eye by Notch signaling. *Dev Cell* **8,** 529-39.

Baonza, A., Murawsky, C. M., Travers, A. A., and Freeman, M. (2002). Pointed and Tramtrack69 establish an EGFR-dependent transcriptional switch to regulate mitosis. *Nat Cell Biol* **4,** 976-80.

Bejsovec, A., and Martinez Arias, A. (1991). Roles of wingless in patterning the larval epidermis of Drosophila. *Development* **113,** 471-85.

Blaumueller, C. M., and Mlodzik, M. (2000). The Drosophila tumor suppressor expanded regulates growth, apoptosis, and patterning during development. *Mech Dev* **92,** 251-62.

Boedigheimer, M., Bryant, P., and Laughon, A. (1993). Expanded, a negative regulator of cell proliferation in Drosophila, shows homology to the NF2 tumor suppressor. *Mech Dev* **44,** 83-4.

Boedigheimer, M., and Laughon, A. (1993). Expanded: a gene involved in the control of cell proliferation in imaginal discs. *Development* **118,** 1291-301.

Boedigheimer, M. J., Nguyen, K. P., and Bryant, P. J. (1997). Expanded functions in the apical cell domain to regulate the growth rate of imaginal discs. *Dev Genet* **20,** 103-10.

Borod, E. R., and Heberlein, U. (1998). Mutual regulation of decapentaplegic and hedgehog during the initiation of differentiation in the Drosophila retina. *Dev Biol* **197,** 187-97.

Brown, K. E., and Freeman, M. (2003). Egfr signalling defines a protective function for ommatidial orientation in the Drosophila eye. *Development* **130,** 5401-12.

Bryant, P. J., Huettner, B., Held, L. I., Jr., Ryerse, J., and Szidonya, J. (1988). Mutations at the fat locus interfere with cell proliferation control and epithelial morphogenesis in Drosophila. *Dev Biol* **129,** 541-54.

Bryant, P. J., and Simpson, P. (1984). Intrinsic and extrinsic control of growth in developing organs. *Q Rev Biol* **59,** 387-415.

Cadigan, K. M., Jou, A. D., and Nusse, R. (2002). Wingless blocks bristle formation and morphogenetic furrow progression in the eye through repression of Daughterless. *Development* **129,** 3393-402.

Cagan, R. L., and Ready, D. F. (1989). The emergence of order in the Drosophila pupal retina. *Dev Biol* **136,** 346-62.

Capdevila, J., Pariente, F., Sampedro, J., Alonso, J. L., and Guerrero, I. (1994). Subcellular localization of the segment polarity protein patched suggests an interaction with the wingless reception complex in Drosophila embryos. *Development* **120,** 987-98.

Casal, J., Struhl, G., and Lawrence, P. A. (2002). Developmental compartments and planar polarity in Drosophila. *Curr Biol* **12,** 1189-98.

Casci, T., Vinos, J., and Freeman, M. (1999). Sprouty, an intracellular inhibitor of Ras signaling. *Cell* **96,** 655-65.

Cavodeassi, F., Diez Del Corral, R., Campuzano, S., and Dominguez, M. (1999). Compartments and organising boundaries in the Drosophila eye: the role of the homeodomain Iroquois proteins. *Development* **126,** 4933-42.

Chalfie, M., Tu, Y., Euskirchen, G., Ward, W. W., and Prasher, D. C. (1994). Green fluorescent protein as a marker for gene expression. *Science* **263,** 802-5.

Chanut, F., and Heberlein, U. (1995). Role of the morphogenetic furrow in establishing polarity in the Drosophila eye. *Development* **121,** 4085-94.

Chanut, F., and Heberlein, U. (1997). Role of decapentaplegic in initiation and progression of the morphogenetic furrow in the developing Drosophila retina. *Development* **124,** 559-67.

Charroux, B., Freeman, M., Kerridge, S., and Baonza, A. (2006). Atrophin contributes to the negative regulation of epidermal growth factor receptor signaling in Drosophila. *Dev Biol* **291,** 278-90.

Chen, Y., and Struhl, G. (1996). Dual roles for patched in sequestering and transducing Hedgehog. *Cell* **87,** 553-63.

Cho, E., and Irvine, K. D. (2004). Action of fat, four-jointed, dachsous and dachs in distal-to-proximal wing signaling. *Development* **131,** 4489-500.

Clark, H. F., Brentrup, D., Schneitz, K., Bieber, A., Goodman, C., and Noll, M. (1995). Dachsous encodes a member of the cadherin superfamily that controls imaginal disc morphogenesis in Drosophila. *Genes Dev* **9,** 1530-42.

Coelho, C. M., Kolevski, B., Bunn, C., Walker, C., Dahanukar, A., and Leevers, S. J. (2005). Growth and cell survival are unevenly impaired in pixie mutant wing discs. *Development* **132,** 5411-24.

Colombani, J., Polesello, C., Josue, F., and Tapon, N. (2006). Dmp53 activates the hippo pathway to promote cell death in response to DNA damage. *Curr Biol* **16,** 1453-8.

Cooper, M. T., and Bray, S. J. (1999). Frizzled regulation of Notch signalling polarizes cell fate in the Drosophila eye. *Nature* **397,** 526-30.

Curtiss, J., and Mlodzik, M. (2000). Morphogenetic furrow initiation and progression during eye development in Drosophila: the roles of decapentaplegic, hedgehog and eyes absent. *Development* **127,** 1325-36.

Dang, D. T., and Perrimon, N. (1992). Use of a yeast site-specific recombinase to generate embryonic mosaics in Drosophila. *Dev Genet* **13,** 367-75.

Das, G., Jenny, A., Klein, T. J., Eaton, S., and Mlodzik, M. (2004). Diego interacts with Prickle and Strabismus/Van Gogh to localize planar cell polarity complexes. *Development* **131,** 4467-76.

Datar, S. A., Jacobs, H. W., de la Cruz, A. F., Lehner, C. F., and Edgar, B. A. (2000). The Drosophila cyclin D-Cdk4 complex promotes cellular growth. *Embo J* **19,** 4543-54.

Dominguez, M. (1999). Dual role for Hedgehog in the regulation of the proneural gene atonal during ommatidia development. *Development* **126,** 2345-53.

Dominguez, M., and Hafen, E. (1997). Hedgehog directly controls initiation and propagation of retinal differentiation in the Drosophila eye. *Genes Dev* **11,** 3254-64.

Dominguez, M., Wasserman, J. D., and Freeman, M. (1998). Multiple functions of the EGF receptor in Drosophila eye development. *Curr Biol* **8,** 1039-48.

Doronkin, S., Djagaeva, I., and Beckendorf, S. K. (2003). The COP9 signalosome promotes degradation of Cyclin E during early Drosophila oogenesis. *Dev Cell* **4,** 699-710.

Dulic, V., Lees, E., and Reed, S. I. (1992). Association of human cyclin E with a periodic G1-S phase protein kinase. *Science* **257,** 1958-61.

Duman-Scheel, M., Weng, L., Xin, S., and Du, W. (2002). Hedgehog regulates cell growth and proliferation by inducing Cyclin D and Cyclin E. *Nature* **417,** 299-304.

Edgar, B. A. (2006). From cell structure to transcription: Hippo forges a new path. *Cell* **124,** 267-73.

Edgar, B. A., and O'Farrell, P. H. (1989). Genetic control of cell division patterns in the Drosophila embryo. *Cell* **57,** 177-87.

Egan, J. E., Hall, A. B., Yatsula, B. A., and Bar-Sagi, D. (2002). The bimodal regulation of epidermal growth factor signaling by human Sprouty proteins. *Proc Natl Acad Sci U S A* **99,** 6041-6.

Fanto, M., Clayton, L., Meredith, J., Hardiman, K., Charroux, B., Kerridge, S., and McNeill, H. (2003). The tumor-suppressor and cell adhesion molecule Fat controls planar polarity via physical interactions with Atrophin, a transcriptional co-repressor. *Development* **130,** 763-74.

Fanto, M., and Mlodzik, M. (1999). Asymmetric Notch activation specifies photoreceptors R3 and R4 and planar polarity in the Drosophila eye. *Nature* **397,** 523-6.

Finley, R. L., Jr., Thomas, B. J., Zipursky, S. L., and Brent, R. (1996). Isolation of Drosophila cyclin D, a protein expressed in the morphogenetic furrow before entry into S phase. *Proc Natl Acad Sci U S A* **93,** 3011-5.

Firth, L. C., and Baker, N. E. (2005). Extracellular signals responsible for spatially regulated proliferation in the differentiating Drosophila eye. *Dev Cell* **8,** 541-51.

Formstecher, E., Aresta, S., Collura, V., Hamburger, A., Meil, A., Trehin, A., Reverdy, C., Betin, V., Maire, S., Brun, C., Jacq, B., Arpin, M., Bellaiche, Y., Bellusci, S., Benaroch, P., Bornens, M., Chanet, R., Chavrier, P., Delattre, O., Doye, V., Fehon, R., Faye, G., Galli, T., Girault, J. A., Goud, B., de Gunzburg, J., Johannes, L., Junier, M. P., Mirouse, V., Mukherjee, A., Papadopoulo, D., Perez, F., Plessis, A., Rosse, C., Saule, S., Stoppa-Lyonnet, D., Vincent, A., White, M., Legrain, P., Wojcik, J., Camonis, J., and Daviet, L. (2005). Protein interaction mapping: a Drosophila case study. *Genome Res* **15,** 376-84.

Frankfort, B. J., Nolo, R., Zhang, Z., Bellen, H., and Mardon, G. (2001). senseless repression of rough is required for R8 photoreceptor differentiation in the developing Drosophila eye. *Neuron* **32,** 403-14.

Freeman, M. (1994). The spitz gene is required for photoreceptor determination in the Drosophila eye where it interacts with the EGF receptor. *Mech Dev* **48,** 25-33.

Freeman, M. (1996). Reiterative use of the EGF receptor triggers differentiation of all cell types in the Drosophila eye. *Cell* **87,** 651-60.

Freilich, S., Oron, E., Kapp, Y., Nevo-Caspi, Y., Orgad, S., Segal, D., and Chamovitz, D. A. (1999). The COP9 signalosome is essential for development of Drosophila melanogaster. *Curr Biol* **9,** 1187-90.

Fu, W., and Baker, N. E. (2003). Deciphering synergistic and redundant roles of Hedgehog, Decapentaplegic and Delta that drive the wave of differentiation in Drosophila eye development. *Development* **130,** 5229-39.

Gabay, L., Scholz, H., Golembo, M., Klaes, A., Shilo, B. Z., and Klambt, C. (1996). EGF receptor signaling induces pointed P1 transcription and inactivates Yan protein in the Drosophila embryonic ventral ectoderm. *Development* **122,** 3355-62.

Gabay, L., Seger, R., and Shilo, B. Z. (1997a). In situ activation pattern of Drosophila EGF receptor pathway during development. *Science* **277,** 1103-6.
Gabay, L., Seger, R., and Shilo, B. Z. (1997b). MAP kinase in situ activation atlas during Drosophila embryogenesis. *Development* **124,** 3535-41.

Gaengel, K., and Mlodzik, M. (2003). Egfr signaling regulates ommatidial rotation and cell motility in the Drosophila eye via MAPK/Pnt signaling and the Ras effector Canoe/AF6. *Development* **130,** 5413-23.

Garoia, F., Grifoni, D., Trotta, V., Guerra, D., Pezzoli, M. C., and Cavicchi, S. (2005). The tumor suppressor gene fat modulates the EGFR-mediated proliferation control in the imaginal tissues of Drosophila melanogaster. *Mech Dev* **122,** 175-87.

Garoia, F., Guerra, D., Pezzoli, M. C., Lopez-Varea, A., Cavicchi, S., and Garcia-Bellido, A. (2000). Cell behaviour of Drosophila fat cadherin mutations in wing development. *Mech Dev* **94,** 95-109.

Gomez, N., and Cohen, P. (1991). Dissection of the protein kinase cascade by which nerve growth factor activates MAP kinases. *Nature* **353,** 170-3.

Greenwood, S., and Struhl, G. (1999). Progression of the morphogenetic furrow in the Drosophila eye: the roles of Hedgehog, Decapentaplegic and the Raf pathway. *Development* **126,** 5795-808.

Hamaratoglu, F., Willecke, M., Kango-Singh, M., Nolo, R., Hyun, E., Tao, C., Jafar-Nejad, H., and Halder, G. (2006). The tumour-suppressor genes NF2/Merlin and Expanded act through Hippo signalling to regulate cell proliferation and apoptosis. *Nat Cell Biol* **8,** 27-36.

Hanafusa, H., Torii, S., Yasunaga, T., and Nishida, E. (2002). Sprouty1 and Sprouty2 provide a control mechanism for the Ras/MAPK signalling pathway. *Nat Cell Biol* **4,** 850-8.

Harvey, K. F., Pfleger, C. M., and Hariharan, I. K. (2003). The Drosophila Mst ortholog, hippo, restricts growth and cell proliferation and promotes apoptosis. *Cell* **114,** 457-67.

Hawkins, R. D., and Lovett, M. (2004). The developmental genetics of auditory hair cells. *Hum Mol Genet* **13 Spec No 2,** R289-96.

Hay, B. A., Maile, R., and Rubin, G. M. (1997). P element insertion-dependent gene activation in the Drosophila eye. *Proc Natl Acad Sci U S A* **94,** 5195-200.

Hay, B. A., Wassarman, D. A., and Rubin, G. M. (1995). Drosophila homologs of baculovirus inhibitor of apoptosis proteins function to block cell death. *Cell* **83,** 1253-62.

Heberlein, U., Borod, E. R., and Chanut, F. A. (1998). Dorsoventral patterning in the Drosophila retina by wingless. *Development* **125,** 567-77.

Heberlein, U., Singh, C. M., Luk, A. Y., and Donohoe, T. J. (1995). Growth and differentiation in the Drosophila eye coordinated by hedgehog. *Nature* **373,** 709-11.

Heberlein, U., Wolff, T., and Rubin, G. M. (1993). The TGF beta homolog dpp and the segment polarity gene hedgehog are required for propagation of a morphogenetic wave in the Drosophila retina. *Cell* **75,** 913-26.

Higashijima, S., Kojima, T., Michiue, T., Ishimaru, S., Emori, Y., and Saigo, K. (1992). Dual Bar homeo box genes of Drosophila required in two photoreceptor cells, R1 and R6, and primary pigment cells for normal eye development. *Genes Dev* **6,** 50-60.

Horsfield, J., Penton, A., Secombe, J., Hoffman, F. M., and Richardson, H. (1998). decapentaplegic is required for arrest in G1 phase during Drosophila eye development. *Development* **125,** 5069-78.

Huang, J., Wu, S., Barrera, J., Matthews, K., and Pan, D. (2005). The Hippo signaling pathway coordinately regulates cell proliferation and apoptosis by inactivating Yorkie, the Drosophila Homolog of YAP. *Cell* **122,** 421-34.

Jaiswal, M., Agrawal, N., and Sinha, P. (2006). Fat and Wingless signaling oppositely regulate epithelial cell-cell adhesion and distal wing development in Drosophila. *Development* **133,** 925-35.

Jarman, A. P., Grell, E. H., Ackerman, L., Jan, L. Y., and Jan, Y. N. (1994). Atonal is the proneural gene for Drosophila photoreceptors. *Nature* **369,** 398-400.

Jaskulski, D., deRiel, J. K., Mercer, W. E., Calabretta, B., and Baserga, R. (1988). Inhibition of cellular proliferation by antisense oligodeoxynucleotides to PCNA cyclin. *Science* **240,** 1544-6.

Jenny, A., Darken, R. S., Wilson, P. A., and Mlodzik, M. (2003). Prickle and Strabismus form a functional complex to generate a correct axis during planar cell polarity signaling. *Embo J* **22,** 4409-20.

Jenny, A., Reynolds-Kenneally, J., Das, G., Burnett, M., and Mlodzik, M. (2005). Diego and Prickle regulate Frizzled planar cell polarity signalling by competing for Dishevelled binding. *Nat Cell Biol* **7,** 691-7.

Jia, J., Amanai, K., Wang, G., Tang, J., Wang, B., and Jiang, J. (2002). Shaggy/GSK3 antagonizes Hedgehog signalling by regulating Cubitus interruptus. *Nature* **416,** 548-52.

Jia, J., Tong, C., Wang, B., Luo, L., and Jiang, J. (2004). Hedgehog signalling activity of Smoothened requires phosphorylation by protein kinase A and casein kinase I. *Nature* **432,** 1045-50.

Jia, J., Zhang, L., Zhang, Q., Tong, C., Wang, B., Hou, F., Amanai, K., and Jiang, J. (2005). Phosphorylation by double-time/CKIepsilon and CKIalpha targets cubitus interruptus for Slimb/beta-TRCP-mediated proteolytic processing. *Dev Cell* **9,** 819-30.

Johnston, L. A., and Edgar, B. A. (1998). Wingless and Notch regulate cell-cycle arrest in the developing Drosophila wing. *Nature* **394,** 82-4.

Jones, L., Richardson, H., and Saint, R. (2000). Tissue-specific regulation of cyclin E transcription during Drosophila melanogaster embryogenesis. *Development* **127,** 4619-30.

Kaltschmidt, J. A., Lawrence, N., Morel, V., Balayo, T., Fernandez, B. G., Pelissier, A., Jacinto, A., and Martinez Arias, A. (2002). Planar polarity and actin dynamics in the epidermis of Drosophila. *Nat Cell Biol* **4,** 937-44.

Kango-Singh, M., Nolo, R., Tao, C., Verstreken, P., Hiesinger, P. R., Bellen, H. J., and Halder, G. (2002). Shar-pei mediates cell proliferation arrest during imaginal disc growth in Drosophila. *Development* **129,** 5719-30.

Kauffmann, R. C., Li, S., Gallagher, P. A., Zhang, J., and Carthew, R. W. (1996). Ras1 signaling and transcriptional competence in the R7 cell of Drosophila. *Genes Dev* **10,** 2167-78.

Kim, J., Johnson, K., Chen, H. J., Carroll, S., and Laughon, A. (1997). Drosophila Mad binds to DNA and directly mediates activation of vestigial by Decapentaplegic. *Nature* **388,** 304-8.

Klein, D. E., Nappi, V. M., Reeves, G. T., Shvartsman, S. Y., and Lemmon, M. A. (2004). Argos inhibits epidermal growth factor receptor signalling by ligand sequestration. *Nature* **430,** 1040-4.

Koff, A., Cross, F., Fisher, A., Schumacher, J., Leguellec, K., Philippe, M., and Roberts, J. M. (1991). Human cyclin E, a new cyclin that interacts with two members of the CDC2 gene family. *Cell* **66,** 1217-28.

Koff, A., Giordano, A., Desai, D., Yamashita, K., Harper, J. W., Elledge, S., Nishimoto, T., Morgan, D. O., Franza, B. R., and Roberts, J. M. (1992). Formation and activation of a cyclin E-cdk2 complex during the G1 phase of the human cell cycle. *Science* **257,** 1689-94.

Kosman, D., Small, S., and Reinitz, J. (1998). Rapid preparation of a panel of polyclonal antibodies to Drosophila segmentation proteins. *Dev Genes Evol* **208,** 290-4.

Kramer, S., Okabe, M., Hacohen, N., Krasnow, M. A., and Hiromi, Y. (1999). Sprouty: a common antagonist of FGF and EGF signaling pathways in Drosophila. *Development* **126,** 2515-25.

Kunisch, M., Haenlin, M., and Campos-Ortega, J. A. (1994). Lateral inhibition mediated by the Drosophila neurogenic gene delta is enhanced by proneural proteins. *Proc Natl Acad Sci U S A* **91,** 10139-43.

Lai, Z. C., Wei, X., Shimizu, T., Ramos, E., Rohrbaugh, M., Nikolaidis, N., Ho, L. L., and Li, Y. (2005). Control of cell proliferation and apoptosis by mob as tumor suppressor, mats. *Cell* **120,** 675-85.

LaJeunesse, D. R., McCartney, B. M., and Fehon, R. G. (1998). Structural analysis of Drosophila merlin reveals functional domains important for growth control and subcellular localization. *J Cell Biol* **141,** 1589-99.

Lawrence, P. A., Casal, J., and Struhl, G. (2004). Cell interactions and planar polarity in the abdominal epidermis of Drosophila. *Development* **131,** 4651-64.

Lee, J. D., and Treisman, J. E. (2001). The role of Wingless signaling in establishing the anteroposterior and dorsoventral axes of the eye disc. *Development* **128,** 1519-29.

Lee, T., and Luo, L. (2001). Mosaic analysis with a repressible cell marker (MARCM) for Drosophila neural development. *Trends Neurosci* **24,** 251-4.

Lehner, C. F., and O'Farrell, P. H. (1990). The roles of Drosophila cyclins A and B in mitotic control. *Cell* **61,** 535-47.

Li, Y., and Baker, N. E. (2001). Proneural enhancement by Notch overcomes Suppressor-of-Hairless repressor function in the developing Drosophila eye. *Curr Biol* **11,** 330-8.

Liu, F., Hata, A., Baker, J. C., Doody, J., Carcamo, J., Harland, R. M., and Massague, J. (1996). A human Mad protein acting as a BMP-regulated transcriptional activator. *Nature* **381,** 620-3.

Lyapina, S., Cope, G., Shevchenko, A., Serino, G., Tsuge, T., Zhou, C., Wolf, D. A., Wei, N., Shevchenko, A., and Deshaies, R. J. (2001). Promotion of NEDD-CUL1 conjugate cleavage by COP9 signalosome. *Science* **292,** 1382-5.

Ma, C., and Moses, K. (1995). Wingless and patched are negative regulators of the morphogenetic furrow and can affect tissue polarity in the developing Drosophila compound eye. *Development* **121,** 2279-89.

Ma, D., Yang, C. H., McNeill, H., Simon, M. A., and Axelrod, J. D. (2003). Fidelity in planar cell polarity signalling. *Nature* **421,** 543-7.

Mahoney, P. A., Weber, U., Onofrechuk, P., Biessmann, H., Bryant, P. J., and Goodman, C. S. (1991). The fat tumor suppressor gene in Drosophila encodes a novel member of the cadherin gene superfamily. *Cell* **67,** 853-68.

Maitra, S., Kulikauskas, R. M., Gavilan, H., and Fehon, R. G. (2006). The tumor suppressors Merlin and expanded function cooperatively to modulate receptor endocytosis and signaling. *Curr Biol* **16,** 702-9.

Mao, Y., Rauskolb, C., Cho, E., Hu, W. L., Hayter, H., Minihan, G., Katz, F. N., and Irvine, K. D. (2006). Dachs: an unconventional myosin that functions downstream of Fat to regulate growth, affinity and gene expression in Drosophila. *Development* **133,** 2539-51.

Marigo, V., Davey, R. A., Zuo, Y., Cunningham, J. M., and Tabin, C. J. (1996). Biochemical evidence that patched is the Hedgehog receptor. *Nature* **384,** 176-9.

Matakatsu, H., and Blair, S. S. (2004). Interactions between Fat and Dachsous and the regulation of planar cell polarity in the Drosophila wing. *Development* **131,** 3785-94.

Matakatsu, H., and Blair, S. S. (2006). Separating the adhesive and signaling functions of the Fat and Dachsous protocadherins. *Development* **133,** 2315-24.

Mathews, M. B., Bernstein, R. M., Franza, B. R., Jr., and Garrels, J. I. (1984). Identity of the proliferating cell nuclear antigen and cyclin. *Nature* **309,** 374-6.

Maurel-Zaffran, C., and Treisman, J. E. (2000). pannier acts upstream of wingless to direct dorsal eye disc development in Drosophila. *Development* **127,** 1007-16.

McCartney, B. M., and Fehon, R. G. (1996). Distinct cellular and subcellular patterns of expression imply distinct functions for the Drosophila homologues of moesin and the neurofibromatosis 2 tumor suppressor, merlin. *J Cell Biol* **133,** 843-52.

McCartney, B. M., Kulikauskas, R. M., LaJeunesse, D. R., and Fehon, R. G. (2000). The neurofibromatosis-2 homologue, Merlin, and the tumor suppressor expanded function together in Drosophila to regulate cell proliferation and differentiation. *Development* **127,** 1315-24.

McNeill, H., Yang, C. H., Brodsky, M., Ungos, J., and Simon, M. A. (1997). mirror encodes a novel PBX-class homeoprotein that functions in the definition of the dorsal-ventral border in the Drosophila eye. *Genes Dev* **11,** 1073-82.

Methot, N., and Basler, K. (1999). Hedgehog controls limb development by regulating the activities of distinct transcriptional activator and repressor forms of Cubitus interruptus. *Cell* **96,** 819-31.

Methot, N., and Basler, K. (2001). An absolute requirement for Cubitus interruptus in Hedgehog signaling. *Development* **128,** 733-42.

Meyer, C. A., Jacobs, H. W., Datar, S. A., Du, W., Edgar, B. A., and Lehner, C. F. (2000). Drosophila Cdk4 is required for normal growth and is dispensable for cell cycle progression. *Embo J* **19,** 4533-42.

Miller, D. T., and Cagan, R. L. (1998). Local induction of patterning and programmed cell death in the developing Drosophila retina. *Development* **125,** 2327-35.

Minshull, J., Golsteyn, R., Hill, C. S., and Hunt, T. (1990). The A- and B-type cyclin associated cdc2 kinases in Xenopus turn on and off at different times in the cell cycle. *Embo J* **9,** 2865-75.

Mohr, O. L. (1929). "Exaggeration and inhibition phenomena encountered in the analysis of an autosomal dominant."

Monnier, V., Dussillol, F., Alves, G., Lamour-Isnard, C., and Plessis, A. (1998). Suppressor of fused links fused and Cubitus interruptus on the hedgehog signalling pathway. *Curr Biol* **8,** 583-6.

Mozer, B. A., and Easwarachandran, K. (1999). Pattern formation in the absence of cell proliferation: tissue-specific regulation of cell cycle progression by string (stg) during Drosophila eye development. *Dev Biol* **213,** 54-69.

Murone, M., Rosenthal, A., and de Sauvage, F. J. (1999). Sonic hedgehog signaling by the patched-smoothened receptor complex. *Curr Biol* **9,** 76-84.

Nolo, R., Abbott, L. A., and Bellen, H. J. (2000). Senseless, a Zn finger transcription factor, is necessary and sufficient for sensory organ development in Drosophila. *Cell* **102,** 349-62.

Nusse, R. (1990). The int genes in mouse mammary tumorigenesis and in normal development. *Ciba Found Symp* **150,** 212-22; discussion 222-6.

Ou, C. Y., Lin, Y. F., Chen, Y. J., and Chien, C. T. (2002). Distinct protein degradation mechanisms mediated by Cul1 and Cul3 controlling Ci stability in Drosophila eye development. *Genes Dev* **16,** 2403-14.

Pantalacci, S., Tapon, N., and Leopold, P. (2003). The Salvador partner Hippo promotes apoptosis and cell-cycle exit in Drosophila. *Nat Cell Biol* **5,** 921-7.

Pappu, K. S., Chen, R., Middlebrooks, B. W., Woo, C., Heberlein, U., and Mardon, G. (2003). Mechanism of hedgehog signaling during Drosophila eye development. *Development* **130,** 3053-62.

Penton, A., Selleck, S. B., and Hoffmann, F. M. (1997). Regulation of cell cycle synchronization by decapentaplegic during Drosophila eye development. *Science* **275,** 203-6.

Pignoni, F., and Zipursky, S. L. (1997). Induction of Drosophila eye development by decapentaplegic. *Development* **124,** 271-8.

Povelones, M., Howes, R., Fish, M., and Nusse, R. (2005). Genetic evidence that Drosophila frizzled controls planar cell polarity and Armadillo signaling by a common mechanism. *Genetics* **171,** 1643-54.

Prelich, G., Tan, C. K., Kostura, M., Mathews, M. B., So, A. G., Downey, K. M., and Stillman, B. (1987). Functional identity of proliferating cell nuclear antigen and a DNA polymerase-delta auxiliary protein. *Nature* **326,** 517-20.

Price, M. A., and Kalderon, D. (1999). Proteolysis of cubitus interruptus in Drosophila requires phosphorylation by protein kinase A. *Development* **126,** 4331-9.

Price, M. A., and Kalderon, D. (2002). Proteolysis of the Hedgehog signaling effector Cubitus interruptus requires phosphorylation by Glycogen Synthase Kinase 3 and Casein Kinase 1. *Cell* **108,** 823-35.

Quiring, R., Walldorf, U., Kloter, U., and Gehring, W. J. (1994). Homology of the eyeless gene of Drosophila to the Small eye gene in mice and Aniridia in humans. *Science* **265,** 785-9.

Rawls, A. S., Guinto, J. B., and Wolff, T. (2002). The cadherins fat and dachsous regulate dorsal/ventral signaling in the Drosophila eye. *Curr Biol* **12,** 1021-6.

Rawls, A. S., and Wolff, T. (2003). Strabismus requires Flamingo and Prickle function to regulate tissue polarity in the Drosophila eye. *Development* **130,** 1877-87.

Ready, D. F., Hanson, T. E., and Benzer, S. (1976). Development of the Drosophila retina, a neurocrystalline lattice. *Dev Biol* **53,** 217-40.

Reich, A., Sapir, A., and Shilo, B. (1999). Sprouty is a general inhibitor of receptor tyrosine kinase signaling. *Development* **126,** 4139-47.

Reifegerste, R., Ma, C., and Moses, K. (1997). A polarity field is established early in the development of the Drosophila compound eye. *Mech Dev* **68,** 69-79.

Riggleman, B., Schedl, P., and Wieschaus, E. (1990). Spatial expression of the Drosophila segment polarity gene armadillo is posttranscriptionally regulated by wingless. *Cell* **63,** 549-60.

Robbins, D. J., Nybakken, K. E., Kobayashi, R., Sisson, J. C., Bishop, J. M., and Therond, P. P. (1997). Hedgehog elicits signal transduction by means of a large complex containing the kinesin-related protein costal2. *Cell* **90,** 225-34.

Rodriguez, A., Terriente, J., Galindo, M. I., Couso, J. P., and Diaz-Benjumea, F. J. (2002). Different mechanisms initiate and maintain wingless expression in the Drosophila wing hinge. *Development* **129,** 3995-4004.

Rodriguez, I. (2004). The dachsous gene, a member of the cadherin family, is required for Wg-dependent pattern formation in the Drosophila wing disc. *Development* **131,** 3195-206.

Rohrbaugh, M., Ramos, E., Nguyen, D., Price, M., Wen, Y., and Lai, Z. C. (2002). Notch activation of yan expression is antagonized by RTK/pointed signaling in the Drosophila eye. *Curr Biol* **12,** 576-81.

Rouleau, G. A., Merel, P., Lutchman, M., Sanson, M., Zucman, J., Marineau, C., Hoang-Xuan, K., Demczuk, S., Desmaze, C., Plougastel, B., and et al. (1993). Alteration in a new gene encoding a putative membrane-organizing protein causes neuro-fibromatosis type 2. *Nature* **363,** 515-21.

Royet, J., and Finkelstein, R. (1997). Establishing primordia in the Drosophila eye-antennal imaginal disc: the roles of decapentaplegic, wingless and hedgehog. *Development* **124,** 4793-800.

Rubin, C., Litvak, V., Medvedovsky, H., Zwang, Y., Lev, S., and Yarden, Y. (2003). Sprouty fine-tunes EGF signaling through interlinked positive and negative feedback loops. *Curr Biol* **13,** 297-307.

Sanson, B., White, P., and Vincent, J. P. (1996). Uncoupling cadherin-based adhesion from wingless signalling in Drosophila. *Nature* **383,** 627-30.

Schweitzer, R., Howes, R., Smith, R., Shilo, B. Z., and Freeman, M. (1995). Inhibition of Drosophila EGF receptor activation by the secreted protein Argos. *Nature* **376,** 699-702.

Simon, M. A. (2004). Planar cell polarity in the Drosophila eye is directed by graded Four-jointed and Dachsous expression. *Development* **131,** 6175-84.

Stone, D. M., Hynes, M., Armanini, M., Swanson, T. A., Gu, Q., Johnson, R. L., Scott, M. P., Pennica, D., Goddard, A., Phillips, H., Noll, M., Hooper, J. E., de Sauvage, F., and Rosenthal, A. (1996). The tumour-suppressor gene patched encodes a candidate receptor for Sonic hedgehog. *Nature* **384,** 129-34.

Strutt, D. I., and Mlodzik, M. (1997). Hedgehog is an indirect regulator of morphogenetic furrow progression in the Drosophila eye disc. *Development* **124,** 3233-40.

Strutt, H., Mundy, J., Hofstra, K., and Strutt, D. (2004). Cleavage and secretion is not required for Four-jointed function in Drosophila patterning. *Development* **131,** 881-90.

Strutt, H., Price, M. A., and Strutt, D. (2006). Planar polarity is positively regulated by casein kinase Iepsilon in Drosophila. *Curr Biol* **16,** 1329-36.

Strutt, H., and Strutt, D. (2002). Nonautonomous planar polarity patterning in Drosophila: dishevelled-independent functions of frizzled. *Dev Cell* **3,** 851-63.

Strutt, H., and Strutt, D. (2003). EGF signaling and ommatidial rotation in the Drosophila eye. *Curr Biol* **13,** 1451-7.

Takada, R., Hijikata, H., Kondoh, H., and Takada, S. (2005). Analysis of combinatorial effects of Wnts and Frizzleds on beta-catenin/armadillo stabilization and Dishevelled phosphorylation. *Genes Cells* **10,** 919-28.

Tapon, N., Harvey, K. F., Bell, D. W., Wahrer, D. C., Schiripo, T. A., Haber, D. A., and Hariharan, I. K. (2002). salvador Promotes both cell cycle exit and apoptosis in Drosophila and is mutated in human cancer cell lines. *Cell* **110,** 467-78.

Teleman, A. A., and Cohen, S. M. (2000). Dpp gradient formation in the Drosophila wing imaginal disc. *Cell* **103,** 971-80.

Thacker, S. A., Bonnette, P. C., and Duronio, R. J. (2003). The contribution of E2F-regulated transcription to Drosophila PCNA gene function. *Curr Biol* **13,** 53-8.

Theisen, H., Haerry, T. E., O'Connor, M. B., and Marsh, J. L. (1996). Developmental territories created by mutual antagonism between Wingless and Decapentaplegic. *Development* **122,** 3939-48.

Thomas, B. J., Gunning, D. A., Cho, J., and Zipursky, L. (1994). Cell cycle progression in the developing Drosophila eye: roughex encodes a novel protein required for the establishment of G1. *Cell* **77,** 1003-14.

Tomlinson, A. (1985). The cellular dynamics of pattern formation in the eye of Drosophila. *J Embryol Exp Morphol* **89,** 313-31.

Tomlinson, A., Strapps, W. R., and Heemskerk, J. (1997). Linking Frizzled and Wnt signaling in Drosophila development. *Development* **124,** 4515-21.

Tomlinson, A., and Struhl, G. (1999). Decoding vectorial information from a gradient: sequential roles of the receptors Frizzled and Notch in establishing planar polarity in the Drosophila eye. *Development* **126,** 5725-38.

Tree, D. R., Shulman, J. M., Rousset, R., Scott, M. P., Gubb, D., and Axelrod, J. D. (2002). Prickle mediates feedback amplification to generate asymmetric planar cell polarity signaling. *Cell* **109,** 371-81.

Treisman, J. E., and Rubin, G. M. (1995). wingless inhibits morphogenetic furrow movement in the Drosophila eye disc. *Development* **121,** 3519-27.

Tsuda, L., Nagaraj, R., Zipursky, S. L., and Banerjee, U. (2002). An EGFR/Ebi/Sno pathway promotes delta expression by inactivating Su(H)/SMRTER repression during inductive notch signaling. *Cell* **110,** 625-37.

Udan, R. S., Kango-Singh, M., Nolo, R., Tao, C., and Halder, G. (2003). Hippo promotes proliferation arrest and apoptosis in the Salvador/Warts pathway. *Nat Cell Biol* **5,** 914-20.

Vincan, E. (2004). Frizzled/WNT signalling: the insidious promoter of tumour growth and progression. *Front Biosci* **9,** 1023-34.

Von Ohlen, T., Lessing, D., Nusse, R., and Hooper, J. E. (1997). Hedgehog signaling regulates transcription through cubitus interruptus, a sequence-specific DNA binding protein. *Proc Natl Acad Sci U S A* **94,** 2404-9.

Wang, G., Wang, B., and Jiang, J. (1999a). Protein kinase A antagonizes Hedgehog signaling by regulating both the activator and repressor forms of Cubitus interruptus. *Genes Dev* **13,** 2828-37.

Wang, S. L., Hawkins, C. J., Yoo, S. J., Muller, H. A., and Hay, B. A. (1999b). The Drosophila caspase inhibitor DIAP1 is essential for cell survival and is negatively regulated by HID. *Cell* **98,** 453-63.

Wasserman, J. D., and Freeman, M. (1998). An autoregulatory cascade of EGF receptor signaling patterns the Drosophila egg. *Cell* **95,** 355-64.

Whitfield, W. G., Gonzalez, C., Maldonado-Codina, G., and Glover, D. M. (1990). The A- and B-type cyclins of Drosophila are accumulated and destroyed in temporally distinct events that define separable phases of the G2-M transition. *Embo J* **9,** 2563-72.

Wiersdorff, V., Lecuit, T., Cohen, S. M., and Mlodzik, M. (1996). Mad acts downstream of Dpp receptors, revealing a differential requirement for dpp signaling in initiation and propagation of morphogenesis in the Drosophila eye. *Development* **122,** 2153-62.

Wolff, B., Sanglier, J. J., and Wang, Y. (1997). Leptomycin B is an inhibitor of nuclear export: inhibition of nucleo-cytoplasmic translocation of the human immunodeficiency virus type 1 (HIV-1) Rev protein and Rev-dependent mRNA. *Chem Biol* **4,** 139-47.

Wolff, T., and Ready, D. F. (1991a). The beginning of pattern formation in the Drosophila compound eye: the morphogenetic furrow and the second mitotic wave. *Development* **113,** 841-50.

Wolff, T., and Ready, D. F. (1991b). Cell death in normal and rough eye mutants of Drosophila. *Development* **113,** 825-39.

Wong, E. S., Fong, C. W., Lim, J., Yusoff, P., Low, B. C., Langdon, W. Y., and Guy, G. R. (2002). Sprouty2 attenuates epidermal growth factor receptor ubiquitylation and endocytosis, and consequently enhances Ras/ERK signalling. *Embo J* **21,** 4796-808.

Woods, D. F., Wu, J. W., and Bryant, P. J. (1997). Localization of proteins to the apico-lateral junctions of Drosophila epithelia. *Dev Genet* **20,** 111-8.

Wu, J. T., Lin, H. C., Hu, Y. C., and Chien, C. T. (2005). Neddylation and deneddylation regulate Cul1 and Cul3 protein accumulation. *Nat Cell Biol* **7,** 1014-20.

Wu, S., Huang, J., Dong, J., and Pan, D. (2003). hippo encodes a Ste-20 family protein kinase that restricts cell proliferation and promotes apoptosis in conjunction with salvador and warts. *Cell* **114,** 445-56.

Xu, D., Wang, Y., Willecke, R., Chen, Z., Ding, T., and Bergmann, A. (2006). The effector caspases drICE and dcp-1 have partially overlapping functions in the apoptotic pathway in Drosophila. *Cell Death Differ.*

Yang, C. H., Axelrod, J. D., and Simon, M. A. (2002). Regulation of Frizzled by fat-like cadherins during planar polarity signaling in the Drosophila compound eye. *Cell* **108,** 675-88.

Yoo, S. J., Huh, J. R., Muro, I., Yu, H., Wang, L., Wang, S. L., Feldman, R. M., Clem, R. J., Muller, H. A., and Hay, B. A. (2002). Hid, Rpr and Grim negatively regulate DIAP1 levels through distinct mechanisms. *Nat Cell Biol* **4,** 416-24.

Zecca, M., Basler, K., and Struhl, G. (1996). Direct and long-range action of a wingless morphogen gradient. *Cell* **87,** 833-44.

Zhang, C., Williams, E. H., Guo, Y., Lum, L., and Beachy, P. A. (2004). Extensive phosphorylation of Smoothened in Hedgehog pathway activation. *Proc Natl Acad Sci U S A* **101,** 17900-7.

Zhang, Y., Feng, X., We, R., and Derynck, R. (1996). Receptor-associated Mad homologues synergize as effectors of the TGF-beta response. *Nature* **383,** 168-72.

Zilian, O., Frei, E., Burke, R., Brentrup, D., Gutjahr, T., Bryant, P. J., and Noll, M. (1999). double-time is identical to discs overgrown, which is required for cell survival, proliferation and growth arrest in Drosophila imaginal discs. *Development* **126,** 5409-20.

Zitnan, D., Sehnal, F., and Bryant, P. J. (1993). Neurons producing specific neuropeptides in the central nervous system of normal and pupariation-delayed Drosophila. *Dev Biol* **156,** 117-35.